Institute for Communications and Navigation

Optimisation of Pseudolite Pulsing Scheme for Participative & Non-Participative Receivers

Jean-Baptiste Gigant

A Thesis submitted for the Degree of
Master Degree

Institute for Communications and Navigation

Prof. Dr. Christoph Günther

Supervised by Francis Soualle (EADS Astrium)
Kaspar Giger (TUM)

October 18, 2012

Institute for Communications and Navigation

Technische Universität München
Theresienstrasse 90
80333 Munich

Abstract

For some applications like guidance of aircrafts, it might be profitable to combine ranging information provided by GNSS like GPS or Galileo with those provided by ground emitters, called pseudolites. Pseudolite signals share many signal characteristics with satellite signals. Because of the Near-Far effect, performance of the tracking of either satellite or pseudolite signals may be highly degraded if no care is taken. The usual technique to limit the tracking degradation consists of transmitting the pseudolite signals in a pulsed way. Then satellite signals are degraded only during pulses. Several solutions for the pulse scheme can be specified: pseudolites can be unsynchronized and transmit randomly or can be synchronized. In the synchronized case, pseudolites can transmit either each at the same time (overlapping pulses) or each at a different time (non-overlapping pulses).

In this paper, two alternative pulse schemes (overlapping and non-overlapping pulses) are compared the using the Cramér-Rao Lower Bound (CRLB). The overlapping pulse scheme has the advantage to leave more time for the reception of the satellite signals and should therefore be recommended to improve compatibility between both systems. In the case of overlapping pulses, a possible architecture implementing the interference cancellation for a participative receiver will allow to reduce the degradation for the reception of pseudolites signals. The interference cancellation consists in estimating the characteristics like the amplitude and the code and phase delays of the interfering (pseudolites) signals and to subtract them from the received signals before the correlation. The performances of the interference cancellation will be evaluated theoretically, with simulations using a Matlab® software simulator and finally with laboratory measurements. It is shown that interference cancellation is a good way to decrease the error on delay estimation, and to approach to the CRLB.

Contents

Acronyms

ADC Analogue to Digital Converter

AGC Automatic Gain Control

AWGN Additive White Gaussian Noise

BaySEF Bavarian Signal Evaluation Facility

BOC Binary Offset Carrier

BPSK Binary Phase Shifting Kay

CDMA Code Division Multiple Access

CRLB Cramér-Rao Lower Bound

D2MAI Double Differential Multiple Access Interference

DLL Delay Locked Loop

DMAI Differential Multiple Access Interference

DWCC Differential Waveform Convolution Coefficient

DOP Dilution Of Precision

GBAS Ground Based Augmentation System

GNSS Global Navigation Satellite System

GPS Global Positioning System

MAI Multiple Access Interference

NSG Navigation Signal Generator

PIC Parallel Interference Cancellation

PPP Pulse Peak Power

PRN Pseudo Random Noise

RTCM Radio Technical Commission for Maritime Services

SIC Sequential Interference Cancellation

SNIR Signal to Noise plus Interferences Ratio

TDMA Time Division Multiple Access

WCC Waveform Convolution Coefficient

Chapter 1

Introduction

1.1 Technical Background

1.1.1 Global Navigation Satellite System

A Global Navigation Satellite System (GNSS) is a system of satellites that provides autonomous positioning with global coverage. For the time being, only the United States NAVSTAR Global Positioning System (GPS) and the Russian GLONASS are fully globally operational GNSSs. The Chinese Compass and the European Galileo system are under development and scheduled to be fully and globally operational in 2016 at the earliest.

GNSSs allow small electronic receivers to determine their location within a few meters using signals transmitted continuously by the satellites of the constellation. Code Division Multiple Access (CDMA) is used to multiplex the signals from the different satellites. Each satellite modulates his down-link message with a specific Pseudo Random Noise (PRN), a repeating predictable noise-like digital code.

The down-link message provides information on the satellite's position and on the satellite's clock. With these information, the receiver can determine its position by using a multilateration algorithm. Since three parameters of position and the receiver's time have to be determined, at least four satellites must be visible. But the more satellites are visible, the higher is the accuracy.

1.1.2 Ground Based Augmentation System

In a GNSS-denied area or wherever GNSS visibility is poor, terrestrial ranging signal transmitters (so called pseudo-satellites, short pseudolites) enhance the positioning performance of the receiver in two respects: firstly they provide additional signals such that enough ranging sources are (always) available and secondly the terrestrial location of these sources improves the spatial geometrical repartition, leading to a better Dilution Of Precision (DOP). Among possible applications are airports, tunnels, mines, shopping malls ...

1.1.3 Near-Far Effect

Drawback of the pseudolite transmissions is the strong signal power as compared to the GNSS signals. This leads to a degradation of the satellite signal ranging precision or even might prevent the receiver from tracking the satellite signals. This is known as the Near-Far effect. The Near-Far problem can be reduced by using pulsed pseudolite transmissions like the one proposed for Ground Based Augmentation System (GBAS) infrastructures (cf. [1] for example). The Near-Far effect can also appear between the pseudolite signals when the receiver is much closer to one pseudolite than to another one. Therefore in the past a high effort was made to find pulsing schemes which reduce or even prevent the concurrent signal reception from more than one pseudolite transmitter (cf. [1,2]).

1.2 Objectives of the Thesis

A non-participative receiver is a receiver that tracks only satellite navigation signals while a participative receiver is a receiver that tracks both satellite and pseudolite navigation signals. The objective of the thesis is to optimize the pseudolite pulse scheme, and to find a scheme that follows these two conditions:

- satellite signals can be acquired and tracked by both participative and non-participative receivers,
- pseudolite signals can be acquired and tracked by participative receivers.

For this purpose the maximum admissible duty cycle for pseudolites will be characterized in chapter 2. Hence, receivers must still be able to track satellite signals despite of the pseudolite pulses. Therefore, a sufficient part of the integration time should be free of pulses. In figure 1.1, the part of the integration time in which pseudolite signals hide satellite signals is too large. Consequently, receivers will not be able to track satellite signals.

Therefore the overall duty cycle for pseudolites has to be limited. Figures 1.2 and 1.3 show two solutions for which the overall duty cycle is reduced and the satellites tracking performs better. Note that for both schemes, the pulses are synchronized. In figure 1.2, the pulses are shorter and are transmitted at different times (non-overlapping pulses), while in figure 1.3, all pseudolites transmit at the same time (overlapping pulses). These two different pulse schemes will be analyzed and the best expected accuracy for code tracking will be compared using the Cramér-Rao Lower Bound (CRLB) in chapter 3. Then in chapter 4, interference cancellation methods are applied to the input signals, in order to improve the tracking performances, and to get close to the theoretical best possible performance given by CRLB. Finally experimental results are presented in chapter 5.

1.3 Simulation Parameters

Throughout the thesis, some simulation results are presented. Except if explicitly mentioned, the following parameters are used:

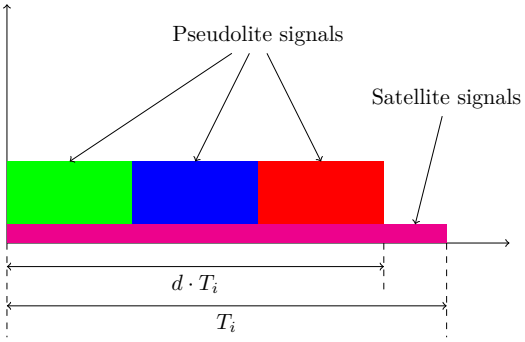

Figure 1.1: Non-overlapping pulses, duty cycle excessive: non-participative receivers can almost not track satellite signals

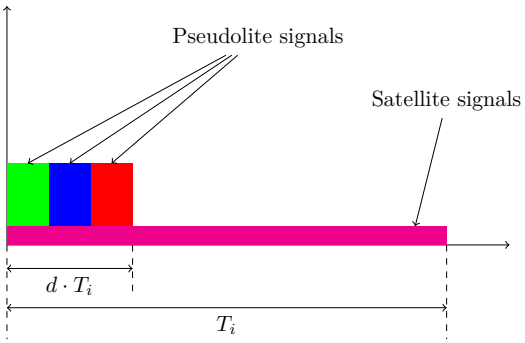

Figure 1.2: Non-overlapping pulses, duty cycle acceptable: non-participative receivers can track satellite signals

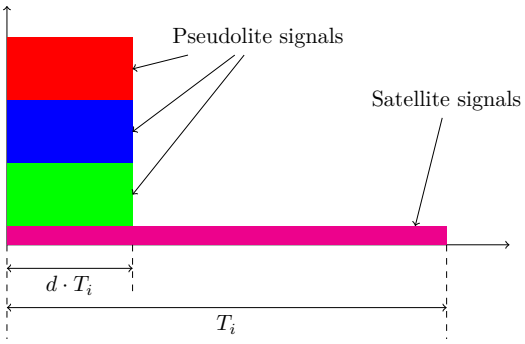

Figure 1.3: Overlapping pulses, duty cycle acceptable: non-participative receivers can track satellite signals

Integration time (code period):	$T_i = 1$ ms
Code:	GPS L1 C/A
Code length:	$L = 1023$ chips per epoch
Noise power spectral density:	$\mathcal{N}_0/2 = -201.5$ dBW/Hz
Received power from satellites:	$\mathcal{P} = -158.5$ dBW
Sampling frequency:	8.18 MHz

Some other parameters are linked to the previous ones, and can consequently be expressed.

Sampling interval:	$\Delta = 12.2\,\mu$s
Chip duration:	$T_c = {}^{T_i}/_{L} = 97.7\ \mu$s
Number of samples per chip:	$N_c = {}^{T_c}/_{\Delta} = 8$
Filter cut-off frequency:	$B = {}^{1}/_{2\cdot\Delta} = 4.092\,$MHz

Chapter 2

SNIR Degradation for Non-Participative Receivers

The aim of this chapter is to determine the degradation of Signal to Noise plus Interferences Ratio (SNIR) for non-participative receivers cause by the presence of pseudolites. Then a maximal acceptable duty cycle will be specified, considering that non-participative receivers must still be able to track satellite navigation signals despite the pseudolite pulses.

2.1 Definition of the Receiver

For now, only the spreading codes are considered, therefore the whole front-end does not have to be taken into account.

Even the simplest receiver must be able to track satellite signals in presence of pseudolite signals. Therefore a low-cost receiver is considered. The front-end used to dimension the maximum pseudolite duty cycle, and partially represented figure 2.1, has no blanker and the quantization is done with only one bit and therefore an Automatic Gain Control (AGC) is not needed.

In this chapter, satellites tracking is studied. Therefore a non-participative receiver is considered. In chapters 3 and 4, pseudolites tracking will be studied. Therefore a participative and highly capable receiver will be considered.

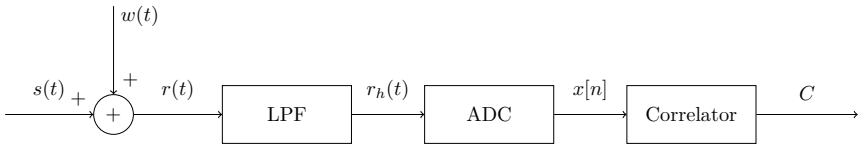

Figure 2.1: Front-end block diagram of a non-participative receiver

2.1.1 Input Signal

The input signal is the sum of all navigation signals from satellites and pseudolites.

$$s(t) = \sum_k s^k(t)$$

$s^k(.)$ represents the navigation signal in baseband from source k, either a satellite or a pseudolite. It corresponds to the delayed spreading code signal scaled with the received amplitude at receiver antenna. The time origin is defined such that the tracked navigation signal is not delayed. For the tracking of the signal of the source l, $\tau^l = 0$ and $s^l(t) = \sqrt{\mathcal{P}^l} \cdot c^l(t)$. In the future, l always represents the index of the tracked pseudolite or satellite, while k represents the index of other interfering pseudolites or satellites.

- For a satellite:
$$s^k(t) = \sqrt{\mathcal{P}^k} \cdot c^k(t - \tau^k)$$
- For a pseudolite transmitting in pulses:
$$s^k(t) = \begin{cases} \sqrt{\mathcal{P}^k} \cdot c^k(t - \tau^k) & \text{if } t \in \text{pulsed interval} \\ 0 & \text{otherwise} \end{cases}$$

$c^k(.)$ is the spreading code signal of source k, defined as:

$$c^k(t) = \sum_{m=-\infty}^{\infty} c_m^k \cdot p(t - mT_c)$$

Notation:

$s^k(.)$	Navigation signal received from source k (satellite or pseudolite)
$\mathcal{P}^k$	Power of signal from source k at receiver
$c^k(.)$	Spreading code signal from source k
τ^k	Delay of the signal from source k, in seconds
c_m^k	Chip bit (index m) of spreading code $c^k(.) \in \{-1, 1\}$
$p(.)$	Chip waveform of spreading code (same for all signals)
T_c	Chip duration (same for all signals)

2.1.2 Noise

The noise component encompasses thermal noise and other similar wide-band interferences. The noise $w(.)$ is assumed to have a Gaussian distribution and to be white, with a power spectral density $\mathcal{N}_0/2$, supposed with an infinite bandwidth before filtering.

2.1.3 Signal After Filtering

To avoid aliasing and respect the Nyquist-Shannon condition, the signal is low-pass filtered at the cut-off frequency B. Thus the signal is band-limited with a maximum frequency B.

$$\begin{aligned} r_h(t) &= h(t) * (s(t) + w(t)) \\ &= h(t) * s(t) + \eta(t) \end{aligned}$$

On the preserved bandwidth, the noise $\eta(.)$ is white with a variance $\sigma^2 = B\mathcal{N}_0$ (the power spectral density is $\mathcal{N}_0/2$ on $[-B\,;B]$).

2.1.4 Signal After ADC

The Analogue to Digital Converter (ADC) samples and quantizes the signal.

- Sampling: The continuous signal is sampled at the sampling interval $\Delta = 1/2 \cdot B$, in order to respect the Nyquist-Shannon condition.
- Quantization: The signal is quantized with a one bit quantizer

At the ADC output:

$$\begin{aligned} x[n] &= \text{sign}\left(r_h(n\Delta)\right) \\ &= \text{sign}\left(\sum_k s^k(n\Delta) + \eta(n\Delta)\right) \end{aligned}$$

2.1.5 Signal After Correlation

For the tracking of signal from source l, the correlator multiplies the signal $x[.]$ with the local replica of the tracked spreading code $c^l[.]$ and integrates it over the integration time T_i, which corresponds to $N = 2 \cdot B \cdot T_i$ samples. Then, when satellite l is tracked, the correlator output is:

$$C^l = \frac{1}{N} \cdot \sum_{n=0}^{N-1} c^l[n] \cdot x[n]$$

2.2 Approximations

In order to make the derivations easier, the following assumptions are supposed to be fulfilled:

Approx. 2.1. All signals are considered real. The down-conversion of received signal into baseband induces actually complex signals, but if the phase is perfectly known, it may be possible to take only the real part.

Approx. 2.2. The power of satellite signals is supposed to be much smaller than the power of the pseudolite signals and the power of the noise (after filtering, the power of the noise is $B\mathcal{N}_0$).

Approx. 2.3. Only noise and navigation signals are considered. Other received signals are not taken into account.

Approx. 2.4. The modulation is Binary Phase Shifting Kay (BPSK) for all navigation signals.

Approx. 2.5. The cut-off frequency of the low-pass filter is considered large. Then the effect of the low-pass filter on the navigation signal is negligible. Consequently $h(t) * s(t) \approx s(t)$.

Approx. 2.6. The spreading codes are supposed to be random and balanced.

Approx. 2.7. The interferences between two navigation signals are maximal when the relative propagation delay is a multiple of the chip duration T_c (cf. equation A.3 in annexe A for justification). Since the worst case is considered, in this chapter, it will be supposed that the chips edges are synchronized ($\forall k, \tau^k = iT_c, i \in \mathbb{Z}$).

2.3 Interval Without Pulses

In this section, the expectation and the variance of the correlator output will be computed for the interval without pulses. The input signal is only composed of satellite signals and noise, and is quantized with one bit. The approach is inspired by the one presented in [3].

2.3.1 Expectation of the Correlator Output

The expectation of the correlator output:

$$\begin{aligned}\mathcal{E}\left[C_{\text{off}}^l\right] &= \mathcal{E}\left[\frac{1}{N}\cdot\sum_{n=0}^{N-1} c^l(n\Delta)\cdot x[n]\right] \\ &= \frac{1}{N}\cdot\sum_{n=0}^{N-1}\mathcal{E}\left[c^l(n\Delta)\cdot x[n]\right]\end{aligned}$$

The expectation can be rewritten as:

$$\begin{aligned}\mathcal{E}\left[c^l(n\Delta)\cdot x[n]\right] = \mathcal{E}&\left[c^l(n\Delta)\cdot x[n] \mid x[n]=1\right]\cdot \mathrm{p}\left(x[n]=1\right) \\ &+ \mathcal{E}\left[c^l(n\Delta)\cdot x[n] \mid x[n]=-1\right]\cdot \mathrm{p}\left(x[n]=-1\right)\end{aligned}$$

Considering that the spreading code is known:

$$\begin{aligned}\mathcal{E}\left[c^l(n\Delta)\cdot x[n] \mid x[n]=1\right] &= c^l(n\Delta) \\ \mathcal{E}\left[c^l(n\Delta)\cdot x[n] \mid x[n]=-1\right] &= -c^l(n\Delta)\end{aligned}$$

It follows:

$$\mathcal{E}\left[c^l(n\Delta)\cdot x[n]\right] = c^l(n\Delta)\cdot\left(\mathrm{p}\left(x[n]=1\right)-\mathrm{p}\left(x[n]=-1\right)\right)$$

The probabilities can be expressed as:

$$\begin{aligned}\mathrm{p}\left(x[n]=1\right) &= \mathrm{p}\left(\sum_k s^k(n\Delta)+\eta[n]>0\right) \\ &= \mathcal{Q}\left(\frac{-\sum_k s^k(n\Delta)}{\sigma}\right)\end{aligned}$$

And:

$$\begin{aligned}\mathrm{p}\left(x[n]=-1\right) &= \mathrm{p}\left(\sum_k s^k(n\Delta)+\eta[n]<0\right) \\ &= \mathcal{Q}\left(\frac{\sum_k s^k(n\Delta)}{\sigma}\right)\end{aligned}$$

Where $\mathcal{Q}(.)$ is the Q-function defined as:

$$\mathcal{Q}(x) = \frac{1}{\sqrt{2\pi}} \cdot \int_x^{\infty} \exp\left(-\frac{u^2}{2}\right) \mathrm{d}u$$

Consequently:

$$\mathcal{E}\left[c^l(n\Delta) \cdot x[n]\right] = c^l(n\Delta) \cdot \left(\mathcal{Q}\left(\frac{-\sum_k s^k(n\Delta)}{\sigma}\right) - \mathcal{Q}\left(\frac{\sum_k s^k(n\Delta)}{\sigma}\right)\right) \quad (2.1)$$

$\sigma \gg \sum s^k[n]$ because the pseudolites are not transmitting. Since the function $\mathcal{Q}(.)$ is differentiable in zero, the previous expression can be approximated by its first order Taylor development:

$$\begin{aligned}\mathcal{Q}(x) &\approx \mathcal{Q}(0) + x \cdot \mathcal{Q}'(0) \\ &= \frac{1}{2} - \frac{x}{\sqrt{2\pi}}\end{aligned}$$

Consequently:

$$\begin{aligned}\mathcal{E}\left[c^l(n\Delta) \cdot x[n]\right] &= \sqrt{\frac{2}{\pi}} \cdot \frac{c^l(n\Delta) \cdot \sum_k s^k(n\Delta)}{\sigma} \\ &= \sqrt{\frac{2}{\pi}} \cdot \frac{\mathcal{P}^l + c^l(n\Delta) \cdot \sum_{k\neq l} s^k(n\Delta)}{\sigma}\end{aligned}$$

Then expectation of the correlator output is:

$$\mathcal{E}\left[C^l_{\text{off}}\right] = \frac{1}{N \cdot \sigma} \cdot \sqrt{\frac{2}{\pi}} \cdot \sum_{n=0}^{N-1} \left(\mathcal{P}^l + c^l(n\Delta) \cdot \sum_{k\neq l} s^k(n\Delta)\right)$$

Finally, since the spreading sequences are independent and balanced:

$$\boxed{\mathcal{E}\left[C^l_{\text{off}}\right] \approx \sqrt{\frac{2}{\pi}} \cdot \frac{\sqrt{\mathcal{P}^l}}{\sigma}}$$

2.3.2 Variance of the Correlator Output

The variance at the correlator output:

$$\begin{aligned}\text{var}\left[C^l_{\text{off}}\right] &= \text{var}\left[\frac{1}{N} \cdot \sum_{n=0}^{N-1} c^l(n\Delta)] \cdot x[n]\right] \\ &= \frac{1}{N^2} \cdot \text{var}\left[\sum_{n=0}^{N-1} c^l(n\Delta) \cdot x[n]\right]\end{aligned}$$

The power of satellites signals is negligible compared to the power of noise, then if $n_1 \neq n_2$, $x[n_1]$ is independent from $x[n_2]$. Consequently the term

$\sum_{n=0}^{N-1} c^l(n\Delta) \cdot x[n]$ can be considered as a sum of independent random variables. It follows:

$$\begin{aligned}
\text{var}\left[C_{\text{off}}^l\right] &= \frac{1}{N^2} \cdot \sum_{n=0}^{N-1} \text{var}\left[c^l(n\Delta) \cdot x[n]\right] \\
&= \frac{1}{N^2} \cdot \sum_{n=0}^{N-1} \left(\mathcal{E}\left[c^l(n\Delta)^2 \cdot x[n]^2\right] - \mathcal{E}\left[c^l(n\Delta) \cdot x[n]\right]^2\right) \\
&= \frac{1}{N^2} \cdot \sum_{n=0}^{N-1} \left(1 + \frac{2}{\pi} \cdot \frac{\mathcal{P}^l}{\sigma^2}\right)
\end{aligned}$$

Since $\mathcal{P}^l \ll \sigma^2$, finally:

$$\boxed{\text{var}\left[C_{\text{off}}^l\right] \approx \frac{1}{N}}$$

2.4 Interval With Pulses

In this section, the expectation and the variance of the correlator output will be computed for an interval with pulses. Therefore satellite signals, pseudolite signals and noise are considered. The satellite l is tracked.

2.4.1 Expectation of the Correlator Output

The expectation of the correlator output is:

$$\begin{aligned}
\mathcal{E}\left[C_{\text{on}}^l\right] &= \mathcal{E}\left[\frac{1}{N} \cdot \sum_{n=0}^{N-1} c^l(n\Delta) \cdot x[n]\right] \\
&= \frac{1}{N} \cdot \sum_{n=0}^{N-1} \mathcal{E}\left[c^l(n\Delta) \cdot x[n]\right]
\end{aligned}$$

Pseudolites are transmitting, then $\sigma \ll \sum s^k[n]$. Then using equation (2.1):

$$\mathcal{E}\left[c^l(n\Delta) \cdot x[n]\right] \approx 0$$

Consequently:

$$\boxed{\mathcal{E}\left[C_{\text{on}}^l\right] \approx 0}$$

2.4.2 Variance of the Correlator Output

The variance at the correlator output is:

$$\begin{aligned}
\text{var}\left[C_{\text{on}}^l\right] &= \text{var}\left[\frac{1}{N} \cdot \sum_{n=0}^{N-1} c^l(n\Delta) \cdot x[n]\right] \\
&= \frac{1}{N^2} \cdot \text{var}\left[\sum_{n=0}^{N-1} c^l(n\Delta) \cdot x[n]\right]
\end{aligned}$$

L is the code length, N_c the number of samples per chip and T_c the chip duration. Note that: $L = {}^{N}/_{N_c}$ and $T_c = \Delta \cdot N_c$. Then:

$$\text{var}\left[C_{\text{on}}^{l}\right] = \frac{1}{N^2} \cdot \text{var}\left[\sum_{k=0}^{L-1}\sum_{i=0}^{N_c-1} c^{l}\left(i\Delta + kT_c\right) \cdot x\left[i + kN_c\right]\right]$$

On a given chip, $c^{l}(.)$ is constant. Since the worst case is considered, the interferences are supposed to be maximal (cf. Approx 2.7). Since the power of the noise is negligible compared to the power of the pseudolites signals, $x[.]$ is constant and consequently:

$$\text{var}\left[C_{\text{on}}^{l}\right] = \frac{N_c^2}{N^2} \cdot \text{var}\left[\sum_{k=0}^{L-1} c^{l}\left(kT_c\right) \cdot x\left[kN_c\right]\right]$$

Since the values are taken on different chip intervals, the sum can be considered as a sum of independent random variables having zero mean and 1 as variance. Consequently:

$$\text{var}\left[\sum_{k=0}^{L-1} c^{l}\left(kT_c\right) \cdot x\left[kN_c\right]\right] = L$$

Finally:

$$\boxed{\text{var}\left[C_{\text{on}}^{l}\right] \approx \frac{1}{L}}$$

Note that the variance of the correlator output does not depend on the pseudolite power. In the case of a one bit quantizer, if the pseudolite power increase, it does not effect the variance. On the contrary, without quantization, if the pseudolite power increase, the variance will also increase and the SNIR can be degraded.

2.5 Global SNIR for a Non-Participative Receiver

The pseudolites transmit during the duty cycle d (and no pseudolites transmit during the duty cycle $1 - d$), then it follows:

$$\begin{aligned}\mathcal{E}\left[C^{l}\right] &= d \cdot \mathcal{E}\left[C_{\text{on}}^{l}\right] + (1-d) \cdot \mathcal{E}\left[C_{\text{off}}^{l}\right] \\ &= (1-d) \cdot \sqrt{\frac{2}{\pi}} \cdot \frac{\sqrt{\mathcal{P}^{l}}}{\sigma}\end{aligned}$$

$$\begin{aligned}\text{var}\left[C^{l}\right] &= d \cdot \text{var}\left[C_{\text{on}}^{l}\right] + (1-d) \cdot \text{var}\left[C_{\text{off}}^{l}\right] \\ &= \frac{1-d}{N} + \frac{d}{L}\end{aligned}$$

$$\begin{aligned}\text{SNIR}^{l} &= \frac{\mathcal{E}\left[C^{l}\right]^2}{\text{var}\left[C^{l}\right]} \\ &= \frac{2 \cdot N \cdot (1-d)^2 \cdot \mathcal{P}^{l}}{\pi \cdot \sigma^2 \cdot \left(1 + d \cdot \left({}^{N}/_{L} - 1\right)\right)}\end{aligned}$$

Finally, since $\sigma^2 = B\mathcal{N}_0$, it follows:

$$\boxed{\mathrm{SNIR}^l = \frac{2 \cdot (1-d)^2 \cdot \mathcal{P}^l}{\pi \cdot \mathcal{N}_0 \cdot B \cdot (1/N + d \cdot (1/L - 1/N))}}$$

Since a simple receiver have been analyzed, the SNIR obtained can be used to dimension the pseudolite duty cycle. Therefore, depending on the tracking algorithm, the lock on satellite signals is maintained if the SNIR is large enough. With this minimal admissible value for the SNIR, the maximal duty cycle d can be obtained. The next objective is to determine which pulse scheme (overlapping or non-overlapping) has to be used, in order to make the most profit of the available duty cycle for the pseudolite pulses.

2.6 Validation of the Theoretical Model

Figure 2.2 shows the mean, the variance and the SNIR at the correlator output in function of the duty cycle for the pseudolite pulses and shows that the simulation and theory curves correspond well. The computation is done using the parameters defined in section 1.3 and 100 Monte-Carlo simulations, with different real GPS PRN codes and different propagation delays. For a duty cycle of 20%, the corresponding SNIR equals to 10 dB (cf. figure 2.2), which is an acceptable value. For the following and without contrary mention, this duty cycle will be used for the numerical simulations.

The SNIR for an infinite-bit quantizer is also plotted. The receiver has no blanker and no AGC. One pseudolite is transmitting and the received power is -120 dBW. Note that the SNIR for this receiver can be worse than for the low-cost receiver. Indeed, depending on the strength of pseudolite signals, quantization leads to a saturation and prevents the correlation results from growing without limit. Therefore a fast AGC or a blanker should be used in receivers with many bits quantizer.

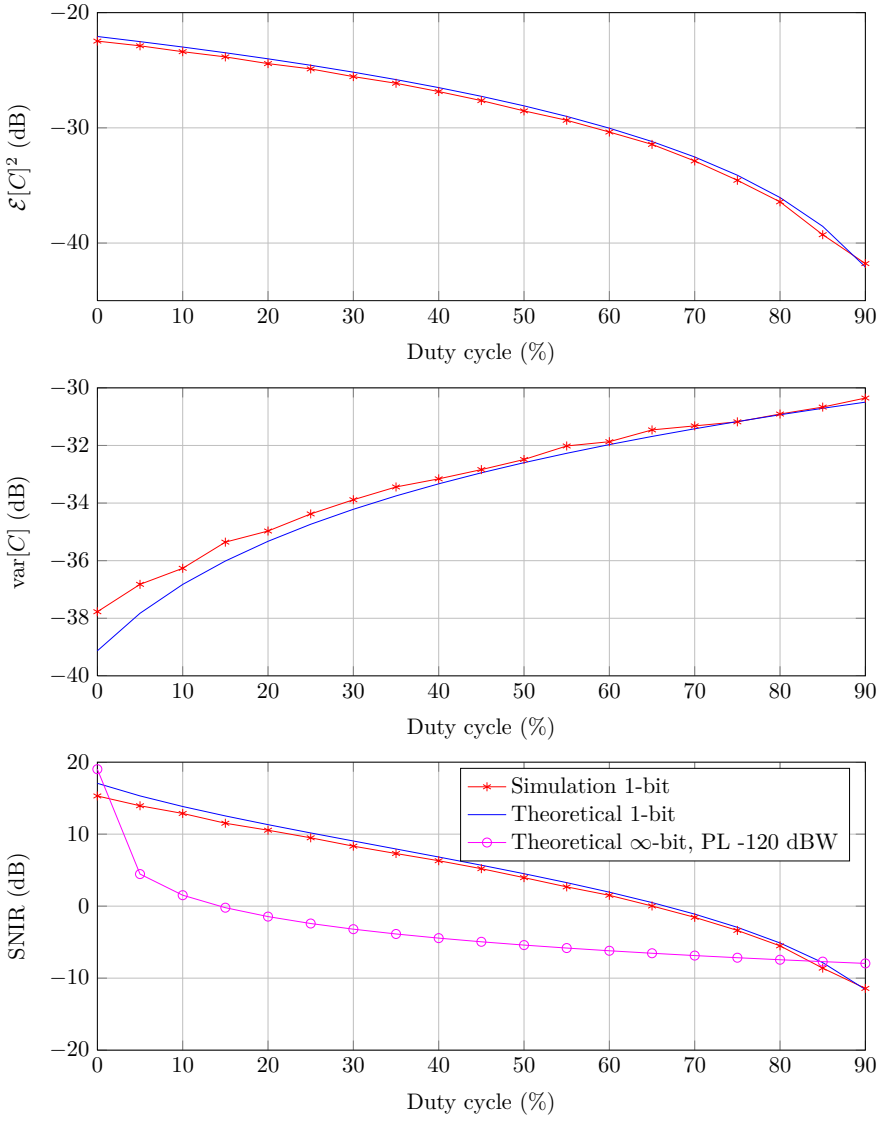

Figure 2.2: Mean, variance and SNIR

Chapter 3

Comparison Between Overlapping and Non-Overlapping Pulses

It is considered that pseudolites share a common time reference and have the possibility to transmit the pulses a dedicated instant in time, according to two different schemes:

- Overlapping pulse scheme: All pseudolites transmit at the same time. The drawback is that pseudolites interfere with each other, but the number of pseudolites is not limited, insofar as the interferences do not prevent tracking the navigation signals. Defining d as the overall duty cycle, $\mathcal{P}^l$ the received power from pseudolite l and T_i the integration time, then each pseudolite transmits at the duty cycle d, and the received power from the pseudolite l during one integration time become $d \cdot T_i \cdot \mathcal{P}^l$.

- Non-overlapping pulse scheme: It is based on a Time Division Multiple Access (TDMA) principe. Each pseudolite transmits at a different time. In this case, pseudolites do not interfere with each other. However the overall duty cycle d is shared between the K pseudolites and only a reduced number of pseudolites can transmit, for a fixed (limited) pulse duty cycle, if one need to limit the effects on the reception of the satellite navigation signals. Then each pseudolite transmits only at the duty cycle d/K and the received energy from pseudolite l becomes $d \cdot T_i \cdot \mathcal{P}^l/K$, that is to say K times smaller than in the overlapping scheme. The transmitted power could be increased to compensate the factor K, but the solution is not realistic since it would request higher classes of power amplifiers and might also not be accepted at ITU level when considering the maximal authorised power flux density.

In this chapter, the objective is to determine which of these two schemes performs the best. It is proposed to determine the bound for the variance of the estimated propagation delays for the two alternative pulse schemes. For that purpose, the Cramér-Rao Lower Bound (CRLB) will be used. Indeed the CRLB describes a fundamental limitation of parameter estimation.

3.1 Definition of the Signals

Since received signal power from the satellites is very weak compared to the one from pseudolites or compared to the noise power, the satellite signals are neglected in this derivation. Then, the received signal $r(t)$ can be described as:

$$r(t) = \sum_{k=0}^{K-1} \sqrt{\mathcal{P}^k} \cdot c^k(t - \tau^k) + \eta(t)$$

Where:

- $\eta(t)$ is a Gaussian white noise process with power spectral density $\mathcal{N}_0/2$
- $\sum_k \sqrt{\mathcal{P}^k} \cdot c^k(t - \tau^k)$ is the sum of the navigation signals transmitted by the K pseudolites.

The received signal is sampled at a sampling time Δ. To avoid aliasing and respect the Shannon condition, the signal is low-pass filtered at the cut-off frequency $B = 1/2 \cdot \Delta$. Thus the signal is band-limited with a maximum frequency B. The number of available samples is called N. N can be expressed as $N = d \cdot T_i/\Delta$, where T_i is the integration time (the signal is correlated with the local replica over a period T_i) and d is the duty cycle allowed for the pseudolites (pulses are allowed only during d percent of the integration time T_i). The vector $\boldsymbol{r} = [r_0; r_1; \cdots r_{N-1}]$ contains the N samples r_i taken at the times $t_i = i \cdot \Delta$. The i^{th} element of $\boldsymbol{r}$ is:

$$r_i = \sum_{k=0}^{K-1} \sqrt{\mathcal{P}^k} \cdot c^k(i\Delta - \tau^k) + \eta(i\Delta)$$

Furthermore, the noise is band-limited with a maximum frequency B equals to the Shannon frequency, therefore the noise after filtering is white on the preserved bandwidth (between $-B$ and B) and the noise variance is $\sigma^2 = B\mathcal{N}_0$. Its probability density function is Gaussian and can be expressed as:

$$f_\eta(x) = \frac{1}{\sigma\sqrt{2\pi}} \cdot \exp\left(-\frac{x^2}{2\sigma^2}\right)$$

3.2 Approximations

In order to make the derivations easier, the following assumptions are supposed fulfilled:

Approx. 3.1. All signals are considered real. The down-conversion of received signal into baseband induces actually complex signals, but if the phase is perfectly known, it may be possible to take the real part only.

Approx. 3.2. Only Gaussian noise and pseudolite navigation signals are considered. Other received signals are not taken into account and satellites signals are neglected, since the satellite signals power is much smaller than the pseudolite signals power and the noise power.

Approx. 3.3. The chip waveform and the chip time are supposed to be the same for all sources.

Approx. 3.4. It is considered that the only unknown parameters are the propagation delays τ^k and the received powers $\mathcal{P}^k$. The phase is considered known. Moreover, it is supposed that the estimators of the delay and of the received power are unbiased estimators.

3.3 Cramér-Rao Lower Bound in the Non Quantized Case

In this section, in a first approach, the quantization losses will not be taken into account.

3.3.1 General Application

The vector $\boldsymbol{\theta} = \left[\tau^1, \tau^2, \cdots, \tau^K, \sqrt{\mathcal{P}^1}, \sqrt{\mathcal{P}^2}, \ldots, \sqrt{\mathcal{P}^K}\right]$ represents the unknown set of parameters and the vector $\hat{\boldsymbol{\theta}}$ contains unbiased estimators of the elements of the vector for $\boldsymbol{\theta}$. Then the CRLB for the covariance matrix of $\hat{\boldsymbol{\theta}}$ is:

$$\operatorname{cov}\left[\hat{\boldsymbol{\theta}}\right] \geq \mathcal{I}(\boldsymbol{\theta})^{-1}$$

Where $\mathcal{I}(\boldsymbol{\theta})$ represents the $2K \times 2K$ Fisher information matrix. Let p and q be integers indexing the pseudolites, and u and v indexing either the delays if equal to one ($\theta_{1p} = \tau^p$), or the amplitudes if equals to two ($\theta_{2p} = \sqrt{\mathcal{P}^p}$). Then the element of the up^{th} row, vq^{th} column is:

$$\mathcal{I}(\theta_{up}, \theta_{vq}) = -\mathcal{E}\left[\frac{\partial^2 \log\left(\mathrm{p}\left(\boldsymbol{r} \mid \boldsymbol{\theta}\right)\right)}{\partial\theta_{up}\partial\theta_{vq}}\right]$$

Note that according to Schwarz's theorem:

$$\frac{\partial^2 \log\left(\mathrm{p}\left(\boldsymbol{r} \mid \boldsymbol{\theta}\right)\right)}{\partial\theta_{up}\partial\theta_{vq}} = \frac{\partial^2 \log\left(\mathrm{p}\left(\boldsymbol{r} \mid \boldsymbol{\theta}\right)\right)}{\partial\theta_{vq}\partial\theta_{up}}$$

Consequently the Fisher Matrix is symmetric. Then the join probability to receive the signal $\boldsymbol{r}$ given the set of parameters $\boldsymbol{\theta}$:

$$\begin{aligned}\mathrm{p}\left(\boldsymbol{r} \mid \boldsymbol{\theta}\right) &= \prod_{i=0}^{N-1} \mathrm{p}\left(r_i \mid \boldsymbol{\theta}\right) \\ &= \prod_{i=0}^{N-1} \frac{1}{\sigma\sqrt{2\pi}} \cdot \exp\left(-\frac{1}{2\sigma^2} \cdot \left(r_i - \sum_{k=0}^{K-1} \sqrt{\mathcal{P}^k} \cdot c^k(i\Delta - \tau^k)\right)^2\right)\end{aligned}$$

The log-likelihood function is:

$$\log\left(\mathrm{p}\left(\boldsymbol{r} \mid \boldsymbol{\theta}\right)\right) = -N \cdot \log\left(\sigma\sqrt{2\pi}\right) - \frac{1}{2\sigma^2} \cdot \sum_{i=0}^{N-1} \left(r_i - \sum_{k=0}^{K-1} \sqrt{\mathcal{P}^k} \cdot c^k(i\Delta - \tau^k)\right)^2$$

By taking the derivative:

$$\begin{aligned}\frac{\partial^2 \log\left(\mathrm{p}\left(\boldsymbol{r} \mid \boldsymbol{\theta}\right)\right)}{\partial\theta_{up}\partial\theta_{vq}} &= \frac{1}{\sigma^2}\sum_{i=0}^{N-1}\left(\left(r_i - \sum_{k=0}^{K-1}\sqrt{\mathcal{P}^k}c^k(i\Delta-\tau^k)\right)\cdot\frac{\partial^2\sqrt{\mathcal{P}^p}c^p(i\Delta-\tau^p)}{\partial\theta_{up}\partial\theta_{vq}}\right.\\ &\qquad\left.-\frac{\partial\sqrt{\mathcal{P}^p}c^p(i\Delta-\tau^p)}{\partial\theta_{up}}\cdot\frac{\partial\sqrt{\mathcal{P}^q}c^q(i\Delta-\tau^q)}{\partial\theta_{vq}}\right)\\ &= \frac{1}{\sigma^2}\sum_{i=0}^{N-1}\left(\eta_i\frac{\partial^2\sqrt{\mathcal{P}^p}c^p(i\Delta-\tau^p)}{\partial\theta_{up}\partial\theta_{vp}}\right.\\ &\qquad\left.-\frac{\partial\sqrt{\mathcal{P}^p}c^p(i\Delta-\tau^p)}{\partial\theta_{up}}\cdot\frac{\partial\sqrt{\mathcal{P}^q}c^q(i\Delta-\tau^q)}{\partial\theta_{vp}}\right)\end{aligned}$$

Since $\mathcal{E}\left[\eta_i\right] = 0$ it follows that the term (up, vq) of the Fisher information matrix can be expressed as:

$$\begin{aligned}\mathcal{I}(\theta_{up},\theta_{vq}) &= -\mathcal{E}\left[\frac{\partial^2\log\left(\mathrm{p}\left(\boldsymbol{r}\mid\boldsymbol{\theta}\right)\right)}{\partial\theta_{up}\partial\theta_{vp}}\right]\\ &= \frac{1}{\sigma^2}\cdot\sum_{i=0}^{N-1}\frac{\partial\sqrt{\mathcal{P}^p}c^p(i\Delta-\tau^p)}{\partial\theta_{up}}\cdot\frac{\partial\sqrt{\mathcal{P}^p}c^q(i\Delta-\tau^q)}{\partial\theta_{vq}}\end{aligned}\tag{3.1}$$

Because the sampling frequency is equal to the Nyquist frequency, the sum can be equally expressed as an integral:

$$\mathcal{I}(\theta_{up},\theta_{vq}) = \frac{1}{\Delta\cdot\sigma^2}\cdot\int_0^{d\cdot T_i}\frac{\partial\sqrt{\mathcal{P}^p}c^p(t-\tau^p)}{\partial\theta_{up}}\cdot\frac{\partial\sqrt{\mathcal{P}^p}c^q(t-\tau^q)}{\partial\theta_{vq}}\,\mathrm{d}t$$

Then by separating the four cases:

- If $\theta_{up} = \sqrt{\mathcal{P}^p}$ and $\theta_{vq} = \sqrt{\mathcal{P}^q}$, then:

  $$\mathcal{I}(\sqrt{\mathcal{P}^p},\sqrt{\mathcal{P}^q}) = \frac{1}{\Delta\cdot\sigma^2}\cdot\int_0^{d\cdot T_i}c^p(t-\tau^p)\cdot c^q(t-\tau^q)\,\mathrm{d}t$$

  Then using equation A.1, it follows:

  $$\begin{aligned}\mathcal{I}(\sqrt{\mathcal{P}^p},\sqrt{\mathcal{P}^q}) &= \frac{1}{\Delta\cdot\sigma^2}\cdot\mathcal{X}_{d\cdot T_i}^{p,q}\\ &= \frac{1}{\Delta\cdot\sigma^2}\sum_{n=0}^{Ld-1}\sum_{m=-\infty}^{\infty}c_n^p\cdot c_m^q\\ &\qquad\cdot\int_{-B}^{B}\left|P(f)\right|^2\cdot\cos\left(2\pi f((n-m)T_c+\tau^q-\tau^p)\right)\mathrm{d}f\end{aligned}$$

  Because of filtering, $f\notin[-B\,;B] \implies P(f) = 0$. Consequently integrating on $]-\infty\,;\infty[$ is the same than integrating on $[-B\,;B]$.

- If $\theta_{up} = \tau^p$ and $\theta_{vq} = \sqrt{\mathcal{P}^q}$, then:

  $$\mathcal{I}(\tau^p,\sqrt{\mathcal{P}^q}) = \frac{\sqrt{\mathcal{P}^p}}{\Delta\cdot\sigma^2}\cdot\int_0^{d\cdot T_i}\frac{\partial c^p(t-\tau^p)}{\partial\tau^p}\cdot c^q(t-\tau^q)\,\mathrm{d}t$$

Then using equation A.4, it follows:

$$\begin{aligned}\mathcal{I}(\tau^p, \sqrt{\mathcal{P}^q}) &= \frac{\sqrt{\mathcal{P}^p}}{\Delta \cdot \sigma^2} \cdot \mathcal{Y}^{q,p}_{d \cdot T_i} \\ &= \frac{\sqrt{\mathcal{P}^p}}{\Delta \cdot \sigma^2} \cdot \sum_{n=0}^{Ld-1} \sum_{m=-\infty}^{\infty} c_n^p \cdot c_m^q \cdot \\ &\qquad \int_{-B}^{B} (2\pi f) \cdot |P(f)|^2 \cdot \sin\left(2\pi f((n-m)T_c + \tau^q - \tau^p)\right) \mathrm{d}f\end{aligned}$$

- If $\theta_{up} = \sqrt{\mathcal{P}^p}$ and $\theta_{vq} = \tau^q$, then:

$$\begin{aligned}\mathcal{I}(\sqrt{\mathcal{P}^q}, \tau^p) &= \frac{\sqrt{\mathcal{P}^q}}{\Delta \cdot \sigma^2} \cdot \int_0^{d \cdot T_i} \frac{\partial c^p(t-\tau^p)}{\partial \tau^p} \cdot c^q(t-\tau^q)\, \mathrm{d}t \\ &= \mathcal{I}(\tau^p, \sqrt{\mathcal{P}^q})\end{aligned}$$

- If $\theta_{up} = \tau^p$ and $\theta_{vq} = \tau^q$, then:

$$\mathcal{I}(\tau^p, \tau^q) = \frac{\sqrt{\mathcal{P}^p \mathcal{P}^q}}{\Delta \cdot \sigma^2} \cdot \int_0^{d \cdot T_i} \frac{\partial c^p(t-\tau^p)}{\partial \tau^p} \cdot \frac{\partial c^q(t-\tau^q)}{\partial \tau^q}\, \mathrm{d}t$$

Then using equation A.7, it follows:

$$\begin{aligned}\mathcal{I}(\tau^p, \tau^q) &= \frac{\sqrt{\mathcal{P}^p \mathcal{P}^q}}{\Delta \cdot \sigma^2} \cdot \mathcal{Z}^{p,q}_{d \cdot T_i} \\ &= \frac{\sqrt{\mathcal{P}^p \mathcal{P}^q}}{\Delta \cdot \sigma^2} \cdot \sum_{n=0}^{Ld-1} \sum_{m=-\infty}^{\infty} c_n^p \cdot c_m^q \cdot \\ &\qquad \int_{-B}^{B} (2\pi f)^2 \cdot |P(f)|^2 \cdot \cos\left(2\pi f((n-m)T_c + \tau^q - \tau^p)\right) \mathrm{d}f\end{aligned}$$

Finally, the Fisher information matrix is:

$$\mathcal{I}(\boldsymbol{\theta}) = \begin{pmatrix} \mathcal{I}_\tau & \mathcal{I}_{\tau,\sqrt{\mathcal{P}}} \\ \mathcal{I}^T_{\tau,\sqrt{\mathcal{P}}} & \mathcal{I}_{\sqrt{\mathcal{P}}} \end{pmatrix}$$

And the CRLB matrix is:

$$\mathrm{cov}\left[\hat{\boldsymbol{\theta}}\right] \geq \mathcal{I}(\boldsymbol{\theta})^{-1}$$

With:

$$\mathcal{I}_\tau = \begin{pmatrix} \mathcal{I}(\tau^1,\tau^1) & \mathcal{I}(\tau^1,\tau^2) & \dots & \mathcal{I}(\tau^1,\tau^K) \\ \mathcal{I}(\tau^2,\tau^1) & \mathcal{I}(\tau^2,\tau^2) & \dots & \mathcal{I}(\tau^2,\tau^K) \\ \dots & \dots & \dots & \dots \\ \mathcal{I}(\tau^K,\tau^1) & \mathcal{I}(\tau^K,\tau^2) & \dots & \mathcal{I}(\tau^K,\tau^K) \end{pmatrix}$$

$$\mathcal{I}_{\sqrt{\mathcal{P}}} = \begin{pmatrix} \mathcal{I}(\sqrt{\mathcal{P}^1},\sqrt{\mathcal{P}^1}) & \mathcal{I}(\sqrt{\mathcal{P}^1},\sqrt{\mathcal{P}^2}) & \dots & \mathcal{I}(\sqrt{\mathcal{P}^1},\sqrt{\mathcal{P}^K}) \\ \mathcal{I}(\sqrt{\mathcal{P}^2},\sqrt{\mathcal{P}^1}) & \mathcal{I}(\sqrt{\mathcal{P}^2},\sqrt{\mathcal{P}^2}) & \dots & \mathcal{I}(\sqrt{\mathcal{P}^2},\sqrt{\mathcal{P}^K}) \\ \dots & \dots & \dots & \dots \\ \mathcal{I}(\sqrt{\mathcal{P}^K},\sqrt{\mathcal{P}^1}) & \mathcal{I}(\sqrt{\mathcal{P}^K},\sqrt{\mathcal{P}^2}) & \dots & \mathcal{I}(\sqrt{\mathcal{P}^K},\sqrt{\mathcal{P}^K}) \end{pmatrix}$$

$$\mathcal{I}_{\tau,\sqrt{\mathcal{P}}} = \begin{pmatrix} \mathcal{I}(\tau^1,\sqrt{\mathcal{P}^1}) & \mathcal{I}(\tau^1,\sqrt{\mathcal{P}^2}) & \dots & \mathcal{I}(\tau^1,\sqrt{\mathcal{P}^K}) \\ \mathcal{I}(\tau^2,\sqrt{\mathcal{P}^1}) & \mathcal{I}(\tau^2,\sqrt{\mathcal{P}^2}) & \dots & \mathcal{I}(\tau^2,\sqrt{\mathcal{P}^K}) \\ \dots & \dots & \dots & \dots \\ \mathcal{I}(\tau^K,\sqrt{\mathcal{P}^1}) & \mathcal{I}(\tau^K,\sqrt{\mathcal{P}^2}) & \dots & \mathcal{I}(\tau^K,\sqrt{\mathcal{P}^K}) \end{pmatrix}$$

3.3.2 One Pseudolite Signal

In order to make the computations easier, it will be assumed for the both cases "One pseudolite signal" and "Two pseudolite signals" that received power of the navigation signals can be estimated with a much better accuracy than the delays. Consequently the reduced set of parameters $\boldsymbol{\theta} = \left[\tau^1, \tau^2, \cdots, \tau^k\right]$ will be considered and therefore cov $\left[\hat{\boldsymbol{\theta}}\right] \geq {\mathcal{I}_\tau}^{-1}$.

General Chip Modulation Waveform

First, only one pseudolite signal is considered:

$$r(t) = \sqrt{\mathcal{P}^1} \cdot c^1(t - \tau^1) + \eta(t)$$

Since the received signal power is supposed to be known, only the parameter $\theta = \tau^1$ has to be estimated. Then the CRLB for the estimator $\hat{\tau}^1$ is var $\left[\hat{\tau}^1\right] \geq \mathcal{I}(\tau^1)^{-1}$, with:

$$\begin{aligned} \mathcal{I}(\tau^1) = \frac{\mathcal{P}^1}{\Delta \cdot \sigma^2} \cdot \sum_{n=0}^{Ld-1} \sum_{m=-\infty}^{\infty} c_n^1 \cdot c_m^1 \cdot \\ \cdot \int_{-B}^{B} (2\pi f)^2 \cdot |P(f)|^2 \cdot \cos\left(2\pi f T_c (m-n)\right) \mathrm{d}f \end{aligned} \tag{3.2}$$

If c^1 is considered balanced, then:

$$\begin{aligned} \mathcal{I}(\tau^1) &= \frac{\mathcal{P}^1}{\Delta \cdot \sigma^2} \cdot \sum_{n=0}^{Ld-1} \int_{-B}^{B} (2\pi f)^2 \cdot |P(f)|^2 \, \mathrm{d}f \\ &= \frac{L \cdot d \cdot \mathcal{P}^1}{\Delta \cdot \sigma^2} \cdot \int_{-B}^{B} (2\pi f)^2 \cdot |P(f)|^2 \, \mathrm{d}f \end{aligned}$$

The energy of the received signal during one code period is:

$$E_1 = L \cdot d \cdot \mathcal{P}^1 \cdot \int_{-B}^{B} |P(f)|^2 \, \mathrm{d}f$$

It follows:

$$\mathcal{I}(\tau^1) = \frac{E_1}{\Delta \cdot \sigma^2} \cdot \frac{\int_{-B}^{B} (2\pi f)^2 \cdot |P(f)|^2 \, \mathrm{d}f}{\int_{-B}^{B} |P(f)|^2 \, \mathrm{d}f}$$

The mean square bandwidth (or Gabor bandwidth) is defined as:

$$\overline{\Delta\omega^2} = \frac{\int_{-B}^{B} (2\pi f)^2 \cdot |P(f)|^2 \, \mathrm{d}f}{\int_{-B}^{B} |P(f)|^2 \, \mathrm{d}f}$$

Consequently, with $\sigma^2 = B\mathcal{N}_0$, it follows:

$$\mathcal{I}(\tau^1) = \frac{E_1}{\mathcal{N}_0/2} \cdot \overline{\Delta\omega^2}$$

And finally, the CRLB is:

$$\boxed{\text{var}\left[\hat{\tau}^1\right] \geq \frac{1}{\frac{E_1}{\mathcal{N}_0/2} \cdot \overline{\Delta\omega^2}}}$$

BPSK Modulation

The case of a BPSK modulation will now be analyzed: the waveform is a low-pass filtered rectangular window. Using equation (A.8), with $L = {}^{T_i}/_{T_c}$ the code length, it leads to:

$$\begin{aligned}
\mathcal{I}(\tau^1) &= \frac{\mathcal{P}^1}{\Delta \cdot \sigma^2} \cdot \mathcal{Z}^{1,1}_{d \cdot T_i} \\
&= \frac{\mathcal{P}^1}{\Delta \cdot \sigma^2} \cdot \sum_{n=0}^{Ld-1} \sum_{m=-\infty}^{+\infty} c^1_n \cdot c^1_m \cdot \\
&\quad (4B \cdot \operatorname{sinc}(2\pi BT_c(m-n)) - 2B \cdot \operatorname{sinc}(2\pi BT_c(n-m-1)) \\
&\quad -2B \cdot \operatorname{sinc}(2\pi BT_c(n-m+1))) \\
&= \frac{4 \cdot \mathcal{P}^1}{\Delta \cdot \mathcal{N}_0} \cdot \sum_{n=0}^{Ld-1} \sum_{m=-\infty}^{+\infty} c^1_n \cdot c^1_m \cdot \\
&\quad \left(\operatorname{sinc}(2\pi BT_c(m-n)) - \frac{1}{2} \cdot \operatorname{sinc}(2\pi BT_c(n-m-1)) \right. \\
&\quad \left. -\frac{1}{2} \cdot \operatorname{sinc}(2\pi BT_c(n-m+1)) \right)
\end{aligned}$$

The function $I(.)$ is defined as:

$$\begin{aligned}
I(m-n) = \operatorname{sinc}(2\pi BT_c(m-n)) &- \frac{1}{2} \cdot \operatorname{sinc}(2\pi BT_c(m-n+1)) \\
&- \frac{1}{2} \cdot \operatorname{sinc}(2\pi BT_c(m-n-1))
\end{aligned}$$

If the lobes of power spectral density are not partially cut (which is the case for usual receivers), then $BT_c(m-n)$ is an integer, and consequently the $\operatorname{sinc}(.)$ functions take a non-null value only in zero, and so can be replaced by Dirac functions (cf. figure 3.1):

$$I(m-n) = \delta(m-n) - \frac{1}{2} \cdot \delta(m-n+1) - \frac{1}{2} \cdot \delta(m-n+1)$$

Then it follows:

$$\begin{aligned}
\mathcal{I}(\tau^1) &= \frac{4 \cdot \mathcal{P}^1}{\Delta \cdot \mathcal{N}_0} \cdot \sum_{n=0}^{Ld-1} \sum_{m=-\infty}^{+\infty} c^1_n \cdot c^1_m \\
&\quad \cdot \left(\delta(m-n) - \frac{1}{2} \cdot \delta(m-n+1) - \frac{1}{2} \cdot \delta(m-n+1) \right) \\
&= \frac{4 \cdot \mathcal{P}^1}{\Delta \cdot \mathcal{N}_0} \cdot \sum_{n=0}^{Ld-1} \left(1 - \frac{1}{2} \cdot c^1_n \cdot (c^1_{n+1} + c^1_{n-1}) \right)
\end{aligned} \tag{3.3}$$

Figure 3.2 represents the CRLB for randomly chosen and randomly shifted GPS C/A codes, with 1023 code length. This figure justifies that:

$$\sum_{n=0}^{Ld-1} \left(1 - \frac{1}{2} \cdot c^1_n \cdot (c^1_{n+1} + c^1_{n-1}) \right) \approx L \cdot d$$

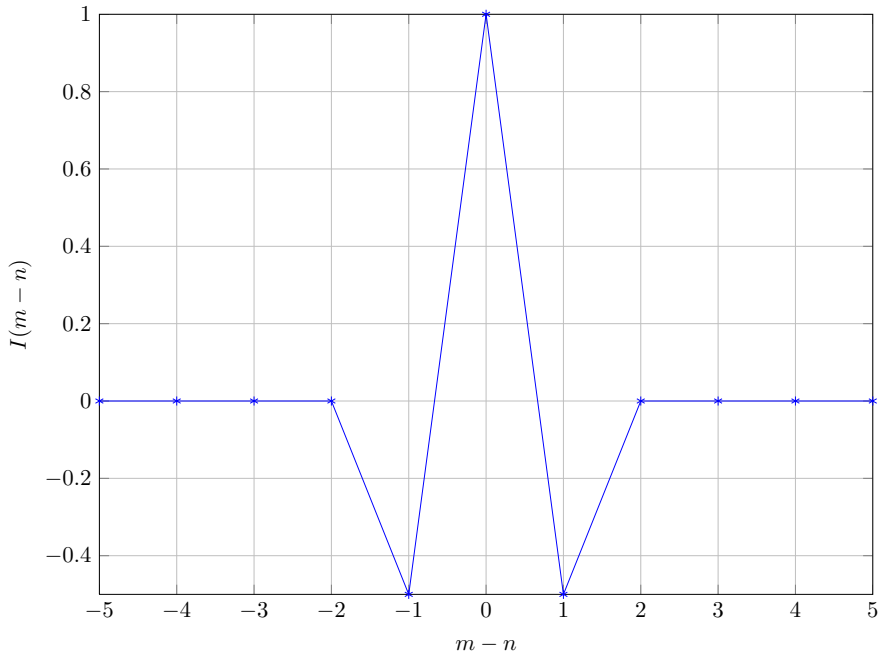

Figure 3.1: $I(m-n)$ with $B = {}^{4}/_{T_c}$

Then the Fisher information can be approximated by its mean value over the chips:

$$\mathcal{I}(\tau^1) \approx \frac{4 \cdot \mathcal{P}^1 \cdot L \cdot d}{\Delta \cdot \mathcal{N}_0} \tag{3.4}$$

Consequently the CRLB for the estimator of τ^1 is can be approximate by its average over all codes:

$$\boxed{\text{var}\left[\hat{\tau}^1\right] \geq \frac{\Delta \cdot \mathcal{N}_0}{4 \cdot \mathcal{P}^1 \cdot L \cdot d}} \tag{3.5}$$

However, in order to dimension the system, the mean value of the CRLB is not adapted. Instead, a work rate can be set to size the system. If x is the work rate, then in x percent of the cases, the real CRLB will be better (lower) and in $100 - x$ percent of cases, the real CRLB will be worse (higher).

For instance the work rate can be set to 90%. Since the CRLB is inversely proportional to the Fisher information, it corresponds to the 10^{th} percentile of the Fisher information. Then, using figure 3.2, in 90% of the cases, the variance of the propagation delay error can be bounded by:

$$\text{var}\left[\hat{\tau}^1\right] \geq \frac{\Delta \cdot \mathcal{N}_0}{4 \cdot 0.9 \cdot \mathcal{P}^1 \cdot L \cdot d}$$

It can be noticed that the CRLB grows with the sampling time and the noise power density, and decreases with the power of the signal, the code length and the duty cycle.

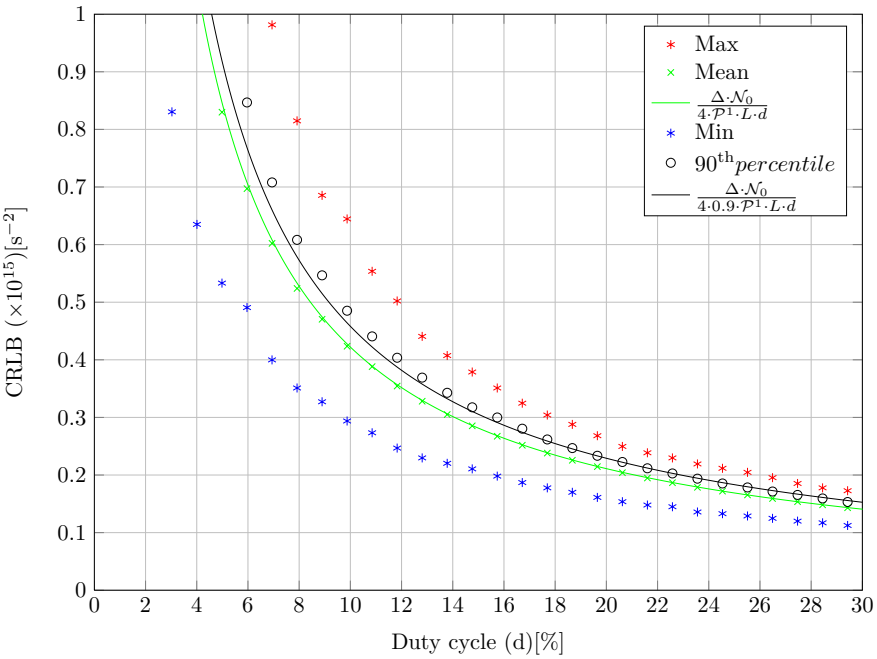

Figure 3.2: CRLB, ∞-bit quantizer, $\mathcal{P}^1 = -120$ dBW

3.3.3 Two Pseudolite Signals

General Chip Modulation Waveform

Two pseudolite signals are considered. The received signal is:

$$r_i = \sqrt{\mathcal{P}^p} \cdot c^p(i\Delta - \tau^p) + \sqrt{\mathcal{P}^q} \cdot c^q(i\Delta - \tau^q) + \eta(i\Delta)$$

Again it is considered that the received power of the navigation signals is already known. Consequently the vector of unknown parameters become $\boldsymbol{\theta} = [\tau^p, \tau^q]$. The CRLB for the estimators $\hat{\boldsymbol{\theta}}$ of $\boldsymbol{\theta}$ is $\text{cov}\left[\hat{\boldsymbol{\theta}}\right] \geq \mathcal{I}(\boldsymbol{\theta})^{-1}$, with $\mathcal{I}(\boldsymbol{\theta})$ the Fisher information Matrix defined as:

$$\mathcal{I}(\boldsymbol{\tau}^p) = \begin{pmatrix} \mathcal{I}(\tau^p, \tau^p) & \mathcal{I}(\tau^p, \tau^q) \\ \mathcal{I}(\tau^q, \tau^p) & \mathcal{I}(\tau^q, \tau^q) \end{pmatrix}$$

Then by inverting the Fisher Matrix, and since $\mathcal{I}(\tau^q, \tau^p) = \mathcal{I}(\tau^p, \tau^q)$:

$$\text{cov}\left[\boldsymbol{\theta}\right] \geq \frac{1}{\mathcal{I}(\tau^p, \tau^p) \cdot \mathcal{I}(\tau^q, \tau^q) - \mathcal{I}(\tau^p, \tau^q)^2} \cdot \begin{pmatrix} \mathcal{I}(\tau^q, \tau^q) & -\mathcal{I}(\tau^p, \tau^q) \\ -\mathcal{I}(\tau^q, \tau^p) & \mathcal{I}(\tau^p, \tau^p) \end{pmatrix}$$

Then CRLB for the estimator of the delay τ^p is:

$$\text{var}\left[\hat{\tau}^p\right] \geq \frac{1}{\mathcal{I}(\tau^p, \tau^p)} \cdot \frac{1}{1 - \frac{\mathcal{I}(\tau^p, \tau^q)^2}{\mathcal{I}(\tau^p, \tau^p) \cdot \mathcal{I}(\tau^q, \tau^q)}}$$

Without consideration of exact shape of the chip waveform:

$$\begin{aligned}
\mathcal{I}(\tau^p, \tau^p) &= \frac{L \cdot d \cdot \mathcal{P}^p}{\Delta \cdot \sigma^2} \cdot \int_{-B}^{B} (2\pi f)^2 \cdot |P(f)|^2 \, \mathrm{d}f \\
&= \frac{E_p}{\mathcal{N}_0/2} \cdot \overline{\Delta\omega^2} \\
\mathcal{I}(\tau^q, \tau^q) &= \frac{E_q}{\mathcal{N}_0/2} \cdot \overline{\Delta\omega^2} \\
\mathcal{I}(\tau^p, \tau^q) &= \frac{\sqrt{\mathcal{P}^p \cdot \mathcal{P}^q}}{\Delta \cdot \sigma^2} \cdot \sum_{n=0}^{Ld-1} \sum_{m=-\infty}^{+\infty} c_n^p \cdot c_m^q \\
&\quad \cdot \int_{-B}^{B} (2\pi f)^2 \cdot |P(f)|^2 \cdot \cos\left(2\pi f((m-n)T_c + \tau^p - \tau^q)\right) \mathrm{d}f
\end{aligned}$$

And consequently the CRLB is:

$$\begin{aligned}
&\mathrm{var}\left[\hat{\tau}^p\right] \geq \frac{1}{\frac{E_p}{\mathcal{N}_0/2} \cdot \overline{\Delta\omega^2}} \\
&\cdot \frac{1}{1 - \left(\frac{\sum_{n=0}^{Ld-1} \sum_{m=-\infty}^{+\infty} c_n^p c_m^q \int_{-B}^{B} (2\pi f)^2 |P(f)|^2 \cos(2\pi f((m-m)T_c + \tau^p - \tau^q)) \, \mathrm{d}f}{L \cdot d \cdot \int_{-B}^{B} (2\pi f)^2 |P(f)|^2 \, \mathrm{d}f} \right)^2}
\end{aligned} \tag{3.6}$$

It can be noticed that the CRLB does not depend on the power of the interfering navigation signal, but only on the correlation between the spreading code of the useful navigation signal and the one of the interfering signal. It shows that, without quantization, an unbiased estimator of the propagation delay error exists, such that the power of the interfering signal has no effect. Therefore if the spreading codes are perfectly orthogonal and in the case of a perfect estimator, then the interfering pseudolites have no effect on the delay error of the tracked signal.

BPSK Modulation

In the case of a BPSK modulation, using equations (3.4) and (3.3), it follows:

$$\begin{aligned}
\mathcal{I}(\tau^p, \tau^p) &\approx \frac{4 \cdot \mathcal{P}^p \cdot L \cdot d}{\Delta \cdot \mathcal{N}_0} \\
\mathcal{I}(\tau^q, \tau^q) &\approx \frac{4 \cdot \mathcal{P}^q \cdot L \cdot d}{\Delta \cdot \mathcal{N}_0}
\end{aligned}$$

Using the knowledge of $P(f)$, the terms $\mathcal{I}(\tau^p, \tau^q) = \mathcal{I}(\tau^q, \tau^p)$ have been further evaluated in annexe A. Using equation (A.8):

$$\begin{aligned}\mathcal{I}(\tau^p, \tau^q) &= \frac{\sqrt{\mathcal{P}^p \cdot \mathcal{P}^q}}{\Delta \cdot \sigma^2} \cdot \mathcal{Z}^{p,q}_{d \cdot T_i} \\ &= \frac{4 \cdot \sqrt{\mathcal{P}^p \cdot \mathcal{P}^q}}{\Delta \cdot \mathcal{N}_0} \cdot \sum_{n=0}^{Ld-1} \sum_{m=-\infty}^{+\infty} c_n^p \cdot c_m^q \\ &\quad \cdot \Big(\operatorname{sinc}\left(2\pi B(\tau^p - \tau^q + T_c(n-m)\right) \\ &\quad - \frac{1}{2} \cdot \operatorname{sinc}\left(2\pi B(\tau^p - \tau^q + T_c(n-m-1)\right)) \\ &\quad - \frac{1}{2} \cdot \operatorname{sinc}\left(2\pi B(\tau^p - \tau^q + T_c(n-m+1)\right)) \Big)\end{aligned}$$

Note that the Fisher information is proportional to $(4 \cdot \sqrt{\mathcal{P}^p \cdot \mathcal{P}^q}) / (\Delta \cdot \mathcal{N}_0)$. Figure 3.3 represents the Fisher information $\mathcal{I}(\tau^p, \tau^q)$ as function of $(\tau^q - \tau^p)/T_c$, the delay in chips between the two signals. It can be noticed that the Fisher information is maximal when $\tau^q - \tau^p = 0 \mod T_c$. When $\mathcal{I}(\tau^p, \tau^q)$ is maximal,

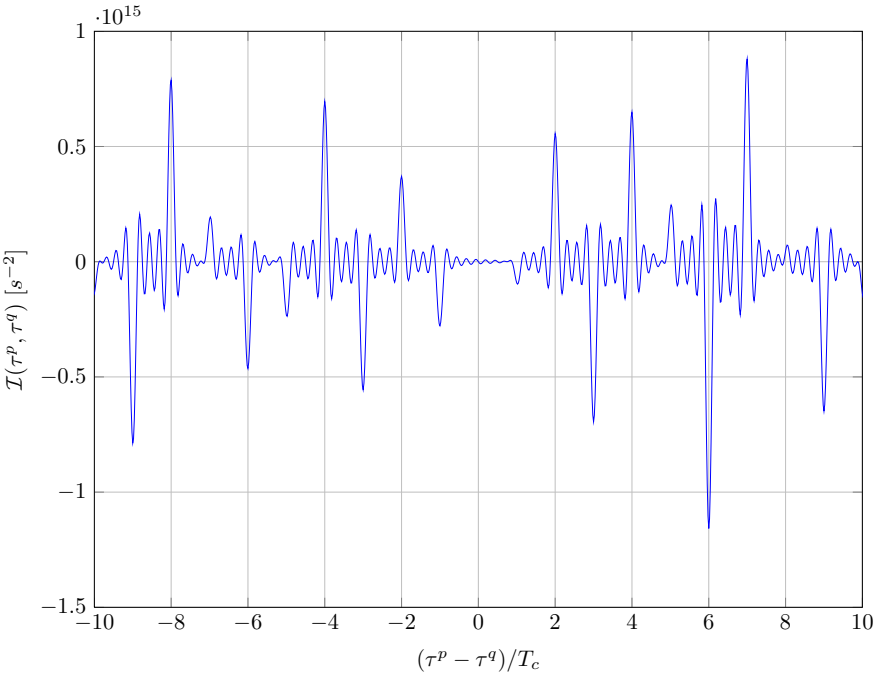

Figure 3.3: Fisher information $\mathcal{I}(\tau^p, \tau^q)$ with $\mathcal{P}^p = \mathcal{P}^q = -120$ dBW and two real GPS codes (PRN 1 and PRN 2)

$1 - \frac{\mathcal{I}(\tau^p, \tau^q)^2}{\mathcal{I}(\tau^q, \tau^q) \cdot \mathcal{I}(\tau^p, \tau^p)}$ is minimal and finally CRLB is maximal. Consequently it corresponds to the worst case situation. Since the aim is to find a lower bound, the worst case situation has to be considered. Consequently it will be considered that $\tau^p - \tau^q$ is a multiple of T_c. Then the $\operatorname{sinc}(.)$ functions are null except in

zero, and so can be replaced by Kronecker delta functions. It follows:

$$\mathcal{I}(\tau^p,\tau^q) = \frac{4\cdot\sqrt{\mathcal{P}^p\cdot\mathcal{P}^q}}{\Delta\cdot\mathcal{N}_0}\cdot\sum_{n=0}^{Ld-1}\sum_{m=-\infty}^{+\infty} c_n^p\cdot c_m^q\cdot\Big(\delta(\tau^p-\tau^q+T_c(n-m)) - \frac{1}{2}\cdot\delta(\tau^p-\tau^q+T_c(n-m-1)) - \frac{1}{2}\cdot\delta(\tau^p-\tau^q+T_c(n-m+1))\Big)$$

Let $a = {}^{(\tau^p-\tau^q)}/_{T_c}$ represents the delay, expressed in chip between the two signals. Then it follows:

$$\begin{aligned}\mathcal{I}(\tau^p,\tau^q) &= \frac{4\cdot\sqrt{\mathcal{P}^p\cdot\mathcal{P}^q}}{\Delta\cdot\mathcal{N}_0}\cdot\sum_{n=0}^{Ld-1}\sum_{m=-\infty}^{+\infty} c_n^p\cdot c_m^q\cdot\Big(\delta(m-n-a) - \frac{1}{2}\cdot\delta(m-n-1-a) - \frac{1}{2}\cdot\delta(m-n+1-a)\Big)\\ &= \frac{4\cdot\sqrt{\mathcal{P}^p\cdot\mathcal{P}^q}}{\Delta\cdot\mathcal{N}_0}\cdot\sum_{n=0}^{Ld-1} c_n^p\left(c_{a+n}^q - \frac{1}{2}\cdot c_{a+n-1}^q - \frac{1}{2}\cdot c_{a+n+1}^q\right)\end{aligned}$$

Figure 3.4 shows the cumulative distribution function of the squared Fisher information between the codes from pseudolite p and pseudolite q. The Fisher information, and consequently the CRLB, depends on the codes and their relative delay a. A work rate can be used to size the system, corresponding to an interference term $\mathcal{I}(\tau^p,\tau^q)$, and consequently to a CRLB. If x is the work rate, then in x percent of cases, the real CRLB will be better and in $100-x$ percent of cases, the real CRLB will be worse. Figure 3.5 shows that the interference term $\frac{\mathcal{I}(\tau^p,\tau^q)^2}{\mathcal{I}(\tau^p,\tau^p)\cdot\mathcal{I}(\tau^q,\tau^q)}$ can be approximated by $k\cdot L\cdot d$, where k is almost constant depending on the tolerance x. The CRLB of the propagation delay estimator, for a specified percent of the cases (depending on the code and the position of the receiver) will be lower than:

$$\boxed{\mathrm{var}\,[\hat{\tau}^p] \geq \frac{\Delta\cdot\mathcal{N}_0}{4\cdot\mathcal{P}^p\cdot L\cdot d}\cdot\frac{1}{1-{}^{k}/_{L\cdot d}}} \tag{3.7}$$

Where k depends on the considered percentile, or the error margin. For instance if the tolerance is set to 1% (cf. 99^{th} percentile on figure 3.5), $\frac{\mathcal{I}(\tau^p,\tau^q)^2}{\mathcal{I}(\tau^p,\tau^p)\cdot\mathcal{I}(\tau^q,\tau^q)}$ can be approximated by ${}^{10}/_{L\cdot d}$, then the CRLB becomes:

$$\boxed{\mathrm{var}\,[\hat{\tau}^p] \geq \frac{\Delta\cdot\mathcal{N}_0}{4\cdot\mathcal{P}^p\cdot L\cdot d}\cdot\frac{1}{1-{}^{10}/_{L\cdot d}}} \tag{3.8}$$

3.3.4 Comparisons Between the Two Pulse Schemes

As reminder, in case of non-overlapping pulses, when the duty cycle is shared between the pseudolites, the transmitted Pulse Peak Power (PPP) power stays the same, and consequently the receiver energy is lower. d represents the aggregated duty cycle, and d_{PL} represents the duty cycle for each pseudolite. In the case of overlapping pulses, $d = d_{\mathrm{PL}}$. In the case of non-overlapping pulses, $d = K\cdot d_{\mathrm{PL}}$.

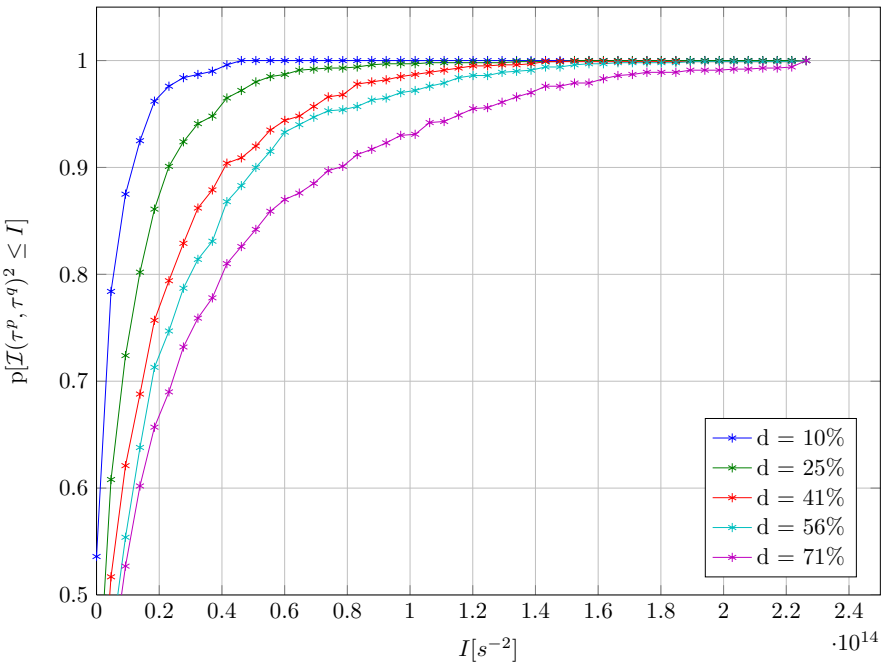

Figure 3.4: Cumulative distribution function of $\mathcal{I}(\tau^p, \tau^q)^2$ for randomly chosen and randomly shifted GPS codes with 1023 chip length, $\mathcal{P}^p = \mathcal{P}^q = -120$ dBW

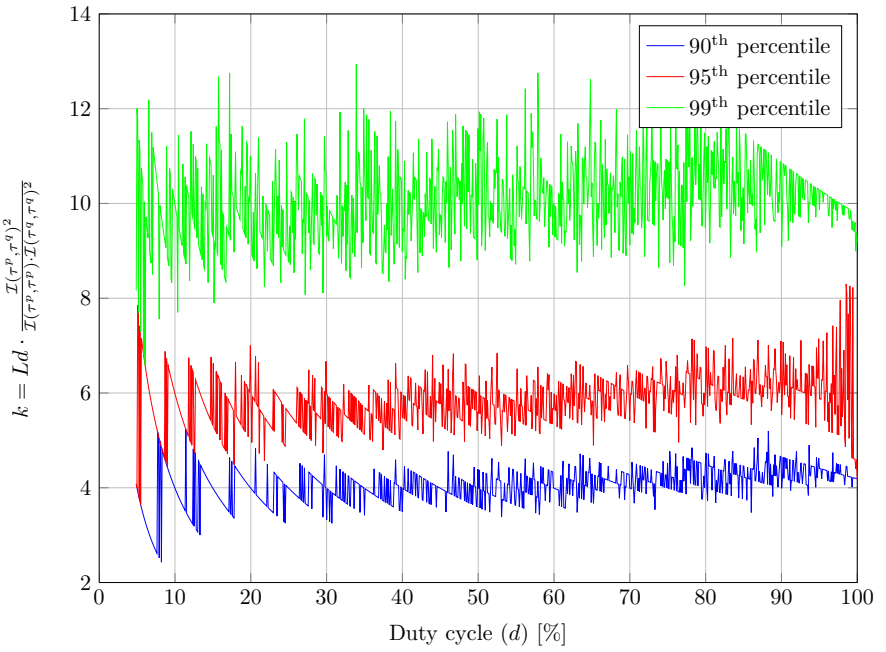

Figure 3.5: Coefficient k that corresponds to a specified percentile

Two pseudolites are Transmitting

The purpose of this section is to compare the two different pulsing schemes. For reasons of simplicity only two pseudolites will be considered firstly. The overall duty cycle d is reserved for pseudolite pulses. Pseudolites transmit successively (non-overlapping pulses) or all at the same time (overlapping pulses). The duty cycle $1 - d$ is reserved for tracking the satellite signals.

- In case of non-overlapping pulses, each of the two pseudolites transmits half of the duty cycle d. The pseudolite l, that transmits with an instantaneous power $\mathcal{P}^l$ at the duty cycle $d_{\mathrm{PL}} = {}^{d}/_{2}$ is tracked. Let $\hat{\tau}^l_{d/2}$ be the estimator of the propagation delay of pseudolite one, measured during ${}^{d \cdot T_i}/_{2}$ of each coherent integration interval, and without interfering pseudolites. Consequently using equation (3.5):

$$\mathrm{var}\left[\hat{\tau}^l_{d/2}\right] \geq \frac{\Delta \cdot \mathcal{N}_0}{2 \cdot \mathcal{P}^l \cdot L \cdot d}$$

- In the case of overlapping pulses, the both pseudolites transmit at the same duty cycle $d = d_{\mathrm{PL}}$. Pseudolite l transmits with the same instantaneous power $\mathcal{P}^l$ as before. Using equation (3.7), the CRLB for the propagation delay of pseudolite l is:

$$\mathrm{var}\left[\hat{\tau}^l\right] \geq \frac{\Delta \cdot \mathcal{N}_0}{4 \cdot \mathcal{P}^l \cdot L \cdot d} \cdot \frac{1}{1 - {}^{k}/_{L \cdot d}}$$

Figure 3.6 shows the evolution of the CRLB for overlapping and non-overlapping pulses, when two pseudolites transmit and when only one pseudolite transmits. It can be noticed that the best CRLB is achieved when only one pseudolite transmits, which is not surprising. However the losses due to the second pseudolite are very low in the case of overlapping pulses.

K Pseudolites are Transmitting

The vector of parameters $\boldsymbol{\theta} = \left[\tau^1, \tau^2, \cdots, \tau^K, \sqrt{\mathcal{P}^1}, \sqrt{\mathcal{P}^2}, \ldots, \sqrt{\mathcal{P}^K}\right]$ is considered, with K the number of pseudolites. Note that now the received powers are also considered as unknown parameters.

- In the case of non-overlapping pulses, the K pseudolites share the duty cycle d. Each pseudolite transmits at the duty cycle $d_{\mathrm{PL}} = {}^{d}/_{K}$ and the duty cycle d is occupied by the different pseudolite pulses. $\hat{\tau}^l_{d/K}$ is the estimator of the propagation delay of pseudolite l, measured during ${}^{d \cdot T_i}/_{K}$, and without interfering signal. Consequently using equation (3.5):

$$\mathrm{var}\left[\hat{\tau}^l_{d/K}\right] \geq \frac{K \cdot \Delta \cdot \mathcal{N}_0}{4 \cdot \mathcal{P}^l \cdot L \cdot d}$$

  Note that in this case, the CRLB grows proportionally with the number of pseudolites.

  On the contrary, if the energy transmitted is supposed constant, then the instantaneous received power is $K \cdot \mathcal{P}^l$, and the CRLB will be:

$$\mathrm{var}\left[\hat{\tau}^l_{d/K}\right] \geq \frac{\Delta \cdot \mathcal{N}_0}{4 \cdot \mathcal{P}^l \cdot L \cdot d}$$

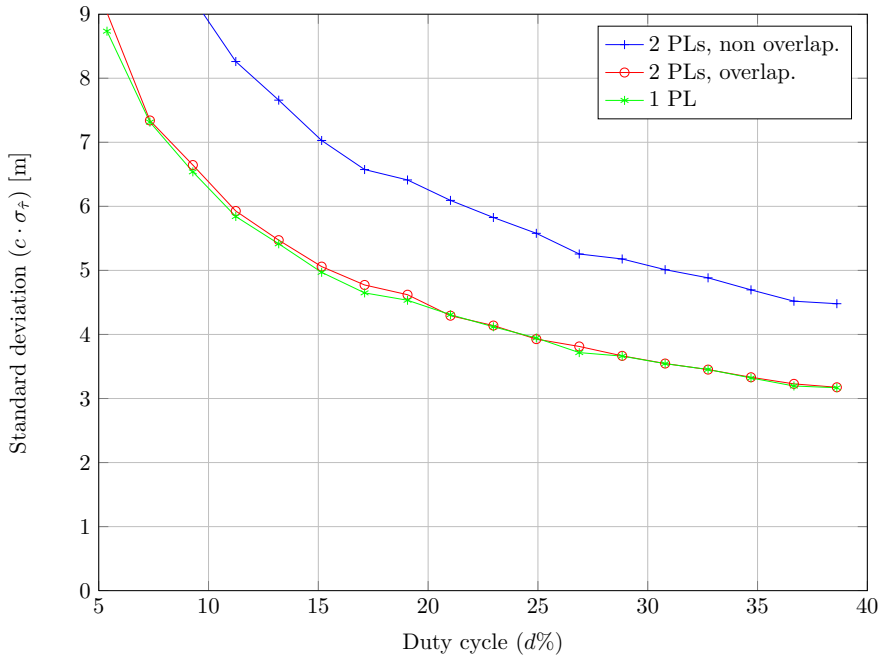

Figure 3.6: CRLB for both cases of overlapping and non-overlapping pulses for a constant received power from all pseudolites

In this case, the CRLB does not depend on the number of pseudolites K anymore, and provides better results than in the case of overlapping pulses. However, as it has been previously explained, this case is not realistic.

- In the case of overlapping pulses, the K pseudolites transmit at the same duty cycle $d = d_{\mathrm{PL}}$, but interfere. The Fisher matrix can be determined using equation (3.1), then inverted to obtain the CRLB. Note that in this case the impact of the estimation of the pseudolite received power is taken into account and the full Fisher information matrix is considered.

The matrix $\mathcal{I}(\boldsymbol{\theta})$ can be numerically inverted. The evolution of the CRLB is plotted in figure 3.7, with $d = 20\%$. The curves show that the CRLB grows very slowly in the case of overlapping pulses, which is therefore a better pulse scheme.

3.4 Cramér-Rao Lower Bound in the Quantized Case

In this section, the CRLB will be refined by taking quantization steps into account. The general approach presented in [4] will be applied to the pseudolite case.

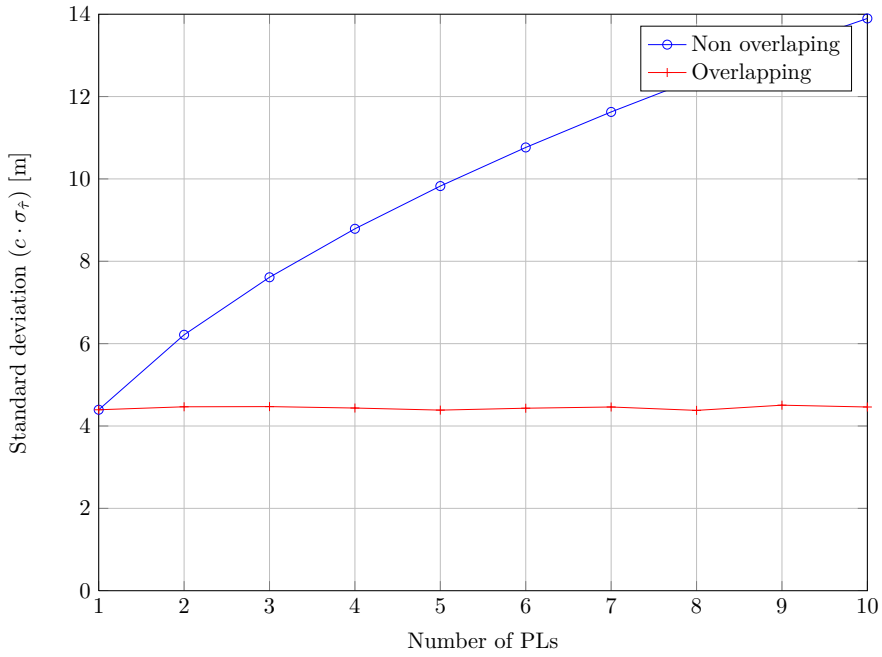

Figure 3.7: CRLB as a function of the number of pseudolites, pseudolites transmit at overall the duty cycle $d = 20\%$ and the received power is constant

3.4.1 Model of the Quantization

The N received samples are:

$$r_i = Q_b\left(\sum_k s^k(i\Delta - \tau^k) + \eta_i\right), i \in \{0, 1, \ldots, N-1\}$$

Where $s^k(i\Delta - \tau^k) = \sqrt{\mathcal{P}^k} \cdot c^k(i\Delta - \tau^k)$ is the received signal from pseudolite k and $Q_b(.)$ is the quantization function of the b-bit quantizer defined as:

$$Q_b(x) = r_i \text{ if } r_i^{\text{low}} \leq x < r_i^{\text{up}}$$

In the case of a uniform symmetric mid-riser type quantizer (cf. figure 3.8), the lower and upper quantization thresholds are:

$$r_i^{\text{low}} = \begin{cases} r_i - \frac{\delta}{2} & \text{if } r_i \geq -\frac{\delta}{2} \cdot (2^b - 1) \\ -\infty & \text{else} \end{cases}$$

$$r_i^{\text{up}} = \begin{cases} r_i + \frac{\delta}{2} & \text{if } r_i \leq \frac{\delta}{2} \cdot (2^b - 1) \\ +\infty & \text{else} \end{cases}$$

And the quantized receive alphabet is given by:

$$r_i \in \left\{\left(-\frac{2^b}{2} - \frac{1}{2} + k\right) \cdot \delta; k = 1, 2, \ldots, 2^b\right\}$$

Where δ is the quantizer step-size and b is the number of quantizer bits.

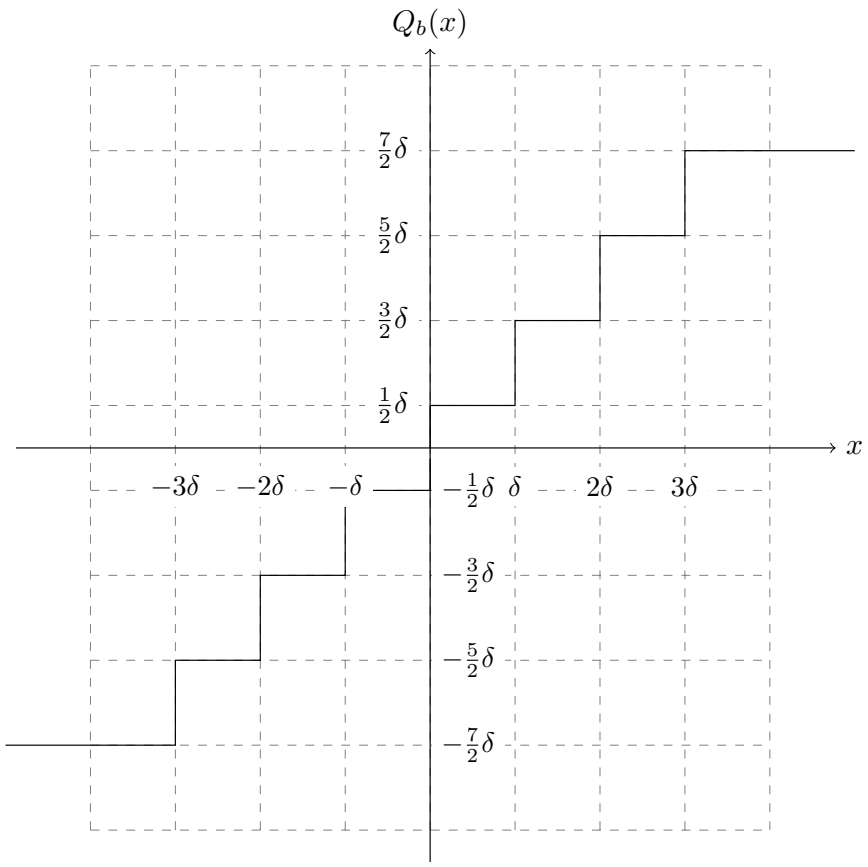

Figure 3.8: Output function of a uniform symmetric mid-riser quantizer

3.4.2 Derivation of the Cramér-Rao Lower Bound

The joint probability density to receive the vector of quantized samples $\boldsymbol{r}$ given the set of parameters $\boldsymbol{\theta} = [\tau^1, \tau^2, \ldots, \tau^k]$ is:

$$\begin{aligned}
\mathrm{p}\left(\boldsymbol{r} \mid \boldsymbol{\theta}\right) &= \prod_{i=0}^{N-1} \mathrm{p}\left(r_i \mid \boldsymbol{\theta}\right) \\
&= \prod_{i=0}^{N-1} \mathrm{p}\left(r_i^{\mathrm{low}} \leq \sum_k s^k(i\Delta - \tau^k) + \eta_i < r_i^{\mathrm{up}} \mid \boldsymbol{\theta}\right) \\
&= \prod_{i=0}^{N-1} \mathrm{p}\left(r_i^{\mathrm{low}} - \sum_k s^k(i\Delta - \tau^k) \leq \eta_i < r_i^{\mathrm{up}} - \sum_k s^k(i\Delta - \tau^k) \mid \boldsymbol{\theta}\right)
\end{aligned}$$

Since η_i is independent on $\boldsymbol{\theta}$:

$$\begin{aligned}
\mathrm{p}\left(\boldsymbol{r} \mid \boldsymbol{\theta}\right) &= \prod_{i=0}^{N-1} \mathrm{p}\left(r_i^{\mathrm{low}} - \sum_k s^k(i\Delta - \tau^k) \leq \eta_i < r_i^{\mathrm{up}} - \sum_k s^k(i\Delta - \tau^k)\right) \\
&= \prod_{i=0}^{N-1} \int_{r_i^{\mathrm{low}} - \sum_k s^k(i\Delta - \tau^k)}^{r_i^{\mathrm{up}} - \sum_k s^k(i\Delta - \tau^k)} \frac{1}{\sigma\sqrt{2\pi}} \cdot \exp\left(-\frac{x^2}{2\sigma^2}\right) \mathrm{d}x \\
&= \prod_{i=0}^{N-1} \mathcal{Q}\left(\frac{r_i^{\mathrm{low}} - \sum_k s^k(i\Delta - \tau^k)}{\sigma}\right) - \mathcal{Q}\left(\frac{r_i^{\mathrm{up}} - \sum_k s^k(i\Delta - \tau^k)}{\sigma}\right)
\end{aligned}$$

Where $\mathcal{Q}(.)$ is the Q-function defined as:

$$\mathcal{Q}(x) = \frac{1}{\sqrt{2\pi}} \cdot \int_x^{+\infty} \exp\left(\frac{-t^2}{2}\right) \mathrm{d}t$$

By taking the logarithm:

$$\begin{aligned}
&\log\left(\mathrm{p}\left(r \mid \boldsymbol{\theta}\right)\right) \\
&= \sum_{i=0}^{N-1} \log\left(\mathcal{Q}\left(\frac{r_i^{\mathrm{low}} - \sum_k s^k(i\Delta - \tau^k)}{\sigma}\right) - \mathcal{Q}\left(\frac{r_i^{\mathrm{up}} - \sum_k s^k(i\Delta - \tau^k)}{\sigma}\right)\right)
\end{aligned}$$

By taking the derivative:

$$\frac{\partial \log\left(\mathrm{p}\left(r \mid \boldsymbol{\theta}\right)\right)}{\partial \tau^p} = \frac{1}{\sigma\sqrt{2\pi}} \cdot \sum_{i=0}^{N-1} f(i, r_i, p)$$

With:

$$f(i, r_i, p) = \frac{\partial s^p(i\Delta - \tau^p)}{\partial \tau^p} \cdot \frac{e^{-\frac{\left(r_i^{\mathrm{up}} - \sum_k s^k(i\Delta - \tau^k)\right)^2}{2\sigma^2}} - e^{-\frac{\left(r_i^{\mathrm{low}} - \sum_k s^k(i\Delta - \tau^k)\right)^2}{2\sigma^2}}}{\mathcal{Q}\left(\frac{r_i^{\mathrm{low}} - \sum_k s^k(i\Delta - \tau^k)}{\sigma}\right) - \mathcal{Q}\left(\frac{r_i^{\mathrm{up}} - \sum_k s^k(i\Delta - \tau^k)}{\sigma}\right)}$$

Then the entries of the Fisher information matrix are given by:

$$\begin{aligned}
\mathcal{I}(\tau^p, \tau^q) &= \mathcal{E}\left[\frac{\partial \log\left(\mathrm{p}\left(r \mid \boldsymbol{\theta}\right)\right)}{\partial \tau^p} \cdot \frac{\partial \log\left(\mathrm{p}\left(r \mid \boldsymbol{\theta}\right)\right)}{\partial \tau^q}\right] \\
&= \frac{1}{2\pi\sigma^2} \cdot \mathcal{E}\left[\sum_{i=0}^{N-1} \sum_{j=0}^{N-1} f(i, r_i, p) \cdot f(j, r_j, q)\right]
\end{aligned}$$

When $i \neq j$, $f(i, r_i, p)$ is independent from $f(j, r_j, q)$, and the corresponding terms vanish. It follows:

$$\begin{aligned}
\mathcal{I}(\tau^p, \tau^q) &= \frac{1}{2\pi\sigma^2} \cdot \mathcal{E}\left[\sum_{i=0}^{N-1} f(i, r_i, p) \cdot f(i, r_i, q)\right] \\
&= \frac{1}{2\pi\sigma^2} \cdot \sum_{i=0}^{N-1} \cdot \sum_{r_i} \mathrm{p}\left(r_i \mid \boldsymbol{\theta}\right) \cdot f(i, r_i, p) \cdot f(i, r_i, q) \\
&= \frac{1}{\sigma^2} \cdot \sum_{i=0}^{N-1} \frac{\partial s^p(i\Delta - \tau^p)}{\partial \tau^p} \cdot \frac{\partial s^q(i\Delta - \tau^q)}{\partial \tau^q} \cdot \rho_{Q_b}
\end{aligned}$$

Where the factor ρ_{Q_b} is defined as:

$$\rho_{Q_b} = \frac{1}{2\pi} \cdot \sum_{r_i} \frac{\left(e^{-\frac{\left(r_i^{\mathrm{up}} - \sum_k s^k(i\Delta - \tau^k)\right)^2}{2\sigma^2}} - e^{-\frac{\left(r_i^{\mathrm{low}} - \sum_k s^k(i\Delta - \tau^k)\right)^2}{2\sigma^2}}\right)^2}{\mathcal{Q}\left(\frac{r_i^{\mathrm{low}} - \sum_k s^k(i\Delta - \tau^k)}{\sigma}\right) - \mathcal{Q}\left(\frac{r_i^{\mathrm{up}} - \sum_k s^k(i\Delta - \tau^k)}{\sigma}\right)}$$

ρ_{Q_b} represents the information loss compared to the unquantified case. Note that in the unquantified case, $\rho_{Q_\infty} = 1$ and equation (3.1) is obtained. In order to optimize the Fisher information, ρ_{Q_b} has to be optimized with respects to the quantizer step size. In the case of a one bit quantizer, the doublet $(r_i^{\mathrm{low}}, r_i^{\mathrm{up}})$ takes two values $(-\infty, 0)$ and $(0, +\infty)$. Then the information loss becomes:

$$\begin{aligned}
\rho_{Q_1} &= \frac{1}{2\pi}\left(\frac{e^{-\frac{\sum_k s^k(i\Delta - \tau^k)}{\sigma^2}}}{1 - \mathcal{Q}\left(-\frac{\sum_k s^k(i\Delta - \tau^k)}{\sigma}\right)} + \frac{e^{-\frac{\sum_k s^k(i\Delta - \tau^k)}{\sigma^2}}}{\mathcal{Q}\left(-\frac{\sum_k s^k(i\Delta - \tau^k)}{\sigma}\right)}\right) \\
&= \frac{e^{\frac{-\sum_k s^k(i\Delta - \tau^k)}{\sigma^2}}}{2\pi} \cdot \left(\frac{1}{\mathcal{Q}\left(\frac{\sum_k s^k(i\Delta - \tau^k)}{\sigma}\right)} + \frac{1}{\mathcal{Q}\left(-\frac{\sum_k s^k(i\Delta - \tau^k)}{\sigma}\right)}\right) \\
&= \frac{\exp\left(-\frac{\sum_k s^k(i\Delta - \tau^k)}{\sigma^2}\right)}{2\pi} \cdot \frac{1}{\mathcal{Q}\left(-\frac{\sum_k s^k(i\Delta - \tau^k)}{\sigma}\right) \cdot \mathcal{Q}\left(\frac{\sum_k s^k(i\Delta - \tau^k)}{\sigma}\right)}
\end{aligned}$$

It can be noticed that at low SNR regime, when $\sigma \gg \sum_k s^k(i\Delta - \tau^k))$, then information loss tends toward to $2/\pi$, which corresponds to the information loss for a one bit quantizer (cf. chapter 2).

3.4.3 Results

Back to the general case (b-bit quantizer), the quantization losses have to be minimized with respect to the number of pseudolites and received power from these pseudolites. Figure 3.9 represents the quantization losses as function of the quantizer step size for different numbers of pseudolites when a 2-bit quantizer

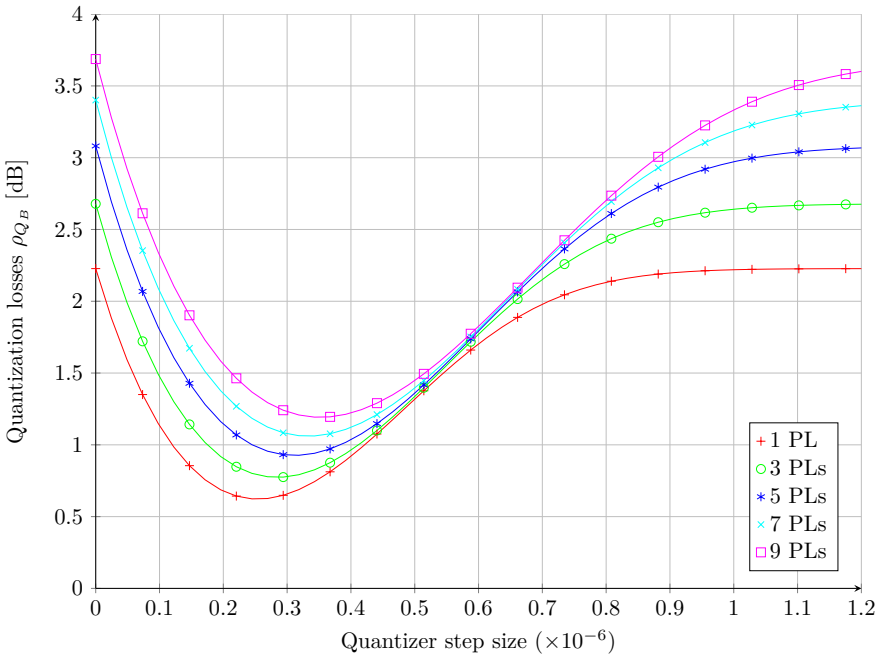

Figure 3.9: Quantization loss for different quantizer step sizes, pseudolites power $\mathcal{P} = -140$dB (the same for all pseudolites), 1023 chips per epoch, duty cycle $d = 20\%$, 2-bit quantizer

is used. Therefore in order to get the minimal quantization losses, and so the minimal CRLB, the quantizer step size has to be optimized.

Then using the optimal quantization step previously determined, the quantization losses as function of the pseudolite number can be plotted (cf. figure 3.10). Finally the CRLB can be determined. Figure 3.11 represents the evolution of the 90^{th} percentile CRLB and figure 3.12 compares the CRLB when the relative power between two pseudolites is varying.

The CRLB in case of non-overlapping pulses grows with the square root of the number of pseudolites. In case of overlapping pulses, the CRLB grows slower than the square root of the number of pseudolites. Then overlapping pulses provide a better CRLB than non-overlapping pulses, and is consequently a better pulse scheme.

3.5 Conclusion

The transmit power is constant whatever the transmitting duration and a maximal overall duty cycle is reserved for the pseudolite pulses. Then using the CRLB, it has been shown in this chapter that overlapping pulses perform better than non-overlapping pulses when pseudolite signals are tracked.

Consequently, in the next chapter, overlapping pulses will be considered. However, pulses have to be synchronized, and it is not sure that the CRLB can be effectively reached. In the next chapter, interference cancellation methods are studied, in order improve the tracking results and to approach the CRLB.

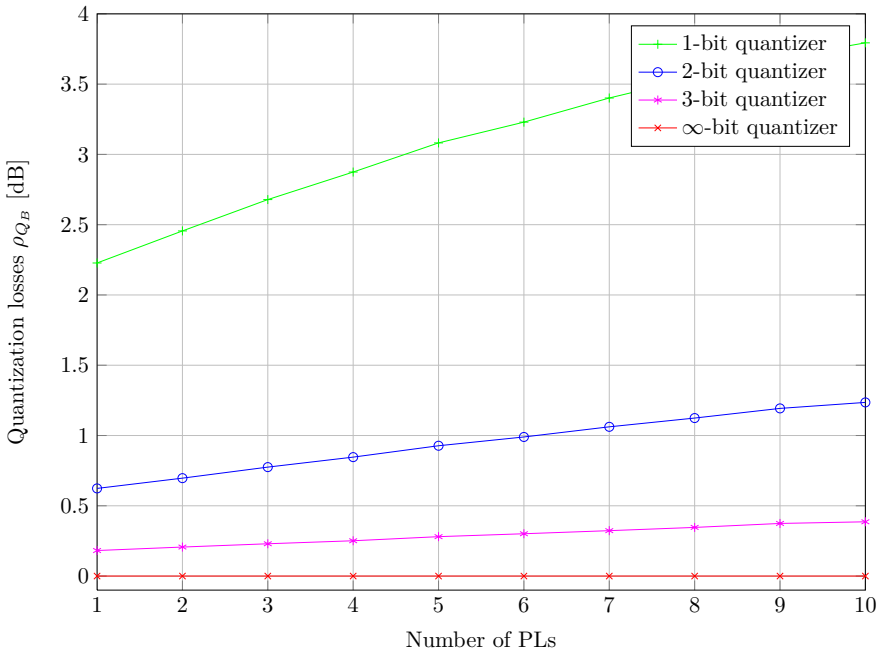

Figure 3.10: Quantization loss, pseudolites power $\mathcal{P} = -140$ dB (the same for all pseudolites), 1023 chip per epoch, duty cycle $d = 20\%$

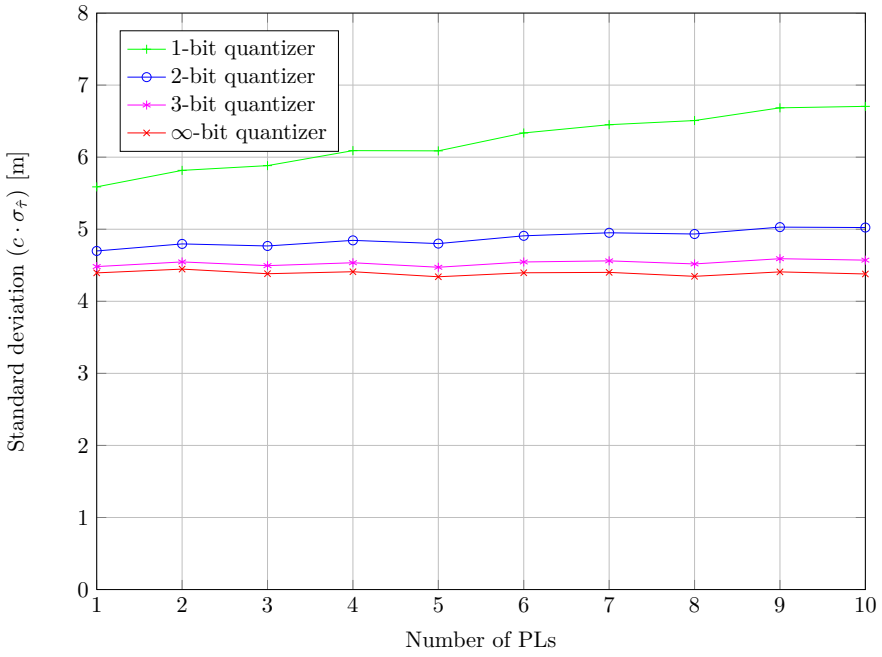

Figure 3.11: CRLB, pseudolites power $\mathcal{P} = -140$ dB (the same for all pseudolites), 1023 chips per epoch, duty cycle $d = 20\%$

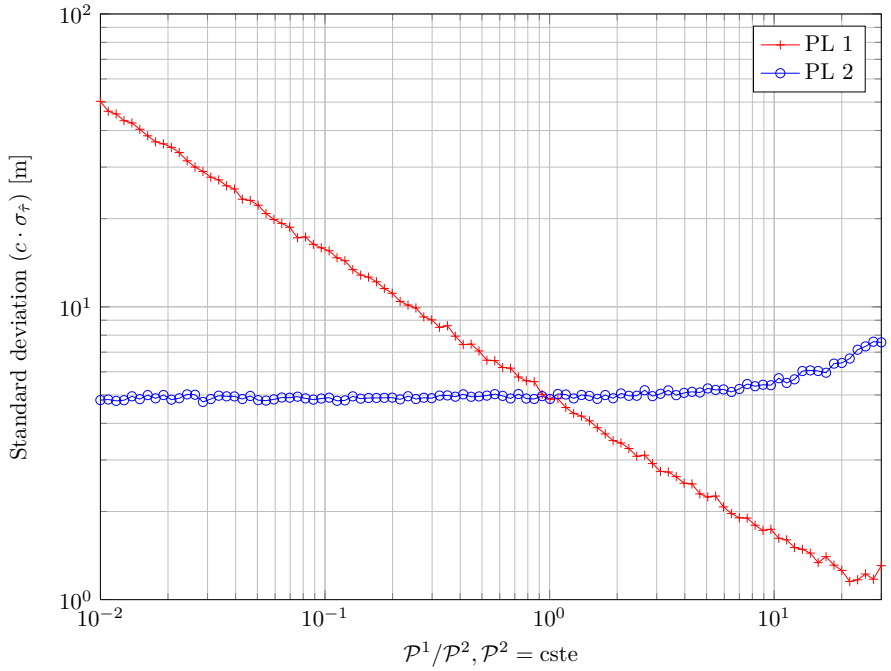

Figure 3.12: Standard deviation, pseudolites power $\mathcal{P}^2 = -140$ dB, 1023 chips per epoch, duty cycle $d = 20\%$, 2-bit quantizer

Chapter 4

Participative Receivers

In order to solve the Near-Far problem, different methods have been proposed:

- Frequency offset schemes involve transmitting pseudolite signals on a carrier frequency offset from the GPS L1 carrier (cf. [5]).
- PRN codes modification: use of longer codes, modified signal polarization, some chipped at higher rate, as proposed in [6].
- Interference cancellation that reduces the effect of inteferences from other navigation signals. Interference cancellation has been firstly proposed for mitigation for the Near-Far problem in cellular systems (cf. [7, 8]).

The first and the second solutions involve modification to the transmitters. Interference cancellation only needs modification in the receiver. Therefore this solution is adopted for the following.

In the previous chapter, it has been shown that at constant PPP and constant aggregated duty cycle, for pseudolite tracking, overlapping pulses provide better results compared to non-overlapping pulses. Consequently from now on, it will be considered that all pseudolites emit simultaneously during a specified duty cycle. The aim of this chapter is to present a possible architecture for a participative receiver that would reduce the effects of the pseudolite signals, to be considered as interfering ones.

4.1 Description of the Receiver Implementing the Interference Cancellation

In this chapter, in the contrary to the chapter 2, a highly capable front-end is considered, in order to track pseudolite signal. A possible structure is presented figure 4.1. T_i is the correlation time and d is the duty cycle.

- The switch directs the signal either to the pseudolite branch if pseudolites are transmitting or to the satellite branch if pseudolites are not transmitting. It is considered that pseudolites transmit during the first part of the integration time ($t \in [0; d \cdot T_i]$) and that the second part the integration time is left free to track the satellites ($t \in [d \cdot T_i, T_i]$).

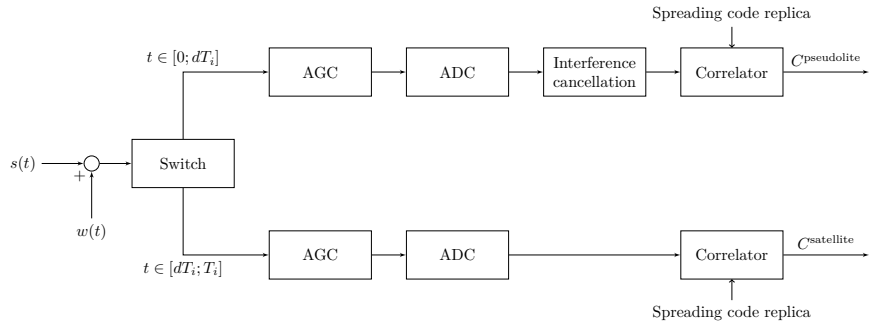

Figure 4.1: Diagram of a participative receiver

- The two AGCs normalize the signal.
- The two ADCs quantize and sample the signals.
- Interference cancellation is used to reduce the Near-Far effect between pseudolites. Note that on the two followings figures (cf. figures 4.2 and 4.3), the upper index refer to the pseudolite numbers and thr lower index refer to the stage numbers. The interference cancellation can be realized in a parallel way (Parallel Interference Cancellation (PIC)) or in a sequential way (Sequential Interference Cancellation (SIC)):
  - SIC: A description and analysis of this method is proposed in [9] and an application for pseudolites is proposed in [10]. In figure 4.2, a diagram of a SIC is presented. At each stage, one pseudolite navigation signal is reconstructed and subtracted to the input signal. The interferences are successively canceled. Consequently at stage k, only the $k-1$ previously estimated signals have been cancelled.

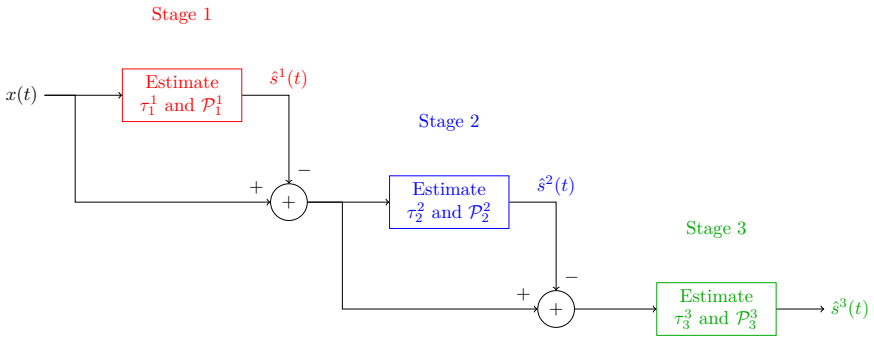

Figure 4.2: Diagram of the first three stages of the sequential interference cancellation

  - PIC consists of a variant of the SIC scheme (cf. [11]). In figure 4.3 a diagram of the PIC method is presented. At each stage, all signals are estimated and all signals other than the tracked one are subtracted from the received signal. k represents the pseudolite index and K the number of pseudolites.

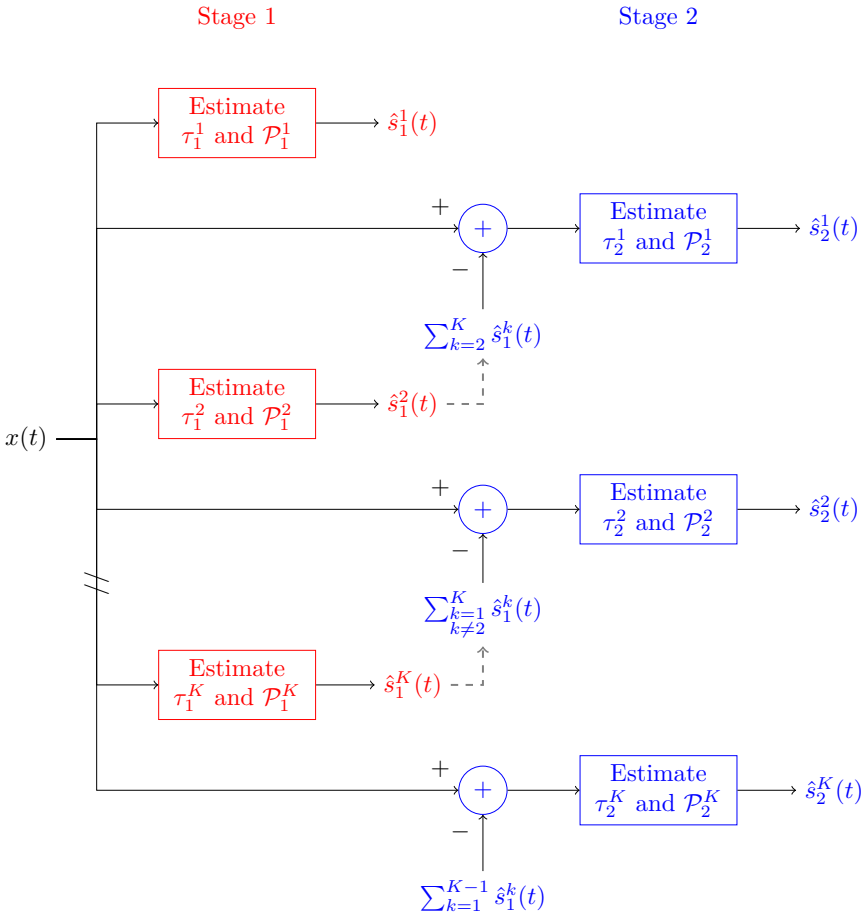

Figure 4.3: Diagram of the first two stages of the parallel interference cancellation

It is the intention of this paper to show that PIC provides better tracking performances than SIC even if the required hardware complexity is greater. It will also be shown that PIC generally provides better performance when all of the strong signals have similar power levels and SIC when they are different (this consolidates assessments proposed in [11] which applies for ICT for communication).

The satellite branch has already been analyzed in chapter 2. Since the satellite tracking is possible for a low-cost receiver (1-bit quantizer, without switch), then the highly capable receiver proposed here (b-bit quantizer, with a switch) is also able to track satellites. Consequently in this chapter the focus will be put on the pseudolites branch. The theoretical analysis is inspired by [12].

4.2 Approximations

Approx. 4.1. All signals are considered real. The down-conversion of the received signal into baseband induces actually complex signals, but if the phase is perfectly known, it may be possible to take only the real part.

Approx. 4.2. Only white Gaussian noise and pseudolite navigation signals are considered. Other interfering signals are not taken into account and satellites interferences are neglected, since the power of the satellite signals is much smaller than the power of the pseudolite signals and the power of the noise in the receiver front-end.

Approx. 4.3. The chip waveform is supposed to be the same for all navigation signals.

Approx. 4.4. The quantization is supposed to be done with enough bits such that the quantization losses can be neglected.

Approx. 4.5. The effect of the low-pass filter on the navigation signals is neglected.

Approx. 4.6. The pulses are supposed to be perfectly synchronized. This can not be the case in reality. Indeed even if the pulses are perfectly synchronized at emission, since distance from each pseudolite to the receiver will be different, the delays will be different, and the pulses will only partially overlap, or even not overlap at all.

Approx. 4.7. The input signals are already acquired. Consequently the relative delay between the tracked signal and the local replica is supposed to be small: $\left|\tau^l - \hat{\tau}_0^l\right| \leq {}^{T_c}/_4$

With these approximations, the received signal is:

$$s(t) = \sum_{k=1}^{K} s^k(t) + w(t)$$

Where K is the number of pseudolites. Since quantization and sampling losses are neglected, the effect of the ADC are ignored. Moreover, the effect of filtering

on the navigation signals is neglected. Consequently, the signal at the ADC output is:

$$x(t) \approx \sum_{k=1}^{K} s^k(t) + \eta(t)$$

The received signal is correlated with the local replica of the code. The local replica is shifted by the estimated delay $\hat{\tau}_0^l$, which fulfils the following constraint at the end of acquisition phase: $\left|\tau^l - \hat{\tau}_0^l\right| \leq {}^{T_c}/_4$ and $\hat{\tau}_0^l$ is the first delay estimate used as input for the first stage of the ICT. Only time intervals containing pulsed signals ($[0\,; d \cdot T_i]$) are taken into account in the correlation function whose expression becomes:

$$C^l = \frac{1}{d \cdot T_i} \cdot \int_0^{d \cdot T_i} c^l(t - \hat{\tau}_0^l) \cdot x(t)\, \mathrm{d}t$$

The aim is to compare the variance of the propagation delay estimators at the correlator output, with and without the application of the interference cancellation, in order to characterize the benefit. Hence the variance of the delay estimation error will be computed without interference cancellation, then after a given number of interference cancellation stages. In order to obtain the variance of the delay error, the SNIR has to be firstly determined. Then a relationship between the SNIR and variance of the delay error is used. This relation will depend on the discriminator which is used to estimate the delay error.

4.3 First Stage of the Interference Cancellation

At the first stage of the interference cancellation no signal is subtracted. Therefore the SNIR that will be computed corresponds to the case without inference cancellation (for both parallel and sequential methods). At the end of this stage, it will be possible to estimate the amplitude and the delay of the navigation signals, and then from stage 2, the reconstructed signals can be subtracted from the received signal. At the first stage, the correlator output for the l^{th} pseudolite is:

$$C_1^l = A_1^l + \mathcal{W}_1^l + \sum_{\substack{k=1 \\ k \neq l}}^{K} I_1^k$$

Where:

- A_1^l represents the contribution of the useful signal. It is considered that $\hat{\tau}_0^l \approx \tau^l$, then:

$$\begin{aligned} A_1^l &= \frac{\sqrt{\mathcal{P}^l}}{d \cdot T_i} \int_0^{d \cdot T_i} c^l(t - \hat{\tau}_0^l) \cdot c^l(t - \tau^l)\, \mathrm{d}t \\ &\approx \sqrt{\mathcal{P}^l} \end{aligned}$$

Consequently:

$$\mathcal{E}\left[A_1^l\right] \approx \sqrt{\mathcal{P}^l}$$
$$\mathrm{var}\left[A_1^l\right] \approx 0$$

- $\mathcal{W}_1^l$ represents the correlation with the Additive White Gaussian Noise (AWGN) process which fulfills the following properties:

$$\mathcal{W}_1^l = \frac{1}{d \cdot T_i} \cdot \int_0^{d \cdot T_i} c^l(t - \hat{\tau}_0^l) \cdot \eta(t)\,\mathrm{d}t$$

Then:

$$\mathcal{E}\left[\mathcal{W}_1^l\right] = 0$$
$$\mathrm{var}\left[\mathcal{W}_1^l\right] = \frac{\mathcal{N}_0/2}{d \cdot T_i}$$

Note that $\mathrm{var}\left[\mathcal{W}_1^l\right]$ does not depends neither on the considered pseudolite nor on the considered stage of interference cancellation.

- I_1^k represents the Multiple Access Interference (MAI) from the k^{th} navigation signal before interference cancellation. It is considered that $\hat{\tau}_0^l \approx \tau^l$, then:

$$\begin{aligned} I_1^k &= \frac{\sqrt{\mathcal{P}^k}}{d \cdot T_i} \cdot \int_0^{d \cdot T_i} c^k(t - \tau^k) \cdot c^l(t - \hat{\tau}_0^l)\,\mathrm{d}t \\ &\approx \frac{\sqrt{\mathcal{P}^k}}{d \cdot T_i} \cdot \int_0^{d \cdot T_i} c^k(t - \tau^k) \cdot c^l(t - \tau^l)\,\mathrm{d}t \end{aligned}$$

The chip values of the underlying spreading sequences $c^l(.)$ and $c^k(.)$ are independent and it is assumed that the spreading sequences are well balanced, then:

$$\mathcal{E}\left[I_1^k\right] = 0$$

Then the variance:

$$\mathrm{var}\left[I_1^k\right] \approx \mathcal{P}^k \cdot \mathrm{var}\left[\frac{1}{d \cdot T_i} \cdot \int_0^{d \cdot T_i} c^k(t - \tau^k) \cdot c^l(t - \tau^l)\,\mathrm{d}t\right]$$

The second multiplicand above is called Waveform Convolution Coefficient (WCC) and is further developed in annexe A. It can be computed using equation A.2 in the general case or using equation A.3 for a BPSK signal if the effect of the low-pass filter is neglected. Consequently, the variance of the MAI can be expressed as:

$$\mathrm{var}\left[I_1^k\right] \approx \mathcal{P}^k \cdot \mathrm{WCC}_{d \cdot T_i}(\tau^l - \tau^k) \tag{4.1}$$

Finally:

$$\mathcal{E}\left[C_1^l\right] \approx \sqrt{\mathcal{P}^l} \tag{4.2}$$

$$\mathrm{var}\left[C_1^l\right] \approx \frac{\mathcal{N}_0/2}{d \cdot T_i} + \sum_{\substack{k=1 \\ k \neq l}}^{K} \mathcal{P}^k \cdot \mathrm{WCC}_{d \cdot T_i}(\tau^l - \tau^k) \tag{4.3}$$

Then the SNIR of the correlator output of the pseudolite l at the first stage (before interference cancellation) is:

$$\boxed{\mathrm{SNIR}_1^l \approx \frac{\mathcal{P}^l}{\frac{\mathcal{N}_0/2}{d \cdot T_i} + \sum_{\substack{k=1 \\ k \neq l}}^{K} \mathrm{WCC}_{d \cdot T_i}(\tau^l - \tau^k) \cdot \mathcal{P}^k}} \tag{4.4}$$

A Non-coherent Early minus Late Power discriminator in open loop is used to track the delay error (cf. annexe B). Consequently, the variance of the delay error can be express as a function of the SNIR:

$$\boxed{\mathrm{var}\left[\tau_1^l - \hat{\tau}_1^l\right] \approx \frac{d_{\mathrm{EL}} \cdot T_c^2}{4 \cdot \mathrm{SNIR}_1^l} \left(1 + \frac{2}{(2 - d_{\mathrm{EL}}) \cdot \mathrm{SNIR}_1^l}\right)} \tag{4.5}$$

Where the early late spacing is $d_{\mathrm{EL}} \cdot T_c$.

4.4 Parallel Interference Cancellation

4.4.1 Signal to Noise plus Interferences Ratio

The received signal power for pseudolite k can be estimated by the square of the correlator output at the previous stage.

$$\begin{aligned} \hat{\mathcal{P}}_s^k &= \left|C_s^k\right|^2 \\ &= \left(C_s^k\right)^2 \text{ since the signal is real} \end{aligned}$$

A reconstructed navigation signal from pseudolite k is $s_s^k(.)$ can be obtained by:

$$\hat{s}_s^k(t) = \sqrt{\hat{\mathcal{P}}_s^k} \cdot c^k(t - \hat{\tau}_s^k)$$

Then the received signal can be improved by subtracting the reconstructed navigation signals corresponding to interfering pseudolites.

$$r_{s+1}^l(t) = \sqrt{\mathcal{P}^l} c^l(t - \tau^l) + \eta(t) + \sum_{\substack{k=1 \\ k \neq l}}^{K} \left(\sqrt{\mathcal{P}^k} \cdot c^k(t - \tau^k) - \sqrt{\hat{\mathcal{P}}_s^k} \cdot c^k(t - \hat{\tau}_s^k)\right)$$

Then the correlator output is:

$$\begin{aligned} C_{s+1}^l &= \frac{1}{d \cdot T_i} \cdot \int_0^{d \cdot T_i} r_{s+1}^l(t) \cdot c^l(t - \hat{\tau}_s^l)\, \mathrm{d}t \\ &= A_{s+1}^l + \mathcal{W}_{s+1}^l + \sum_{\substack{k=1 \\ k \neq l}}^{K} I_{s+1}^k \end{aligned}$$

The three terms will be computed separately:

- A_{s+1}^l represents the useful part of the signal. It is considered that $\hat{\tau}_s^l \approx \tau^l$, then:

$$\begin{aligned} A_{s+1}^l &= \frac{\sqrt{\mathcal{P}^l}}{d \cdot T_i} \int_0^{d \cdot T_i} c^l(t - \tau^l) \cdot c^l(t - \hat{\tau}_s^l)\, \mathrm{d}t \\ &\approx \sqrt{\mathcal{P}^l} \end{aligned}$$

Then:

$$\begin{aligned}\mathcal{E}\left[A_{s+1}^{l}\right] &\approx \sqrt{\mathcal{P}^{l}}\\ \operatorname{var}\left[A_{s+1}^{l}\right] &= 0\end{aligned}$$

- $\mathcal{W}_{s+1}^{l}$ represents the AWGN process.

$$\mathcal{W}_{s+1}^{l} = \frac{1}{d\cdot T_i}\cdot\int_{0}^{d\cdot T_i}\eta(t)\cdot c^{l}(t-\hat{\tau}_{s}^{l})\,\mathrm{d}t$$

Then:

$$\begin{aligned}\mathcal{E}\left[\mathcal{W}_{s+1}^{l}\right] &= 0\\ \operatorname{var}\left[\mathcal{W}_{s+1}^{l}\right] &= \frac{\mathcal{N}_0/2}{d\cdot T_i}\end{aligned}$$

- I_{s+1}^{k} represents the residual MAI from the k^{th} pseudolite at stage $s+1$:

$$I_{s+1}^{k} = \frac{1}{d\cdot T_i}\cdot\int_{0}^{d\cdot T_i}\left(\sqrt{\mathcal{P}^{k}}\cdot c^{k}(t-\tau^{k}) - \sqrt{\hat{\mathcal{P}}_{s}^{k}}\cdot c^{k}(t-\hat{\tau}_{s}^{k})\right)\cdot c^{l}(t-\hat{\tau}_{s}^{l})\,\mathrm{d}t$$

The chip values of the spreading sequences $c^{l}(.)$ and $c^{k}(.)$ are independent and the spreading sequences are balanced, then:

$$\mathcal{E}\left[I_{s+1}^{k}\right] = 0$$

In order to derive the variance, I_{s}^{k} can be rewritten as:

$$I_{s+1}^{k} = \gamma_{s+1}^{k} + \lambda_{s+1}^{k}$$

Where:

$$\begin{aligned}\gamma_{s+1}^{k} &= \frac{\sqrt{\mathcal{P}^{k}} - \sqrt{\hat{\mathcal{P}}_{s}^{k}}}{d\cdot T_i}\cdot\int_{0}^{d\cdot T_i} c^{l}(t-\hat{\tau}_{s}^{l})\cdot c^{k}(t-\tau^{k})\,\mathrm{d}t\\ \lambda_{s+1}^{k} &= \frac{\sqrt{\hat{\mathcal{P}}_{s}^{k}}}{d\cdot T_i}\cdot\int_{0}^{d\cdot T_i} c^{l}(t-\hat{\tau}_{s}^{l})\cdot\left(c^{k}(t-\tau^{k}) - c^{k}(t-\hat{\tau}_{s}^{k})\right)\mathrm{d}t\end{aligned}$$

Note that γ_{s+1}^{k} represents the residual due to the error on the amplitude estimation $\sqrt{\hat{\mathcal{P}}_{s}^{k}}$ and λ_{s+1}^{k} the one due to the error of delay estimation $\hat{\tau}_{s}^{l}$. Considering that $\hat{\tau}_{s+1}^{l} \approx \tau^{l}$, it follows:

$$\gamma_{s+1}^{k} \approx \frac{\sqrt{\mathcal{P}^{k}} - \sqrt{\hat{\mathcal{P}}_{s}^{k}}}{d\cdot T_i}\cdot\int_{0}^{d\cdot T_i} c^{l}(t-\tau_{s}^{l})\cdot c^{k}(t-\tau^{k})\,\mathrm{d}t$$

Since $\hat{\tau}_{s}^{k} \approx \tau^{k}$, then using Taylor development around τ^{k}, the estimated spreading code can be approximated by:

$$c^{k}(t-\hat{\tau}_{s}^{k}) \approx c^{k}(t-\tau_{s}^{k}) + (\tau^{k}-\hat{\tau}_{s}^{k})\cdot\frac{\mathrm{d}c^{k}(t-\hat{\tau}^{k})}{\mathrm{d}t}$$

Then the error between the real spreading code and the estimated spreading code becomes:

$$c^k(t-\tau^k) - c^k(t-\hat{\tau}_s^k) \approx (\tau^k - \hat{\tau}_s^k) \cdot \frac{\mathrm{d}c^k(t-\tau^k)}{\mathrm{d}t}$$

Consequently λ_{s+1}^k can be approximated by:

$$\lambda_{s+1}^k \approx \frac{\sqrt{\hat{\mathcal{P}}_s^k}}{d \cdot T_i} \cdot (\tau^k - \hat{\tau}_s^k) \cdot \int_0^{d \cdot T_i} c^l(t-\tau_s^l) \cdot \frac{\mathrm{d}c^k(t-\tau^k)}{\mathrm{d}t}\,\mathrm{d}t$$

The variance of the residual MAI can be rewritten as:

$$\mathrm{var}\left[I_{s+1}^k\right] = \mathrm{var}\left[\gamma_{s+1}^k\right] + 2 \cdot \mathrm{cov}\left[\gamma_{s+1}^k, \lambda_{s+1}^k\right] + \mathrm{var}\left[\lambda_{s+1}^k\right]$$

The three terms will be derived separately:

– Derivation of $\mathrm{var}\left[\gamma_{s+1}^k\right]$

$$\mathrm{var}\left[\gamma_{s+1}^k\right] \approx \mathrm{var}\left[\frac{\sqrt{\mathcal{P}^k} - \sqrt{\hat{\mathcal{P}}_s^k}}{d \cdot T_i} \cdot \int_0^{d \cdot T_i} c^l(t-\tau_s^l) \cdot c^k(t-\tau^k)\,\mathrm{d}t\right]$$

Since the power estimation error does not depends on the correlation between the chip sequences:

$$\begin{aligned}\mathrm{var}\left[\gamma_{s+1}^k\right] &\approx \mathrm{var}\left[\sqrt{\mathcal{P}^k} - \sqrt{\hat{\mathcal{P}}_s^k}\right] \cdot \mathrm{var}\left[\frac{1}{d \cdot T_i}\int_0^{d \cdot T_i} c^l(t-\tau_s^l) \cdot c^k(t-\tau^k)\,\mathrm{d}t\right] \\ &= \mathrm{var}\left[\sqrt{\hat{\mathcal{P}}_s^k}\right] \cdot \mathrm{WCC}_{d \cdot T_i}(\tau^l - \tau^k) \\ &= \mathrm{var}\left[C_s^k\right] \cdot \mathrm{WCC}_{d \cdot T_i}(\tau^l - \tau^k)\end{aligned}$$

– Derivation of $\mathrm{cov}\left[\gamma_{s+1}^k, \lambda_{s+1}^k\right]$

$$\mathrm{cov}\left[\gamma_{s+1}^k, \lambda_{s+1}^k\right] = \mathcal{E}\left[\gamma_{s+1}^k \lambda_{s+1}^k\right] - \mathcal{E}\left[\gamma_{s+1}^k\right] \cdot \mathcal{E}\left[\lambda_{s+1}^k\right]$$

$$\begin{aligned}\mathcal{E}\left[\gamma_{s+1}^k \lambda_{s+1}^k\right] \approx \mathcal{E}\Bigg[&\frac{1}{(d \cdot T_i)^2} \cdot \sqrt{\hat{\mathcal{P}}_s^k} \cdot \left(\sqrt{\mathcal{P}^k} - \sqrt{\hat{\mathcal{P}}_s^k}\right) \\ &\cdot \int_0^{d \cdot T_i} c^k(t-\tau^k) \cdot c^l(t-\tau_s^l)\,\mathrm{d}t \\ &\cdot \left(\tau^k - \hat{\tau}_s^k\right) \cdot \int_0^{d \cdot T_i} c^l(t-\tau_s^l) \cdot \frac{\mathrm{d}c^k(t-\tau^k)}{\mathrm{d}t}\,\mathrm{d}t\Bigg]\end{aligned}$$

Since the estimated propagation delay error does not depends on

power estimation error and on the chip sequences:

$$\begin{aligned}\mathcal{E}\left[\gamma_{s+1}^k \lambda_{s+1}^k\right] \approx \mathcal{E}\left[\left(\tau^k - \hat{\tau}_s^k\right)\right] \\ \cdot \mathcal{E}\left[\frac{1}{(d\cdot T_i)^2}\cdot\sqrt{\hat{\mathcal{P}}_s^k}\cdot\left(\sqrt{\mathcal{P}^k}-\sqrt{\hat{\mathcal{P}}_s^k}\right)\right. \\ \cdot\int_0^{d\cdot T_i} c^k(t-\tau^k)\cdot c^l(t-\tau_s^l)\,\mathrm{d}t \\ \left.\cdot\int_0^{d\cdot T_i} c^l(t-\tau_s^l)\cdot\frac{\mathrm{d}c^k(t-\tau^k)}{\mathrm{d}t}\,\mathrm{d}t\right] \\ = 0\end{aligned}$$

Since $\hat{\tau}_s^k$ is an unbiased estimator of τ^k. Moreover:

$$\begin{aligned}\mathcal{E}\left[\gamma_{s+1}^k\right] &= \frac{1}{d\cdot T_i}\cdot\mathcal{E}\left[\left(\sqrt{\mathcal{P}^k}-\sqrt{\hat{\mathcal{P}}_s^k}\right)\cdot\int_0^{d\cdot T_i} c^k(t-\tau^k)\cdot c^l(t-\hat{\tau}_s^l)\,\mathrm{d}t\right] \\ &= \frac{1}{d\cdot T_i}\cdot\mathcal{E}\left[\sqrt{\mathcal{P}^k}-\sqrt{\hat{\mathcal{P}}_s^k}\right]\cdot\mathcal{E}\left[\int_0^{d\cdot T_i} c^k(t-\tau^k)\cdot c^l(t-\hat{\tau}_s^l)\right] \\ &= 0\end{aligned}$$

Then:

$$\mathrm{cov}\left[\gamma_{s+1}^k, \lambda_{s+1}^k\right] = 0$$

– Derivation of $\mathrm{var}\left[\lambda_{s+1}^k\right]$

$$\begin{aligned}\mathrm{var}\left[\lambda_{s+1}^k\right] &\approx \mathrm{var}\left[\sqrt{\hat{\mathcal{P}}_s^k}\cdot\frac{\tau^k-\hat{\tau}_s^k}{d\cdot T_i}\cdot\int_0^{d\cdot T_i} c^l(t-\tau_s^l)\cdot\frac{\mathrm{d}c^k(t-\tau^k)}{\mathrm{d}t}\,\mathrm{d}t\right] \\ &= \mathrm{var}\left[\sqrt{\hat{\mathcal{P}}_s^k}\right] \\ &\quad\cdot\mathrm{var}\left[\frac{\tau^k-\hat{\tau}_s^k}{d\cdot T_i}\cdot\int_0^{d\cdot T_i} c^l(t-\tau_s^l)\cdot\frac{\mathrm{d}c^k(t-\tau^k)}{\mathrm{d}t}\,\mathrm{d}t\right]\end{aligned}$$

Estimated power, propagation delay error and chip sequences are independent, therefore:

$$\begin{aligned}\mathrm{var}\left[\lambda_{s+1}^k\right] &\approx \mathrm{var}\left[\sqrt{\hat{\mathcal{P}}_s^k}\right]\cdot\mathrm{var}\left[\hat{\tau}_s^k-\tau^k\right] \\ &\quad\cdot\mathrm{var}\left[\frac{1}{d\cdot T_i}\cdot\int_0^{d\cdot T_i} c^l(t-\tau_s^l)\cdot\frac{\mathrm{d}c^k(t-\tau^k)}{\mathrm{d}t}\,\mathrm{d}t\right] \\ &= \mathrm{var}\left[\sqrt{\hat{\mathcal{P}}_s^k}\right]\cdot\mathrm{var}\left[\hat{\tau}_s^k-\tau^k\right]\cdot\mathrm{DWCC}_{d\cdot T_i}(\tau^l-\tau^k) \\ &= \mathrm{var}\left[C_s^k\right]\cdot\mathrm{var}\left[\hat{\tau}_s^k-\tau^k\right]\cdot\mathrm{DWCC}_{d\cdot T_i}(\tau^l-\tau^k)\end{aligned}$$

Where $\mathrm{DWCC}_{d\cdot T_i}(\tau^l-\tau^k)$ is called the Differential Waveform Convolution Coefficient (DWCC) (cf. annexe A). This coefficient can be computed using equation A.5 in the general case or with equation A.6 for a BPSK signal and if the effect of the low-pass filter are neglected.

Then the variance of the interference contribution from pseudolite k at stage $s+1$ is:

$$\begin{aligned}\operatorname{var}\left[I_{s+1}^{k}\right] \approx & \operatorname{var}\left[C_{s}^{k}\right] \\ & \cdot\left(\mathrm{WCC}_{d\cdot T_i}(\tau^{l}-\tau^{k})+\operatorname{var}\left[\hat{\tau}_{s}^{k}-\tau^{k}\right]\cdot\mathrm{DWCC}_{d\cdot T_i}(\tau^{l}-\tau^{k})\right)\end{aligned}$$

Since $\mathrm{SNIR}_{s}^{k} = {}^{\mathcal{P}^{k}}/_{\mathrm{var}[C_{s}^{k}]}$, it follows:

$$\begin{aligned}\operatorname{var}\left[I_{s+1}^{k}\right] = \frac{\mathcal{P}^{k}}{\mathrm{SNIR}_{s}^{k}}\cdot\big(&\mathrm{WCC}_{d\cdot T_i}(\tau^{l}-\tau^{k}) \\ &+\operatorname{var}\left[\hat{\tau}_{s}^{k}-\tau^{k}\right]\cdot\mathrm{DWCC}_{d\cdot T_i}(\tau^{l}-\tau^{k})\big)\end{aligned} \tag{4.6}$$

Then the variance of the correlator output for pseudolite l, at stage $s+1$ is:

$$\begin{aligned}\operatorname{var}\left[C_{s+1}^{l}\right] = & \frac{{}^{\mathcal{N}_0}/_{2}}{d\cdot T_i} \\ & +\sum_{\substack{k=1\\k\neq l}}^{K}\frac{\mathcal{P}^{k}}{\mathrm{SNIR}_{s}^{k}}\cdot\left(\mathrm{WCC}_{d\cdot T_i}(\tau^{l}-\tau^{k})+\operatorname{var}\left[\hat{\tau}_{s}^{k}-\tau^{k}\right]\cdot\mathrm{DWCC}_{d\cdot T_i}(\tau^{l}-\tau^{k})\right)\end{aligned}$$

And consequently the SNIR of the correlator output for pseudolite l, at stage $s+1$ can be expressed indirectly as a function of the SNIR at stage s:

$$\boxed{\mathrm{SNIR}_{s+1}^{l} = \frac{\mathcal{P}^{l}}{\frac{\mathcal{N}_0/2}{d\cdot T_i}+\sum_{\substack{k=1\\k\neq l}}^{K}\frac{\mathcal{P}^{k}}{\mathrm{SNIR}_{s}^{k}}\cdot\left(\mathrm{WCC}_{d\cdot T_i}(\tau^{l}-\tau^{k})+\operatorname{var}\left[\hat{\tau}_{s}^{k}-\tau^{k}\right]\mathrm{DWCC}_{d\cdot T_i}(\tau^{l}-\tau^{k})\right)}} \tag{4.7}$$

Using annexe B, the variance of the propagation delay error can be expressed as a function of the SNIR:

$$\boxed{\operatorname{var}\left[\hat{\tau}_{s}^{k}-\tau_{s}^{k}\right] \approx \frac{d_{\mathrm{EL}}\cdot T_{c}^{2}}{4\cdot\mathrm{SNIR}_{s}^{k}}\left(1+\frac{2}{(2-d_{\mathrm{EL}})\cdot\mathrm{SNIR}_{s}^{k}}\right)} \tag{4.8}$$

Finally using equations (4.4) , (4.7) and (4.8), the value of the SNIR^{l} and consequently of the variance delay error can be determined recursively at each stage.

4.4.2 Limit and Convergence Properties (BPSK)

The sequence composed of the var $\left[C_{s+1}^l\right]$ will be now studied at the different stages.

$$\text{var}\left[C_1^l\right] = \frac{\mathcal{N}_0/2}{d \cdot T_i} + \sum_{\substack{k=1 \\ k \neq l}}^{K} \text{WCC}_{d \cdot T_i}(\tau^l - \tau^k) \cdot \mathcal{P}^k$$

$$\text{var}\left[C_{s+1}^l\right] = \frac{\mathcal{N}_0/2}{d \cdot T_i} + \sum_{\substack{k=1 \\ k \neq l}}^{K} \text{var}\left[C_s^k\right] \left(\text{WCC}_{d \cdot T_i}(\tau^l - \tau^k) + \text{var}\left[\hat{\tau}_s^k - \tau^k\right] \cdot \text{DWCC}_{d \cdot T_i}(\tau^l - \tau^k)\right)$$

Note that at the first stage, the interferences are proportional to the power of the interfering signals $\mathcal{P}^k$. At the next stages, the interferences are proportional to the error on the power estimations var $\left[C_s^k\right]$. Using results in the case of a BPSK signal from annexe A:

$$\frac{T_c}{2 \cdot d \cdot T_i} < \text{WCC}_{d \cdot T_i}(\tau^l - \tau^k)$$

$$\text{DWCC}_{d \cdot T_i}(\tau^l - \tau^k) = \frac{2}{d \cdot T_i \cdot T_c}$$

$\forall k$, $\left|\hat{\tau}_s^k - \tau^k\right| < {}^{T_c}/_4$ (cf. Approx. 4.7), then the variance can be bounded:

$$\text{var}\left[\hat{\tau}_s^k - \tau^k\right] \leq \left(\frac{T_c}{4}\right)^2$$

Consequently:

$$\text{var}\left[\hat{\tau}_s^k - \tau^k\right] \text{DWCC}_{d \cdot T_i}(\tau^l - \tau^k) < \frac{T_c}{32 \cdot d \cdot T_i} \ll \frac{T_c}{2 \cdot d \cdot T_i} < \text{WCC}_{d \cdot T_i}(\tau^l - \tau^k)$$

Therefore the term var $\left[\hat{\tau}_s^k - \tau^k\right] \cdot \text{DWCC}_{d \cdot T_i}(\tau^l - \tau^k)$ can be neglected in comparison to $\text{WCC}_{d \cdot T_i}(\tau^l - \tau^k)$.

Moreover, in order to simplify the computation, the worst case is considered, which consists in setting the relative delay between all signals as a multiple of T_c ($\forall (l,k)\ \tau^l - \tau^k = 0 \mod T_c$). Consequently the WCC can be factorized, leading to:

$$\text{var}\left[C_1^l\right] \approx \frac{\mathcal{N}_0/2}{d \cdot T_i} + \text{WCC}_{d \cdot T_i} \cdot \sum_{\substack{k=1 \\ k \neq l}}^{K} \mathcal{P}^k$$

$$\text{var}\left[C_{s+1}^l\right] \approx \frac{\mathcal{N}_0/2}{d \cdot T_i} + \text{WCC}_{d \cdot T_i} \cdot \sum_{\substack{k=1 \\ k \neq l}}^{K} \text{var}\left[C_s^k\right]$$

Where:

$$\text{WCC}_{d \cdot T_i} = \max_{\tau^l - \tau^k} \text{WCC}_{d \cdot T_i}(\tau^l - \tau^k)$$

For a BPSK signal, using equation (A.3), $\mathrm{WCC}_{d\cdot T_i} = \frac{T_c}{d\cdot T_i}$. At the second stage, the variance of the correlator output is:

$$\begin{aligned}
\mathrm{var}\left[C_2^l\right] &= \frac{\mathcal{N}_0/2}{d\cdot T_i} + \mathrm{WCC}_{d\cdot T_i}\cdot\sum_{\substack{k=1\\k\neq l}}^{K}\mathrm{var}\left[C_1^k\right] \\
&= \left(1+(K-1)\cdot\mathrm{WCC}_{d\cdot T_i}\right)\cdot\frac{\mathcal{N}_0/2}{d\cdot T_i} + \mathrm{WCC}_{d\cdot T_i}^2\cdot\sum_{\substack{k=1\\k\neq l}}^{K}\sum_{\substack{q=1\\q\neq k}}^{K}\mathcal{P}^q \\
&= \sum_{k=0}^{1}\left((K-1)\cdot\mathrm{WCC}_{d\cdot T_i}\right)^k\cdot\frac{\mathcal{N}_0/2}{d\cdot T_i} \\
&\quad + \mathrm{WCC}_{d\cdot T_i}^2\cdot\left((K-2)\cdot\sum_{k=1}^{K}\mathcal{P}^k + \mathcal{P}^l\right)
\end{aligned}$$

The term $(K-2)$ can be rewritten as:

$$K-2 = \frac{(K-1)^2-1}{K}$$

And consequently:

$$\begin{aligned}
\mathrm{var}\left[C_2^l\right] &= \sum_{k=0}^{1}\left((K-1)\cdot\mathrm{WCC}_{d\cdot T_i}\right)^k\cdot\frac{\mathcal{N}_0/2}{d\cdot T_i} \\
&\quad + \mathrm{WCC}_{d\cdot T_i}^2\cdot\left(\frac{(K-1)^2-1}{K}\cdot\sum_{k=1}^{K}\mathcal{P}^k + \mathcal{P}^l\right)
\end{aligned}$$

At the third stage, the variance of the correlator output is:

$$\begin{aligned}
\mathrm{var}\left[C_3^l\right] &= \frac{\mathcal{N}_0/2}{d\cdot T_i} + \mathrm{WCC}_{d\cdot T_i}\cdot\sum_{\substack{k=1\\k\neq l}}^{K}\mathrm{var}\left[C_2^k\right] \\
&= \sum_{k=0}^{2}\left((K-1)\cdot\mathrm{WCC}_{d\cdot T_i}\right)^k\cdot\frac{\mathcal{N}_0/2}{d\cdot T_i} \\
&\quad + \mathrm{WCC}_{d\cdot T_i}^3\cdot\sum_{\substack{k=1\\k\neq l}}^{K}\left((K-2)\cdot\sum_{q=1}^{K}\mathcal{P}^q + \mathcal{P}^k\right) \\
&= \sum_{k=0}^{2}\left((K-1)\cdot\mathrm{WCC}_{d\cdot T_i}\right)^k\cdot\frac{\mathcal{N}_0/2}{d\cdot T_i} \\
&\quad + \mathrm{WCC}_{d\cdot T_i}^3\cdot\left(((K-2)\cdot(K-1)+1)\cdot\sum_{q=1}^{K}\mathcal{P}^q - \mathcal{P}^l\right)
\end{aligned}$$

The term $((K-2)\cdot(K-1)+1)$ can be rewritten as:

$$(K-2)\cdot(K-1)+1 = \frac{(K-1)^3+1}{K}$$

Consequently:

$$\begin{aligned}\mathrm{var}\left[C_3^l\right] = \sum_{k=0}^{2}\left((K-1)\cdot \mathrm{WCC}_{d\cdot T_i}\right)^k \cdot \frac{\mathcal{N}_0/2}{d\cdot T_i} \\ + \mathrm{WCC}_{d\cdot T_i}^3 \cdot \left(\frac{(K-1)^3+1}{K}\cdot\sum_{q=1}^{K}\mathcal{P}^q - \mathcal{P}^l\right)\end{aligned}$$

Then at stage s, it can be conjectured that the variance is:

$$\begin{aligned}\mathrm{var}\left[C_s^l\right] &= \sum_{k=0}^{s-1}\left((K-1)\cdot \mathrm{WCC}_{d\cdot T_i}\right)^k \cdot \frac{\mathcal{N}_0/2}{d\cdot T_i} \\ &\quad + \mathrm{WCC}_{d\cdot T_i}^s \cdot \left(\frac{(K-1)^s-(-1)^s}{K}\cdot\sum_{q=1}^{K}\mathcal{P}^q + (-1)^s\cdot\mathcal{P}^l\right) \\ &= \frac{1-\left((K-1)\cdot \mathrm{WCC}_{d\cdot T_i}\right)^s}{1-(K-1)\cdot \mathrm{WCC}_{d\cdot T_i}} \cdot \frac{\mathcal{N}_0/2}{d\cdot T_i} \\ &\quad + \mathrm{WCC}_{d\cdot T_i}^s \cdot \left(\frac{(K-1)^s-(-1)^s}{K}\cdot\sum_{q=1}^{K}\mathcal{P}^q + (-1)^s\cdot\mathcal{P}^l\right)\end{aligned}$$

This relationship can be proved by induction: at stage 1 the relation is true. Let assume the relation true at stage s. Then at stage $s+1$:

$$\begin{aligned}\mathrm{var}\left[C_{s+1}^l\right] &= \frac{\mathcal{N}_0/2}{d\cdot T_i} + \mathrm{WCC}_{d\cdot T_i}\cdot\sum_{\substack{k=1\\k\neq l}}^{K}\mathrm{var}\left[C_s^k\right] \\ &= \left(1+(K-1)\mathrm{WCC}_{d\cdot T_i}\cdot\sum_{k=0}^{s-1}(K-1)\cdot\mathrm{WCC}_{d\cdot T_i}^k\right)\cdot\frac{\mathcal{N}_0/2}{d\cdot T_i} \\ &\quad + \mathrm{WCC}_{d\cdot T_i}^{s+1}\cdot\sum_{\substack{k=1\\k\neq l}}^{K}\left(\frac{(K-1)^s-(-1)^s}{K}\cdot\sum_{q=1}^{K}\mathcal{P}^q + (-1)^s\cdot\mathcal{P}^k\right) \\ &= \sum_{k=0}^{s}\left((K-1)\cdot\mathrm{WCC}_{d\cdot T_i}\right)^k\cdot\frac{\mathcal{N}_0/2}{d\cdot T_i} \\ &\quad + \mathrm{WCC}_{d\cdot T_i}^{s+1}\cdot\left(\frac{(K-1)^{s+1}-(-1)^{s+1}}{K}\cdot\sum_{q=1}^{K}\mathcal{P}^q + (-1)^{s+1}\cdot\mathcal{P}^l\right)\end{aligned}$$

Consequently, by mathematical induction, the relationship is true at all stages. Finally the SNIR of pseudolite l at stage s is:

$$\boxed{\begin{aligned}\mathrm{SNIR}_s^l = \Bigg[&\frac{1-\left((K-1)\cdot\mathrm{WCC}_{d\cdot T_i}\right)^s}{1-(K-1)\cdot\mathrm{WCC}_{d\cdot T_i}}\cdot\frac{\mathcal{N}_0/2}{\mathcal{P}^l\cdot d\cdot T_i} \\ &+\mathrm{WCC}_{d\cdot T_i}^{s+1}\cdot\left(\frac{(K-1)^{s+1}+(-1)^{s+1}}{K}\cdot\frac{\sum_{q=1}^{K}\mathcal{P}^q}{\mathcal{P}^l}+(-1)^{s+1}\right)\Bigg]^{-1}\end{aligned}} \quad (4.9)$$

The sequence of the SNIR_s^l converges and admits a limit SNIR_∞^l if:

$$\begin{aligned} & (K-1)\cdot \mathrm{WCC}_{d\cdot T_i} < 1 \\ \iff & K < \frac{1}{\mathrm{WCC}_{d\cdot T_i}} + 1 \\ \iff & K \leq \frac{1}{\mathrm{WCC}_{d\cdot T_i}} \end{aligned}$$

For a BPSK signal, $\mathrm{WCC}_{d\cdot T_i} = {T_c}/{d\cdot T_i}$ and consequently $K < {d\cdot Ti}/{T_c}$. Therefore convergence is achieved if the number of satellites is smaller than the number of chips per integration time. Assuming this condition fulfilled, the limit of the sequence becomes:

$$\boxed{\mathrm{SNIR}_\infty^l = (1-(K-1)\cdot \mathrm{WCC}_{d\cdot T_i}))\cdot \frac{\mathcal{P}^l \cdot d \cdot T_i}{\mathcal{N}_0/2}} \tag{4.10}$$

Note that this limit is independent on the power of the interfering signals. In chapter 3 as well, in case of unquantized signals, the CRLB does not depends on the power of the interfering signals (cf. equation (3.6)). The two results are consequently coherent. The PIC provides improvement of the SNIR if $\mathrm{SNIR}_\infty^l > \mathrm{SNIR}_0^l$. This condition yields to:

$$\begin{aligned} & \mathrm{SNIR}_\infty^l > \mathrm{SNIR}_0^l \\ \iff & (1-((K-1)\cdot \mathrm{WCC}_{d\cdot T_i})\cdot \frac{d\cdot T_i}{\mathcal{N}_0/2} > \frac{1}{\frac{\mathcal{N}_0/2}{d\cdot T_i} + \mathrm{WCC}_{d\cdot T_i}\cdot \sum_{\substack{k=1\\k\neq l}}^{K} \mathcal{P}^k} \\ \iff & \frac{\sum_{\substack{k=1\\k\neq l}}^{K} \mathcal{P}^k}{\mathcal{N}_0/2} > \frac{K-1}{d\cdot T_i\cdot (1-(K-1)\cdot \mathrm{WCC}_{d\cdot T_i})} \end{aligned}$$

Consequently if the received power of the interfering signals is too low compared to the noise power, the PIC degrades the SNIR and should not be applied.

4.4.3 Simulation Results

Figure 4.4 represents theoretical results using equation (4.7), simulation results and the CRLB using results from chapter 3, when the received power from each pseudolite is the same (here -130 dBW. It can be noticed that the results, both theoretical and simulated, tends to the CRLB. Consequently PIC is a good way to approach the CRLB. Figures 4.5 compares simulation, theoretical results and CRLB when the received power from each pseudolite is different. Again parallel interference cancellation provides a great improvement of the standard deviation. But it also shows that the CRLB is not reached for the smallest received powers

4.5 Sequential Interference Cancellation

In this section, a SIC will be analyzed. At stage $s+1$, s navigation signals have been cancelled. It is considered that pseudolite one is tracked and estimated at stage one and cancelled at stage two, pseudolite two tracked and estimated at stage two and cancelled at stage three and so on, as depicted on figure 4.2

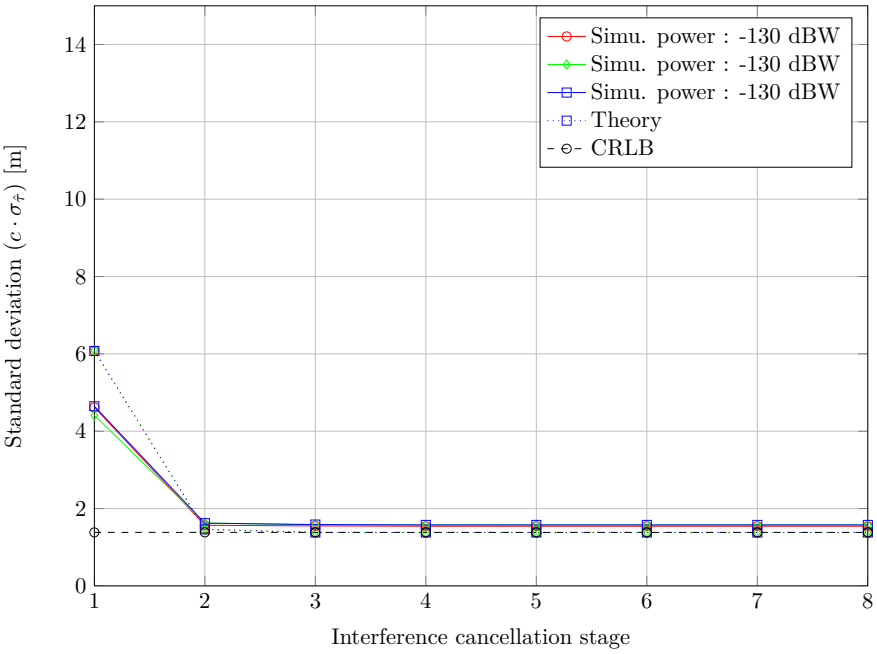

Figure 4.4: PIC, 20% duty cycle and same powers

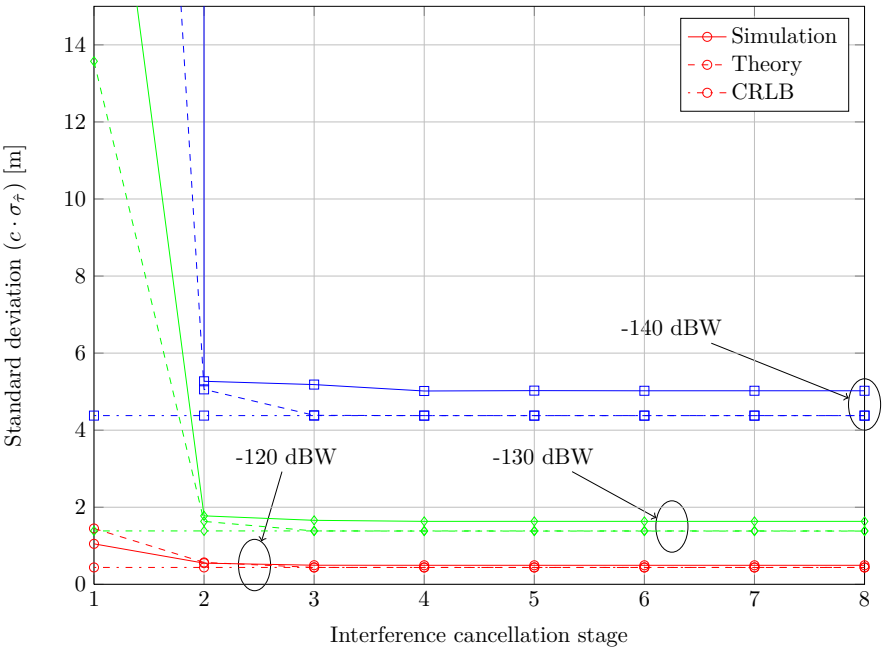

Figure 4.5: PIC, 20% duty cycle and different powers

4.5.1 Signal to Noise plus Interferences Ratio

Pseudolite l is tracked at stage $l = s + 1$. Then pseudolites from 1 to $s = l - 1$ have been canceled. To improve the readability, when the lower index equals the upper ones (estimation is done at the stage corresponding to the pseudolite number), the lower index is not written. Consequently the correlator output is:

$$r^l(t) = \eta(t) + \sqrt{\mathcal{P}^l} \cdot c^l(t - \tau^l) + \sum_{k=1}^{l-1} \left(\sqrt{\mathcal{P}^k} \cdot c^k(t - \tau^k) - \sqrt{\hat{\mathcal{P}}^k} \cdot c^k(t - \hat{\tau}^k) \right) + \sum_{k=l+1}^{K} \sqrt{\mathcal{P}^k} \cdot c^k(t - \tau^k)$$

Then the correlator output for pseudolite l, at stage l is:

$$\begin{aligned} C^l &= \frac{1}{d \cdot T_i} \cdot \int_0^{d \cdot T_i} r^l(t) \cdot c^l(t - \hat{\tau}^l) \, \mathrm{d}t \\ &= A^l + \mathcal{W}^l + \sum_{k=l+1}^{K} I_1^k + \sum_{k=1}^{l-1} J^k \end{aligned}$$

- A^l represents the useful part of the signal. It is considered that $\hat{\tau}^l \approx \tau^l$, then:

$$\begin{aligned} A^l &= \frac{\sqrt{\mathcal{P}^l}}{d \cdot T_i} \cdot \int_0^{d \cdot T_i} c^l(t - \tau^l) \cdot c^l(t - \hat{\tau}^l) \, \mathrm{d}t \\ &\approx \sqrt{\mathcal{P}^l} \end{aligned}$$

  Then:

$$\begin{aligned} \mathcal{E}\left[A^l\right] &\approx \sqrt{\mathcal{P}^l} \\ \mathrm{var}\left[A^l\right] &\approx 0 \end{aligned}$$

- $\mathcal{W}_l^l$ represents the AWGN process:

$$\mathcal{W}^l = \frac{\sqrt{\mathcal{P}^l}}{d \cdot T_i} \cdot \int_0^{d \cdot T_i} \eta(t) \cdot c^l(t - \hat{\tau}^l) \, \mathrm{d}t$$

  Then:

$$\begin{aligned} \mathcal{E}\left[\mathcal{W}^l\right] &= 0 \\ \mathrm{var}\left[\mathcal{W}^l\right] &= \frac{\mathcal{N}_0/2}{d \cdot T_i} \end{aligned}$$

- I_1^k represents the MAI from the k^{th} navigation signal before interference cancellation (pseudolite navigation signals that have not been cancelled yet)

$$I_1^k = \frac{\sqrt{\mathcal{P}^k}}{d \cdot T_i} \cdot \int_0^{d \cdot T_i} c^k(t - \tau^k) \cdot c^l(t - \hat{\tau}_0^l) \, \mathrm{d}t$$

Then:

$$\mathcal{E}\left[I_1^k\right] = 0$$

Because $\hat{\tau}_0^l \approx \tau^l$, using equation (4.1)

$$\text{var}\left[I_1^k\right] \approx \text{WCC}_{d\cdot T_i}(\tau^l - \tau^k) \cdot \mathcal{P}^k$$

- J^k represents the residual MAI from the k^{th} pseudolite from stage k (pseudolite signals that have been cancelled):

$$J^k = \frac{\sqrt{\mathcal{P}^l}}{d \cdot T_i} \cdot \int_0^{d\cdot T_i} \left(\sqrt{\mathcal{P}^k} \cdot c^k(t - \tau^k) - \sqrt{\hat{\mathcal{P}}^k} \cdot c^k(t - \hat{\tau}^k)\right) \cdot c^l(t - \hat{\tau}^l)\,\mathrm{d}t$$

Then:

$$\mathcal{E}\left[J^k\right] = 0$$

Using equation (4.6):

$$\text{var}\left[J^k\right] \approx \frac{\mathcal{P}^k}{\text{SNIR}^k} \cdot (\text{WCC}_{d\cdot T_i}(\tau^l - \tau^k) + \text{var}\left[\hat{\tau}^k - \tau^k\right] \cdot \text{DWCC}_{d\cdot T_i}(\tau^l - \tau^k))$$

Then the expectation and the variance of the correlator output are:

$$\begin{aligned}
\mathcal{E}\left[C^l\right] &\approx \sqrt{\mathcal{P}^l} \\
\text{var}\left[C^l\right] &\approx \frac{\mathcal{N}_0/2}{d \cdot T_i} \\
&\quad + \sum_{k=1}^{l-1} \frac{\mathcal{P}^k}{\text{SNIR}^k} \cdot \big(\text{WCC}_{d\cdot T_i}(\tau^l - \tau^k) \\
&\quad + \big(\text{var}\left[\hat{\tau}^k - \tau^k\right] \cdot \text{DWCC}_{d\cdot T_i}(\tau^l - \tau^k)\big) \\
&\quad + \sum_{k=l+1}^{K} \text{WCC}_{d\cdot T_i}(\tau^l - \tau^k) \cdot \mathcal{P}^k
\end{aligned}$$

Then the SNIR can be determined recursively using:

$$\text{SNIR}^l = \frac{\mathcal{E}\left[C^l\right]^2}{\text{var}\left[C^l\right]}$$

4.5.2 Simulation Results

Figure 4.6 compares simulation results, theoretical results and the CRLB using chapter 3 when the received power from each peudolite is the same. Figure 4.7 provides the same comparison when pseudolites are at different distances from the receiver.

At stage one, no signals is canceled, therefore it corresponds to the case without interference cancellation. At stage two, signal 1 is canceled. Then the standard deviation of signals 2 and 3 is improved. Finally, at stage three, signal 2 is canceled. Then the standard deviation of signal 3 is improved.

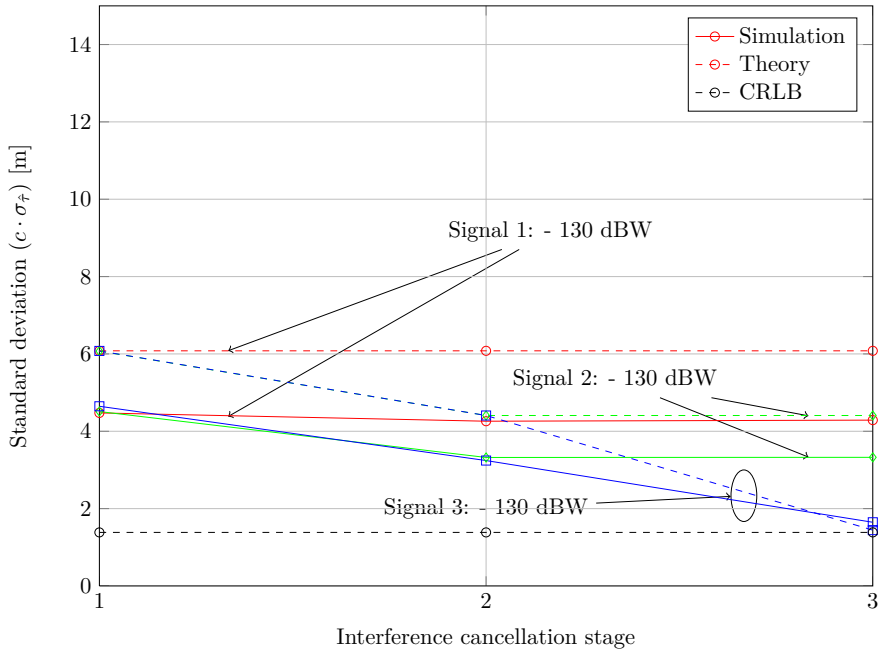

Figure 4.6: Sequential Interference Cancellation with 20 % duty cycle and same powers

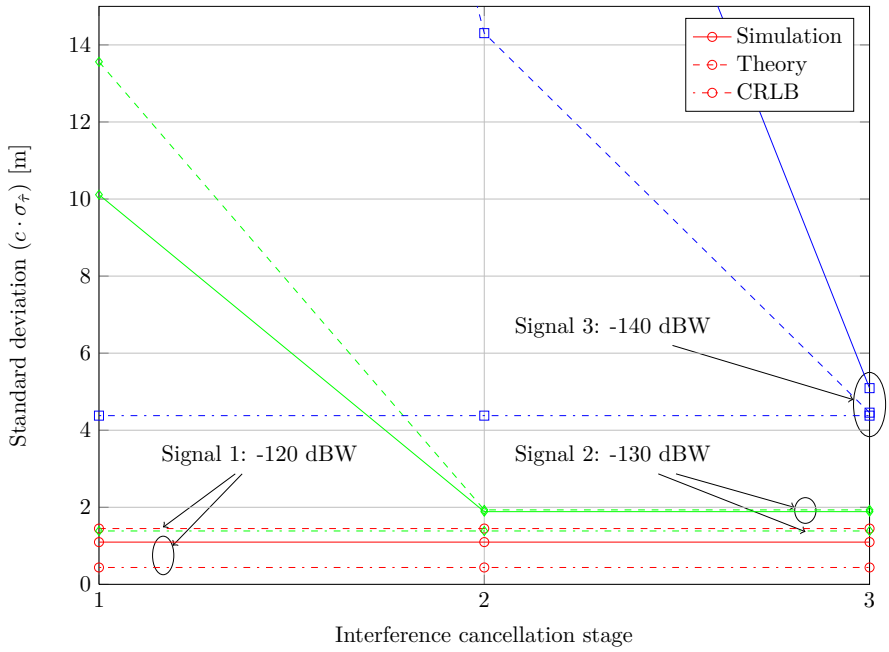

Figure 4.7: Sequential Interference Cancellation with 20 % duty cycle and different powers

4.6 Conclusion

PIC provides the best results: it reaches the lowest standard deviation and converges more rapidly. However, PIC is more complex to implement than SIC and needs more computation time. Moreover, PIC provides better performance compared to SIC when all the strong signals have similar power levels.

Both methods of interference cancellation improve the SNIR, and consequently the tracking results. Consequently the Near-Far problem between the pseudolites can be reduced. In the next chapter, experimental measurements are presented and interference cancellation is applied to real pseudolite signals. Only PIC is implemented, since it leads to the best tracking performance.

Chapter 5

Experimental Measurements

5.1 Presentation of the Experimentation

Experimental tests have been executed at the Astrium laboratory. Three pseudolite signals are considered, generated by three Navigation Signal Generators (NSGs). Figure 5.1 shows the experimental set-up and figure 5.2 a photo of the experimentation. The objectives are:

- To verify that application of interference cancellation improves performance of pseudolite acquisition and tracking for overlapping/synchronised pulses
- To verify that tracking of GPS signals is improved for overlapping and synchronised pulses

5.1.1 Pseudolites Pulses

The pseudolite signal properties are defined in the Radio Technical Commission for Maritime Services (RTCM) SC-104 specification (cf. [13]). A pseudolite employs one of the 51 non-GPS, 1023 chips, Gold codes. The signal is transmitted by pulses of 90.91 μs (or 93 chips, one-eleventh of a code). There are 11 pulses per 10 ms interval. In case of synchronized overlapping pulses, the pseudolite signals will interfere with the GPS signals during an average of $^{11 \cdot 90.91 \mu s}/_{10 \text{ms}} = 10\%$ of the time. In case of synchronized non overlapping pulses, the pseudolite signals will interfere during $k \cdot 10\%$ of the time, where k is the number of pseudolites. Moreover the pulse position is changed from millisecond to millisecond, both to randomize the spectrum and to assure that one complete code sequence is transmitted every 10 ms. All pulses change from one interval of 10 ms to the next, over a 200 ms interval, so that all pulse positions have been transmitted after 200 ms. In case of non-overlapping pulses, a shifted RTCM pattern will be used (each pseudolite has a different RTCM pattern). On the contrary, in case of overlapping pulses, the same RTCM pattern will be used for all pseudolites. In both cases, the NSGs have to be synchronized.

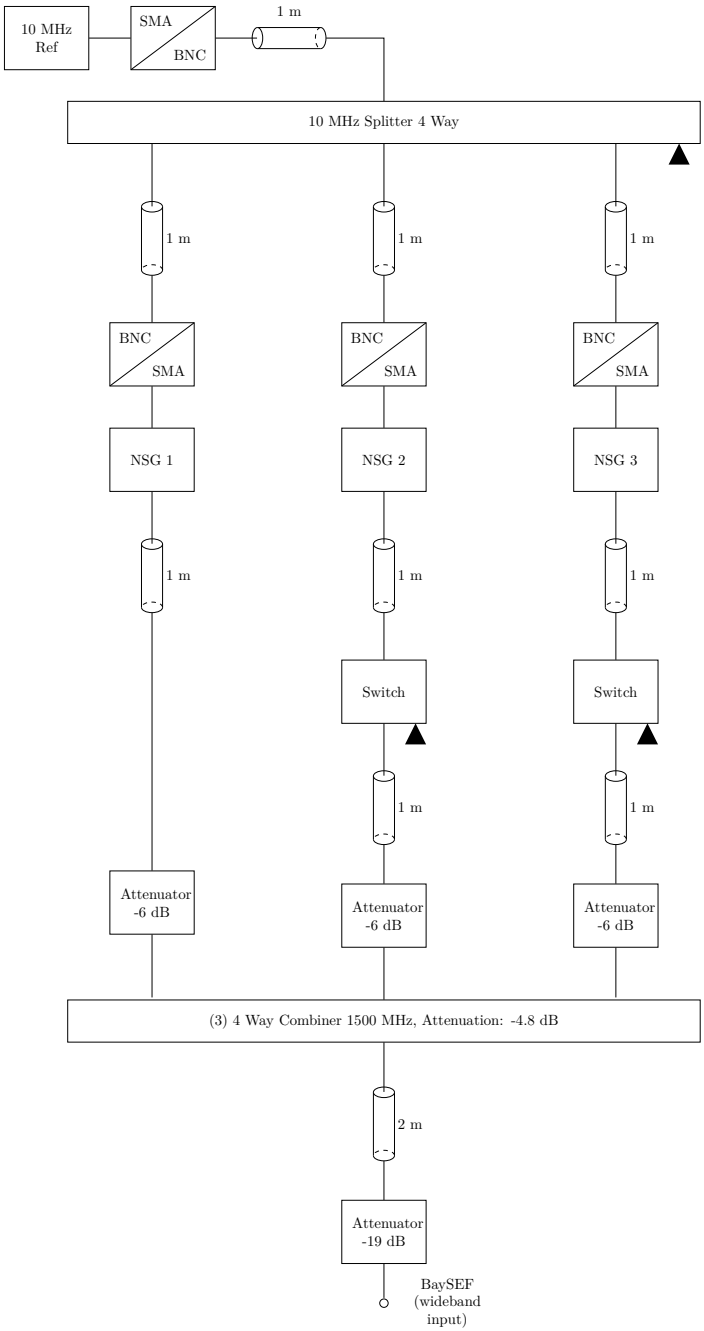

Figure 5.1: Schema of the experimentation

Figure 5.2: Photo of the experimentation. The BaySEF is on the right, the three NSGs are in the bottom left corner.

However the pulses will never be perfectly synchronized, firstly because of errors in the hardware synchronization, secondly because the pseudolites will not be at the same distance from the receiver. If the distance between two pseudolites is $d = 2$ m, then the synchronization error is:

$$\frac{d}{c} = \frac{2}{3 \cdot 10^8} \approx 6.6 \text{ ns} \approx \frac{1}{150} \text{ chips}$$

Consequently in our experiment, the pulses overlap well and the synchronization error is negligible. But it will not be the case in reality, since the distance between the pseudolites can be several kilometers. Note that the PPP represents the instantaneous transmitted power by the pseudolite during the pulse. Consequently, since the duty cycle is 10%, a PPP of -110 dBm corresponds to an average power of -120 dBm for a continuous signal.

5.1.2 Acquisition and Tracking

The input signal is acquired by the BaySEF. At the BaySEF output, the signal has been down-converted, low-pass filtered, normalised, sampled and quantized. The sampling frequency is 57.2 MHz and the signal is quantized with 8 bits. A slow AGC is used to normalize the signal.

Then the signal is post-processed by software receiver, written in Matlab, based on [14]).

Both satellite and pseudolite signals are tracked. But because of the pseudolite pulses, if nothing is done, the acquisition and tracking of the satellite signals is degraded, or even impossible for large PPPs. The main problem is that the pseudolite pulses can be much stronger than the noise and the satellite signals. Then the correlation peak between the received signal and the satellite code replica is "hidden" by interfering peaks. Fortunately different solutions exist

to reduce these interferences and enable a better tracking of the GPS signals (cf. [15]):

- Clear the pseudolite pulses by using either a blanker or interference cancellation. These two solutions are adapted when a slow AGC is used. If the AGC is fast, the pulses are at the same level than the noise, and are consequently difficult to blank or to cancel. Interference cancellation is probably not a good solution since the remaining part of the pseudolite signals after interference cancellation can still interfere too much with the satellite signals.

- Put the pseudolite pulses at the same level than the rest of the signal by using either a fast AGC or a 1-bit quantizer (case of the low-cost receivers, cf. chapter 2).

In case of non-participative receivers, complexity and cost have to be reduced, and the second solution might be preferred (fast AGC or 1-bit quantizer). In case of participative receivers, higher complexity and cost can be afforded, and the first solution might be preferred (interference cancellation, blanker).

The BaySEF includes a slow AGC. In the Matlab tool, a blanker is used. Then when a GPS signal is tracked, the pseudolite pulses are cleared by the blanker.

Moreover pseudolite signals acquisition and tracking can also be degraded by the noise. Consequently, when a pseudolite signal is tracked, a blanker is also used to clear intervals without pulses.

Different scenarios have been tested, in order to see the effects of the interference cancellation and of the pulse scheme synchronisation. The NSGs use PRNs which are not used by visible satellites. In the experiment, NSG 1 corresponds to PRN1, NSG 2 to PRN 2 and NSG 3 to PRN 3.

5.2 Interference Cancellation

Parallel Interference Cancellation between the pseudolites is used to improve acquisition and tracking of the navigation signals:

- Acquisition Phase:
  - Step 1: Try to acquire the pseudolite navigation signals
  - Step 2: For all acquired signals, estimate the phase, delay and received power
  - Step 3: Reconstruct and subtract pseudolite signals to the input signal
  - Step 4: Go back to step 1 or stop if the loop has been iterated a sufficient number of times.

- Tracking Phase
  - At each integration time, estimate the phase, delay and received power of each pseudolite signal
  - Apply interference cancellation to the same signal a specified number of times (can be zero).

– Go to next integration time, and apply interference cancellation.

Two different scenarios have been tested, where the received power from one pseudolite is varying.

The Received PPP from each NSG is the Same (-52 dBm):

Figures 5.3 and 5.4 compare the acquisition results without and with PIC. The acquisition metric is the ratio of the two biggest correlation peaks between input signal and local replica. Navigation signals are considered acquired if the acquisition metric exceeds a threshold. The acquisition metrics is higher when using PIC, consequently PIC improves acquisition performances.

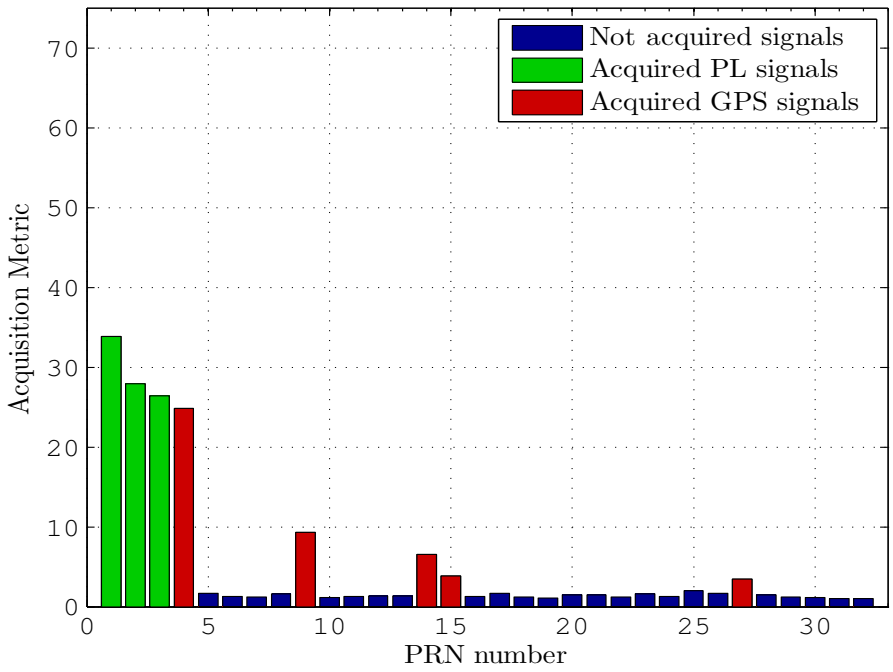

Figure 5.3: Acquisition results without PIC, same received PPP, overlapping pulses

Figures 5.5 and 5.6 compare the tracking results without and with PIC. The Real part of prompt correlation is the result of the correlation between prompt replica and in-phase signal, normalized by the number of samples contained in one integration time. Since the signal is quantized, the result of the prompt correlation is also quantized. A pseudolite transmits 11 times per interval of 10 ms. Therefore 10% of the integration time holds two pulses. The remaining 90% holds only one pulse and the correlation result is consequently twice lower. This is why there are peaks on the curves. By comparing the two figures, it is noticeable that using PIC, the frequency error and position error have a lower variance and that the the real part of prompt correlation is bigger. Consequently the tracking performance is improved by PIC.

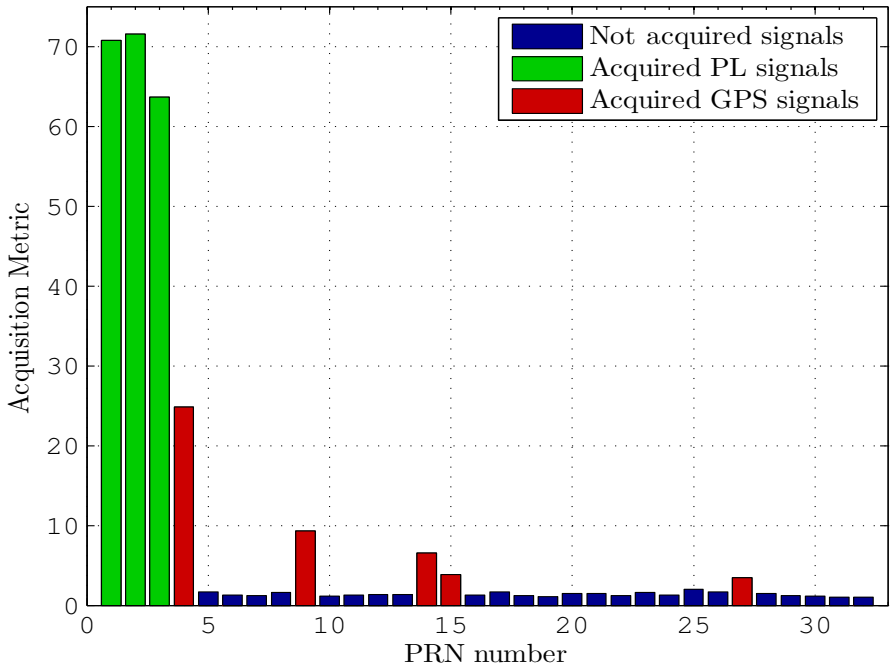

Figure 5.4: Acquisition results with PIC, same received PPP, overlapping pulses

The Received PPP from NSGs 2 and 3 Stays the Same (-52 dBm), and the Received PPP from NSG 1 is 10 dB Lower (-62 dBm):

Acquisition results without PIC are plotted in figure 5.7 and with PIC in figure 5.8. Tracking results without PIC are plotted in figure 5.9 and with PIC in figure 5.10. It can be noticed that again PIC improves acquisition and tracking performance and provides an even better improvement than in the previous case (same received powers).

5.3 Comparison Between Overlapping and Non-Overlapping Pulses

In both cases, the NSG are synchronized. In case of overlapping pulses, the same RTCM pulse scheme is used. On the contrary, in case of non-overlapping pulses, shifted RTCM pulse schemes are used. The aim is to compare tracking performance of GPS signals between the two pulse schemes. In both experiments, the received PPP is the same for all pseudolites (-52 dBm). A satellite signal is tracked (PRN 4). Tracking results in case of overlapping pulses are plotted in figure 5.11 and in case of non-overlapping pulses in figure 5.12.

By comparing the two figures, it is noticeable that overlapping pulses provide better performance than non-overlapping pulses. Indeed frequency error and position error have a lower variance and the average power is bigger. This is not surprising, since the available duty cycle in case of overlapping pulses is 90%, whereas only 70% is available in case of non overlapping pulses.

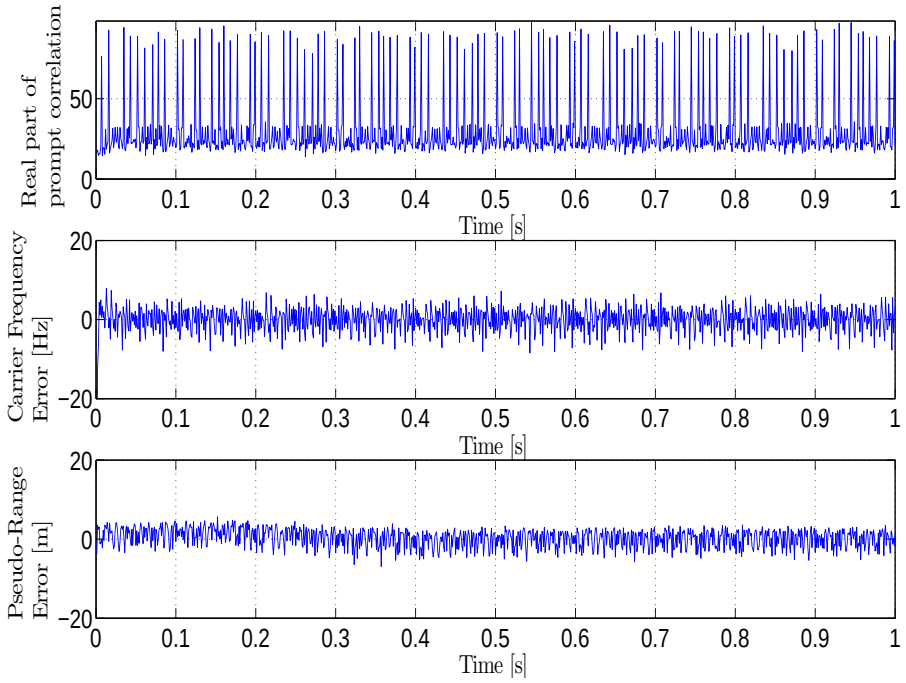

Figure 5.5: Tracking results for NSG 1, without PIC , same received PPP, overlapping pulses

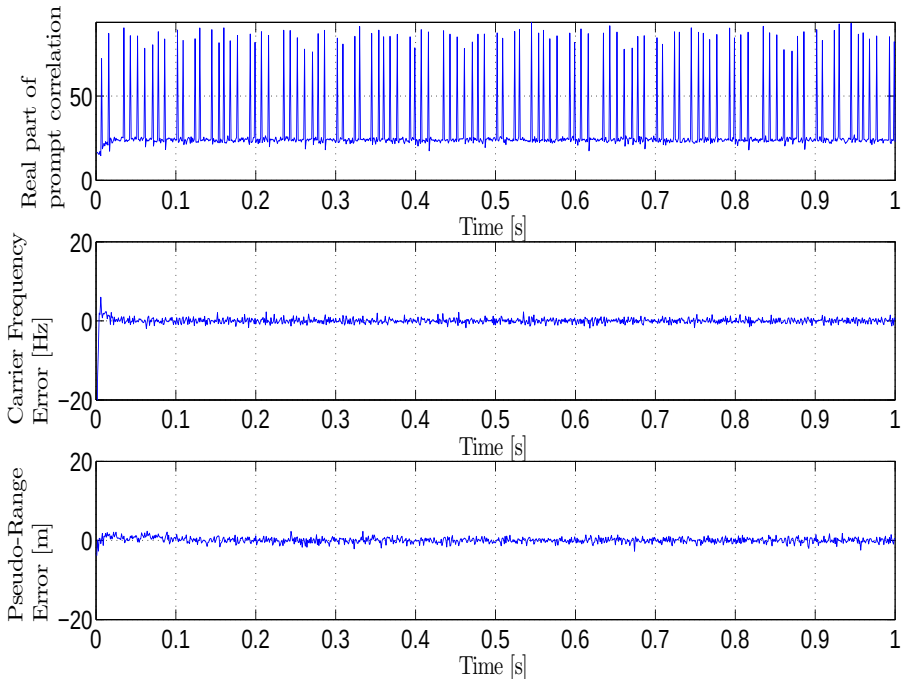

Figure 5.6: Tracking results for NSG 1, with PIC, same received PPP, overlapping pulses

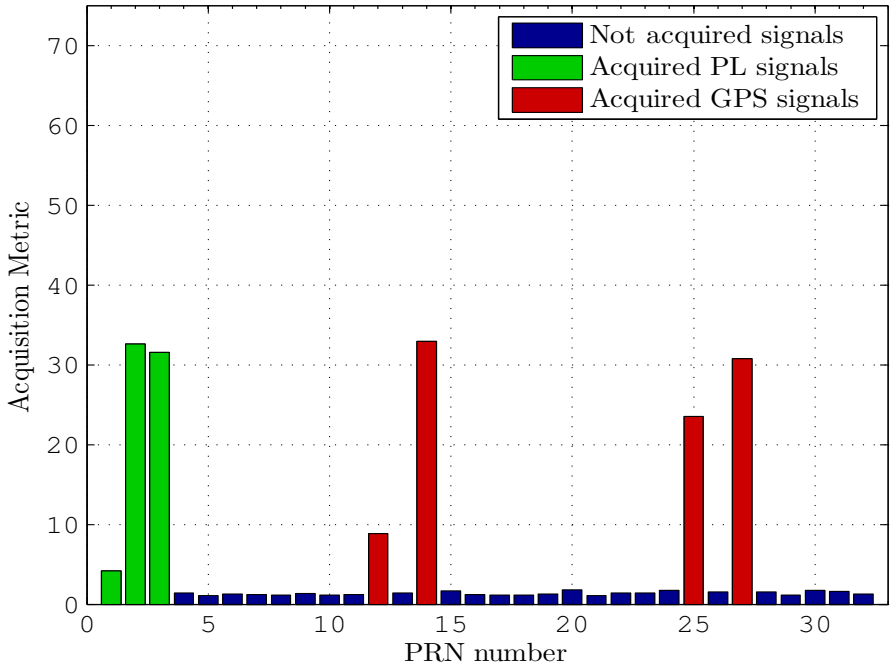

Figure 5.7: Acquisition results without PIC, received PPP from NSG 1 is 10 dB lower, overlapping pulses

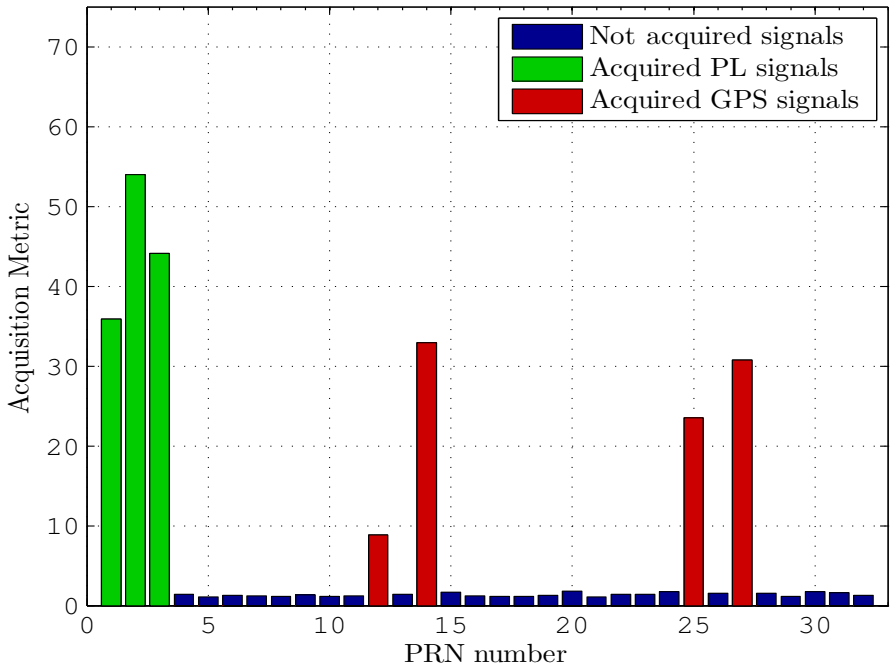

Figure 5.8: Acquisition results with PIC, received PPP from NSG 1 is 10 dB lower, overlapping pulses

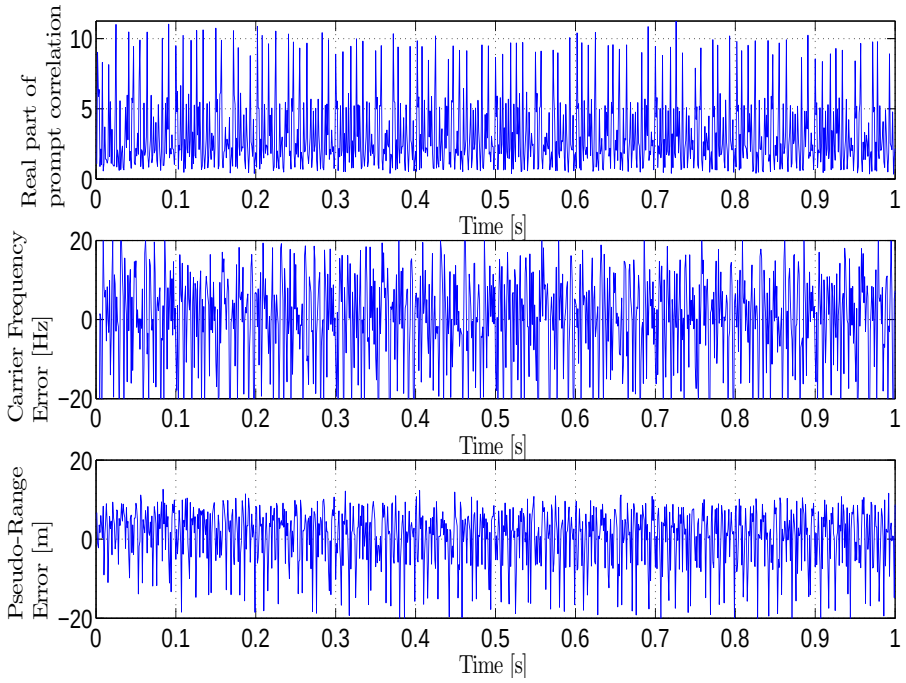

Figure 5.9: Tracking results for NSG 1, without PIC, received PPP from NSG 1 is 10 dB lower, overlapping pulses

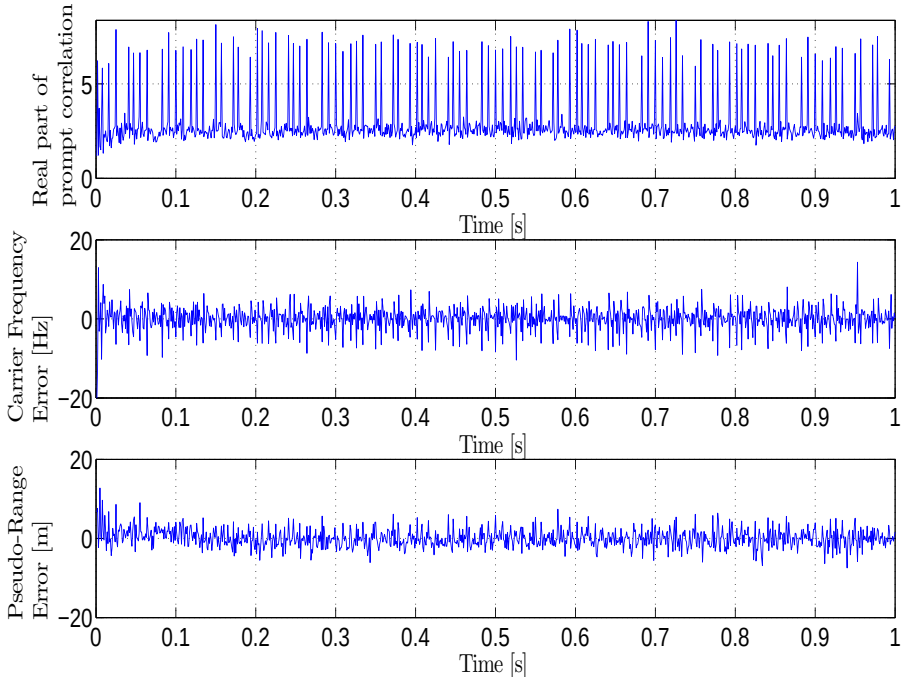

Figure 5.10: Tracking results for NSG 1, with PIC, received PPP from NSG 1 is 10 dB lower, overlapping pulses

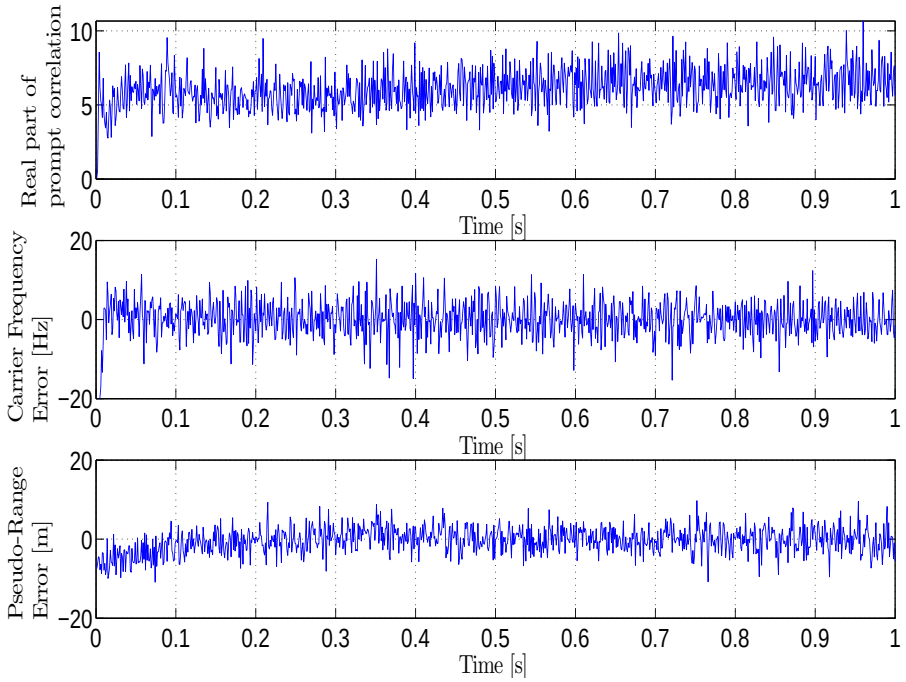

Figure 5.11: Tracking results for a GPS signal (PRN 4), same received PPP, overlapping pulses

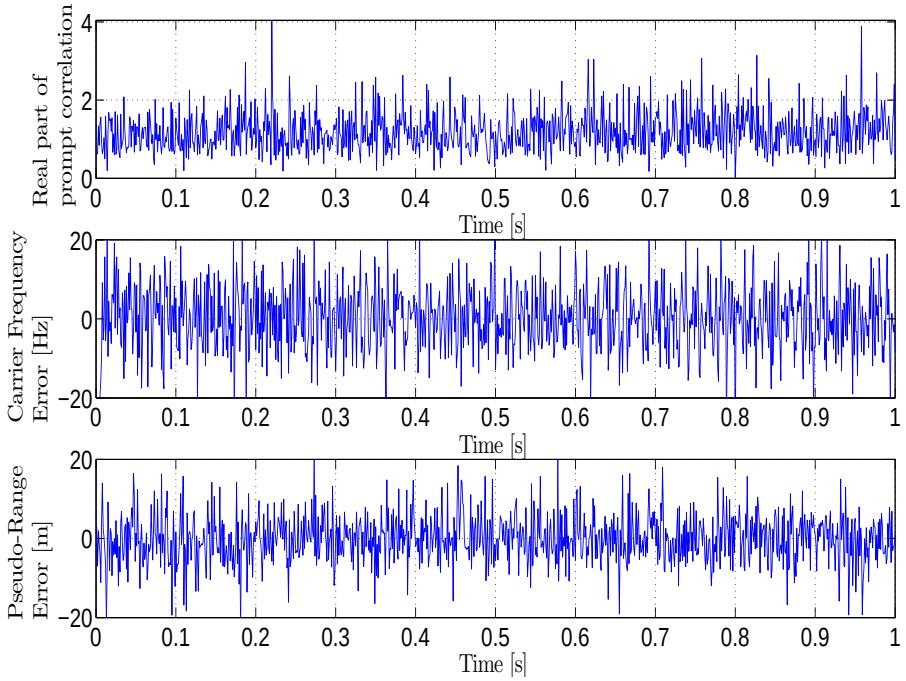

Figure 5.12: Tracking results for a GPS signal (PRN 4), same received PPP, non overlapping pulses

Chapter 6

Conclusion and Future Work

6.1 Conclusion

Throughout this thesis, it has been shown theoretically, by simulation and by experimental measurements that it is possible for non-participative receivers to track the satellite signals (if a sufficient part of the duty cycle is left free of pulses) while a participative receiver can track the pseudolite signals. Indeed, in chapter 2, it has been shown that if a sufficient part of the duty cycle is left free of pseudolite pulses, low-cost non-participative receivers can track satellite without technological modifications. Then it has been shown in chapter 3 that in terms of CRLB, overlapping pulses provide a lower propagation delay error than non-overlapping pulses. Finally, in chapter 4, a real architecture of the participative receiver is presented, and it has been shown that interference cancellation can be used to reduce interferences between the pseudolites and to approach the CRLB. Finally in chapter 5, experimental measurements are presented, and it is shown that interference cancellation improves tracking performance.

6.2 Future Work

6.2.1 Modulation Waveform

In some derivations in chapter 3, in annexe A and for all simulations, only the BPSK modulation has been considered. It could be interesting to extend the derivations and the simulations to others waveforms (i.e Binary Offset Carrier (BOC)).

6.2.2 Quantization

The derivations and the simulations concerning interference cancellation (cf. chapter 4) do not take into account the quantization losses. It is probably not possible to extend the derivations, but simulations could be done in order to analyze the effect of quantization on the interference cancellation.

6.2.3 Phase Estimation

In the proposed work, the phase estimation has been considered perfect. This is not the case in reality. Then the computations and simulations could be extended by considering it.

6.2.4 Locked Loop

The tracking simulations from chapter 4 are done in open loop and could also be extended to the locked loop case.

6.2.5 Sequential Interference Cancellation

Only PIC has been tested experimentally. Sequential Interference Cancellation could also be tested implemented, in order to compare the tracking performance and computation time.

Appendix A

Waveform Convolution Coefficients And Multiple Access Interference

The aim of this chapter is to derive different coefficients that are used in chapters 3 and 4.

A.1 Waveform Convolution Coefficient and Multiple Access Interference

The Waveform Convolution Coefficient (WCC) is defined as:

$$\mathrm{WCC}_T(\tau^l - \tau^k) = \mathrm{var}\left[\frac{1}{T} \cdot \int_0^T c^k(t-\tau^k) \cdot c^l(t-\tau^l)\,\mathrm{d}t\right]$$

The term $\mathcal{X}_T^{l,k}$ represents the Multiple Access Interference (MAI):

$$\mathcal{X}_T^{l,k} = \int_0^T c^k(t-\tau^k) \cdot c^l(t-\tau^l)\,\mathrm{d}t$$

The sequences $c^k(.)$ and $c^l(.)$ are independent. Then by taking the expectation with respect to the chip sequences:

$$\mathcal{E}\left[\mathcal{X}_T^{l,k}\right] = 0$$

A.1.1 General Case

$\mathcal{X}_T^{l,k}$ can be developed by using definition of the spreading code signals:

$$c^l(t) = \sum_{n=-\infty}^{+\infty} c_n^l \cdot p(t - nT_c)$$

$$c^k(t) = \sum_{m=-\infty}^{+\infty} c_m^k \cdot p(t - mT_c)$$

Then it follows:

$$\mathcal{X}_T^{l,k} = \sum_{n=-\infty}^{+\infty} \sum_{m=-\infty}^{+\infty} c_n^l \cdot c_m^k \cdot \int_0^T p(t - nT_c - \tau^l) \cdot p(t - mT_c - \tau^k)\,\mathrm{d}t$$

Integrating the product of the two waveforms over $[0\,;T]$ is the same as integrating the waveforms over $]-\infty\,;+\infty[$ when one is null outside the interval $[0\,;T]$ (cf. figure A.1). Let consider that $p(t - nT_c - \tau^l)$ is null outside $[0\,;T]$. Then $n \in \left[-\tau^l/T_c\,;T-\tau^l/T_c - 1\right]$. If $\tau^l = 0 \mod T_c$, the result is exact. If not, this is an approximation. But since there is a large number of chips per integration interval, the error is small. Let $\tilde{\tau}^l = \mathrm{round}(\tau^l/T_c)$. Then:

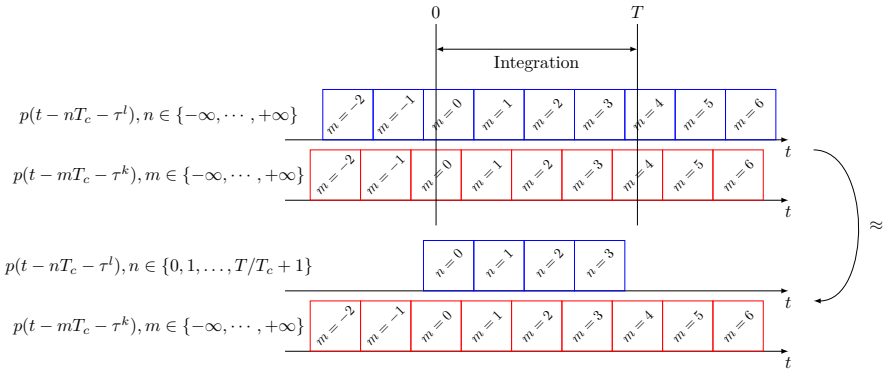

Figure A.1: Interval where the waveform is non-null

$$\begin{aligned}\mathcal{X}_T^{l,k} &\approx \sum_{n=-\tilde{\tau}^l}^{T/T_c-\tilde{\tau}^l-1} \sum_{m=-\infty}^{+\infty} c_n^l \cdot c_m^k \cdot \int_{-\infty}^{+\infty} p(t - nT_c - \tau^l) \cdot p(t - mT_c - \tau^k)\,\mathrm{d}t \\ &\approx \sum_{n=0}^{T/T_c-1} \sum_{m=-\infty}^{+\infty} c_{n+\tilde{\tau}^l}^l \cdot c_{m+\tilde{\tau}^l}^k \cdot \int_{-\infty}^{+\infty} p(t - nT_c - \tau^l) \cdot p(t - mT_c - \tau^k)\,\mathrm{d}t\end{aligned}$$

Finally, since the codes are random:

$$\mathcal{X}_T^{l,k} \approx \sum_{n=0}^{T/T_c-1} \sum_{m=-\infty}^{+\infty} c_n^l \cdot c_m^k \cdot \int_{-\infty}^{+\infty} p(t - nT_c - \tau^l) \cdot p(t - mT_c - \tau^k)\,\mathrm{d}t$$

Using the Parseval identity, the MAI becomes:

$$\mathcal{X}_T^{l,k} \approx \sum_{n=0}^{T/T_c-1} \sum_{m=-\infty}^{+\infty} c_n^l \cdot c_m^k \cdot \int_{-\infty}^{+\infty} |P(f)|^2 \cdot e^{j2\pi f(\tau^l - \tau^k + T_c \cdot (n-m))}\,\mathrm{d}f$$

Since the waveform $p(.)$ is real, the module of its Fourier transform $P(.)$ is even. Consequently:

$$\boxed{\begin{aligned}\mathcal{X}_T^{l,k} \approx \sum_{n=0}^{T/T_c-1} \sum_{m=-\infty}^{+\infty} & c_n^l \cdot c_m^k \\ & \cdot \int_{-\infty}^{+\infty} |P(f)|^2 \cdot \cos\left(2\pi f(\tau^l - \tau^k + T_c \cdot (n-m))\right)\mathrm{d}f\end{aligned}} \quad (A.1)$$

When variance and expectation are taken with respect to to the random spreading sequences, the variance is:

$$\begin{aligned}
\operatorname{var}\left[\mathcal{X}_T^{l,k}\right] &= \mathcal{E}\left[\mathcal{X}_T^{l,k\,2}\right] - \mathcal{E}\left[\mathcal{X}_T^{l,k}\right]^2 \\
&= \mathcal{E}\left[\mathcal{X}_T^{l,k\,2}\right] \\
&= \sum_{n=0}^{T/T_c-1} \sum_{m=-\infty}^{+\infty} \sum_{\tilde{n}=0}^{T/T_c-1} \sum_{\tilde{m}=-\infty}^{+\infty} \mathcal{E}\left[c_n^l c_m^k c_{\tilde{n}}^l c_{\tilde{m}}^k\right] \\
&\quad \cdot \int_{-\infty}^{+\infty} |P(f)|^2 \cdot \cos\left(2\pi f(\tau^l - \tau^k + T_c \cdot (n-m))\right) \mathrm{d}f \\
&\quad \cdot \int_{-\infty}^{+\infty} |P(f)|^2 \cdot \cos\left(2\pi f(\tau^l - \tau^k + T_c \cdot (\tilde{n}-\tilde{m}))\right) \mathrm{d}f
\end{aligned}$$

Since $\mathcal{E}\left[c_n^l c_m^k c_{\tilde{n}}^l c_{\tilde{m}}^k\right] = 0$ if $n \neq \tilde{n}$ or $m \neq \tilde{m}$ and $\mathcal{E}\left[c_n^l c_m^k c_{\tilde{n}}^l c_{\tilde{m}}^k\right] = 1$ if $n = \tilde{n}$ and $m = \tilde{m}$, finally:

$$\begin{aligned}
\mathrm{WCC}_T(\tau^l - \tau^k) = \frac{1}{T^2} \cdot \sum_{n=0}^{T/T_c-1} \sum_{m=-\infty}^{+\infty} \\
\left(\int_{-\infty}^{+\infty} |P(f)|^2 \cdot \cos\left(2\pi f(\tau^l - \tau^k + T_c \cdot (n-m))\right) \mathrm{d}f \right)^2
\end{aligned} \tag{A.2}$$

A.1.2 BPSK Case

The case of a BPSK signal will be now analysed. The effect of the low-pass filter will be neglected. The chip modulation waveform is:

$$p(t) = \begin{cases} 1 & \text{if } -\frac{T_c}{2} < t < \frac{T_c}{2} \\ 0 & \text{otherwise} \end{cases}$$

Then the Fourier transform is:

$$P(f) = T_c \cdot \operatorname{sinc}(\pi f T_c)$$

With the function $\operatorname{sinc}(.)$ defined as:

$$\operatorname{sinc}(x) = \frac{\sin(x)}{x}$$

Let $\delta = \tau^l - \tau^k + T_c \cdot (n - m)$. Then it follows:

$$\begin{aligned}
&\int_{-\infty}^{+\infty} |P(f)|^2 \cdot \cos(2\pi f \delta)\,\mathrm{d}f \\
&= \frac{1}{\pi^2} \cdot \int_{-\infty}^{+\infty} \frac{1}{f^2} \cdot \sin^2(\pi f T_c) \cdot \cos(2\pi f \delta)\,\mathrm{d}f \\
&= \frac{1}{2\pi^2} \cdot \int_{-\infty}^{+\infty} \frac{1}{f^2} \cdot (1 - \cos(2\pi f T_c)) \cdot \cos(2\pi f \delta)\,\mathrm{d}f \\
&= \frac{1}{2\pi^2} \cdot \int_{-\infty}^{+\infty} \frac{\cos(2\pi f \delta)}{f^2}\,\mathrm{d}f - \frac{1}{4\pi^2} \cdot \int_{-\infty}^{+\infty} \frac{\cos(2\pi f(\delta - T_c))}{f^2}\,\mathrm{d}f \\
&\quad - \frac{1}{4\pi^2} \cdot \int_{-\infty}^{+\infty} \frac{\cos(2\pi f(\delta + T_c))}{f^2}\,\mathrm{d}f
\end{aligned}$$

Then by variable substitution:

$$\int_{-\infty}^{+\infty} \frac{\cos(2\pi f \delta)}{f^2}\,\mathrm{d}f = 2\pi \cdot |\delta| \cdot \int_{-\infty}^{+\infty} \frac{\cos(x)}{x^2}\,\mathrm{d}x, \qquad x = 2\pi f \delta$$

$$\int_{-\infty}^{+\infty} \frac{\cos(2\pi f(\delta - T_c))}{f^2}\,\mathrm{d}f = 2\pi \cdot |\delta - T_c| \cdot \int_{-\infty}^{+\infty} \frac{\cos(x)}{x^2}\,\mathrm{d}x, \quad x = 2\pi f(\delta - T_c)$$

$$\int_{-\infty}^{+\infty} \frac{\cos(2\pi f(\delta + T_c))}{f^2}\,\mathrm{d}f = 2\pi \cdot |\delta + T_c| \cdot \int_{-\infty}^{+\infty} \frac{\cos(x)}{x^2}\,\mathrm{d}x, \quad x = 2\pi f(\delta + T_c)$$

Then:

$$\int_{-\infty}^{+\infty} |P(f)|^2 \cdot e^{j2\pi f \delta}\,\mathrm{d}f = \left(\frac{|\delta|}{\pi} - \frac{|\delta - T_c|}{2\pi} - \frac{|\delta + T_c|}{2\pi}\right) \cdot \int_{-\infty}^{+\infty} \frac{\cos(x)}{x^2}\,\mathrm{d}x$$

$\int_{-\infty}^{+\infty} \frac{\cos(x)}{x^2}\,\mathrm{d}x$ can be further developed by partial integration:

$$\int_{-\infty}^{+\infty} \frac{\cos(x)}{x^2}\,\mathrm{d}x = \left[-\frac{\cos(x)}{x}\right]_{-\infty}^{\infty} - \int_{-\infty}^{\infty} \frac{\sin(x)}{x}\,\mathrm{d}x$$

$\left[-\frac{\cos(x)}{x}\right]_{-\infty}^{\infty} = 0$ and $\int_{-\infty}^{\infty} \frac{\sin(x)}{x}\,\mathrm{d}x$ is called the Dirichlet integral and is equal to π. Then:

$$\int_{-\infty}^{+\infty} \frac{\cos(x)}{x^2}\,\mathrm{d}x = -\pi$$

And consequently:

$$\int_{-\infty}^{+\infty} |P(f)|^2 \cdot e^{j2\pi f \delta}\,\mathrm{d}f = \frac{1}{2} \cdot (|\delta + T_c| + |\delta - T_c| - 2|\delta|)$$

Then four cases can be distinguished:

- If $\delta \leq -T_c$, then:

$$\int_{-\infty}^{+\infty} |P(f)|^2 \cdot e^{j2\pi f \delta}\,\mathrm{d}f = 0$$

- If $-T_c < \delta \leq 0$, then:

$$\int_{-\infty}^{+\infty} |P(f)|^2 \cdot e^{j2\pi f\delta} \, \mathrm{d}f = T_c + \delta$$

- If $0 < \delta < T_c$, then:

$$\int_{-\infty}^{+\infty} |P(f)|^2 \cdot e^{j2\pi f\delta} \, \mathrm{d}f = T_c - \delta$$

- If $\delta \geq T_c$, then:

$$\int_{-\infty}^{+\infty} |P(f)|^2 \cdot e^{j2\pi f\delta} \, \mathrm{d}f = 0$$

Note that for a given n, only one value of m results a δ in that $T_c < \delta \leq 0$ and one other such as $0 < \delta < T_c$. Then it follows:

$$\mathrm{WCC}_T(\tau^l - \tau^k) = \frac{1}{T^2} \cdot \sum_{n=0}^{T/T_c - 1} (T_c + \delta_a)^2 + (T_c - \delta_b)^2$$

Where:

$$\delta_b = \Delta_{l,k}$$
$$\delta_a = \Delta_{l,k} - T_c$$

With $\Delta_{l,k} = \tau^l - \tau^k \mod T_c$ such that $\Delta_{l,k} \in [0\,; T_c[$. Consequently:

$$\boxed{\mathrm{WCC}_T(\tau^l - \tau^k) = \frac{\Delta_{l,k}^2 + (\Delta_{l,k} - T_c)^2}{T \cdot T_c}} \tag{A.3}$$

Note that the WCC is maximal (which corresponds to the biggest interference contribution) when the relative propagation delay between the two emitters is proportional to the chip duration ($\tau^l - \tau^k = 0 \mod T_c$). In this case, $\mathrm{WCC}_T(0) = {T_c}/{T}$. On the contrary, the WCC is minimal (which corresponds to the loweest interference contribution) when the relative delay between the two emitters is proportional to the half of the chip duration ($\tau^l - \tau^k = {T_c}/{2} \mod T_c$). In this case, $\mathrm{WCC}_T({T_c}/{2}) = {T_c}/{2 \cdot T}$. In average, the WCC is equals to ${2 \cdot T_c}/{3 \cdot T}$

A.2 Differential Waveform Convolution Coefficient and Differential Multiple Access Interference

The Differential Waveform Convolution Coefficient (DWCC) is defined as:

$$\begin{aligned}\mathrm{DWCC}_T(\tau^l - \tau^k) &= \mathrm{var}\left[\frac{1}{T} \cdot \int_0^T \frac{\partial c^k(t - \tau^k)}{\partial t} \cdot c^l(t - \tau^l) \, \mathrm{d}t\right] \\ &= \mathrm{var}\left[\frac{1}{T} \cdot \int_0^T \frac{\partial c^k(t - \tau^k)}{\partial \tau^k} \cdot c^l(t - \tau^l) \, \mathrm{d}t\right]\end{aligned}$$

The term $\mathcal{Y}_T^{l,k}$ represents the Differential Multiple Access Interference (DMAI):

$$\begin{aligned}\mathcal{Y}_T^{l,k} &= \int_0^T \frac{\partial c^k(t-\tau^k)}{\partial \tau^k} \cdot c^l(t-\tau^l)\,\mathrm{d}t \\ &= -\int_0^T \frac{\partial c^k(t-\tau^k)}{\partial t} \cdot c^l(t-\tau^l)\,\mathrm{d}t\end{aligned}$$

The sequences $c^k(.)$ and $c^l(.)$ are independent, then:

$$\mathcal{E}\left[\mathcal{Y}_T^{l,k}\right] = 0$$

A.2.1 General Case

The term $\mathcal{Y}_T^{l,k}$ can be developed by using the spreading code signals: Then it follows:

$$\begin{aligned}\mathcal{Y}_T^{l,k} &= -\sum_{n=-\infty}^{+\infty}\sum_{m=-\infty}^{+\infty} c_n^l \cdot c_m^k \cdot \int_0^T p(t-nT_c-\tau^l)\cdot\frac{\partial p(t-mT_c-\tau^k)}{\partial t}\,\mathrm{d}t \\ &\approx -\sum_{n=0}^{T/T_c-1}\sum_{m=-\infty}^{+\infty} c_n^l \cdot c_m^k \cdot \int_{-\infty}^{+\infty} p(t-nT_c-\tau^l)\cdot\frac{\partial p(t-mT_c-\tau^k)}{\partial t}\,\mathrm{d}t\end{aligned}$$

For the same reasons as in the derivation of the WCC. Then using the Parseval identity, the DMAI can be rewritten as:

$$\mathcal{Y}_T^{l,k} = -\sum_{n=0}^{T/T_c-1}\sum_{m=-\infty}^{+\infty} c_n^l \cdot c_m^k \cdot \int_{-\infty}^{+\infty} (j2\pi f)\cdot|P(f)|^2 \cdot e^{j2\pi f(\tau^l-\tau^k+T_c\cdot(n-m))}\,\mathrm{d}f$$

Since the waveform $p(.)$ is real, the module of its Fourier transform $P(.)$ is even. Consequently:

$$\boxed{\begin{aligned}\mathcal{Y}_T^{l,k} = &\sum_{n=0}^{T/T_c-1}\sum_{m=-\infty}^{+\infty} c_n^l \cdot c_m^k \cdot \\ &\int_{-\infty}^{+\infty}(2\pi f)\cdot|P(f)|^2\cdot\sin\left(2\pi f(\tau^l-\tau^k+T_c\cdot(n-m))\right)\mathrm{d}f\end{aligned}} \quad \text{(A.4)}$$

Then the variance:

$$\begin{aligned}\mathrm{var}\left[\mathcal{Y}_T^{l,k}\right] &= \mathcal{E}\left[\left(\mathcal{Y}_T^{l,k}\right)^2\right] - \mathcal{E}\left[\mathcal{Y}_T^{l,k}\right]^2 \\ &= \mathcal{E}\left[\left(\mathcal{Y}_T^{l,k}\right)^2\right] \\ &= \sum_{n=0}^{T/T_c-1}\sum_{m=-\infty}^{+\infty}\sum_{\tilde{n}=0}^{T/T_c-1}\sum_{\tilde{m}=-\infty}^{+\infty}\mathcal{E}\left[c_n^l c_m^k c_{\tilde{n}}^l c_{\tilde{m}}^k\right] \\ &\quad\cdot\int_{-\infty}^{+\infty}(2\pi f)\cdot|P(f)|^2\cdot\sin\left(2\pi f(\tau^l-\tau^k+T_c\cdot(n-m))\right)\mathrm{d}f \\ &\quad\cdot\int_{-\infty}^{+\infty}(2\pi f)\cdot|P(f)|^2\cdot\sin\left(2\pi f(\tau^l-\tau^k+T_c\cdot(\tilde{n}-\tilde{m}))\right)\mathrm{d}f\end{aligned}$$

Since $\mathcal{E}\left[c_n^l c_m^k c_{\tilde{n}}^l c_{\tilde{m}}^k\right] = 0$ if $n \neq \tilde{n}$ or $m \neq \tilde{m}$ and $\mathcal{E}\left[c_n^l c_m^k c_{\tilde{n}}^l c_{\tilde{m}}^k\right] = 1$ if $n = \tilde{n}$ and $m = \tilde{m}$, finally:

$$\boxed{\begin{aligned}\mathrm{DWCC}_T(\tau^l - \tau^k) = \frac{1}{T^2} \cdot \sum_{n=0}^{T/T_c-1} \sum_{m=-\infty}^{+\infty} \\ \left(\int_{-\infty}^{+\infty} (2\pi f) \cdot |P(f)|^2 \cdot \sin\left(2\pi f(\tau^l - \tau^k + T_c(n-m))\right) \mathrm{d}f\right)^2\end{aligned}} \quad \text{(A.5)}$$

A.2.2 BPSK Case

The case of a BPSK signal will be now analysed. The effect of the low-pass filter will be neglected.

Let $\delta = \tau^l - \tau^k + T_c \cdot (n-m)$ as before. Then it follows:

$$\begin{aligned}&\int_{-\infty}^{+\infty} (j2\pi f) \cdot |P(f)|^2 \cdot e^{j2\pi f\delta} \,\mathrm{d}f \\ &= \frac{2j}{\pi} \cdot \int_{-\infty}^{+\infty} \frac{1}{f} \cdot \sin^2(\pi f T_c) \cdot e^{j2\pi f\delta} \,\mathrm{d}f \\ &= -\frac{2}{\pi} \cdot \int_{-\infty}^{+\infty} \frac{1}{f} \cdot \sin^2(\pi f T_c) \cdot \sin(2\pi f\delta) \,\mathrm{d}f \\ &= -\frac{1}{\pi} \cdot \int_{-\infty}^{+\infty} \frac{1}{f} \cdot (1 - \cos(2\pi f T_c)) \cdot \sin(2\pi f\delta) \,\mathrm{d}f \\ &= -\frac{1}{\pi} \cdot \int_{-\infty}^{+\infty} \frac{\sin(2\pi f\delta)}{f} \,\mathrm{d}f + \frac{1}{2\pi} \cdot \int_{-\infty}^{+\infty} \frac{\sin(2\pi f(\delta - T_c))}{f} \,\mathrm{d}f \\ &\quad + \frac{1}{2\pi} \cdot \int_{-\infty}^{+\infty} \frac{\sin(2\pi f(\delta + T_c))}{f} \,\mathrm{d}f\end{aligned}$$

Since:

$$\int_{-\infty}^{+\infty} \frac{\sin(kx)}{x} \,\mathrm{d}x = \pi \cdot \mathrm{sign}(k)$$

Then:

$$\begin{aligned}&\int_{-\infty}^{+\infty} (j2\pi f) \cdot |P(f)|^2 \cdot e^{j2\pi f\delta} \,\mathrm{d}f \\ &= \frac{1}{2} \cdot \Big(\mathrm{sign}(\delta + T_c) + \mathrm{sign}(\delta - T_c) - 2 \cdot \mathrm{sign}(\delta)\Big)\end{aligned}$$

Then four cases can be distinguished:

- If $\delta \leq -T_c$, then:

$$\int_{-\infty}^{+\infty} |P(f)|^2 \cdot e^{j2\pi f\delta} \,\mathrm{d}f = 0$$

- If $-T_c < \delta \leq 0$, then:

$$\int_{-\infty}^{+\infty} |P(f)|^2 \cdot e^{j2\pi f\delta} \,\mathrm{d}f = 1$$

- If $0 < \delta < T_c$, then:

$$\int_{-\infty}^{+\infty} |P(f)|^2 \cdot e^{j2\pi f\delta} \, \mathrm{d}f = -1$$

- If $\delta \geq T_c$, then:

$$\int_{-\infty}^{+\infty} |P(f)|^2 \cdot e^{j2\pi f\delta} \, \mathrm{d}f = 0$$

Note that for a given n, only one value of m results a δ in such that $T_c < \delta \leq 0$ and one other such that $0 < \delta < T_c$. Then it follows:

$$\mathrm{DWCC}_T(\tau^l - \tau^k) = \frac{1}{T^2} \cdot \sum_{n=0}^{T/T_c} (1)^2 + (-1)^2$$

Consequently:

$$\boxed{\mathrm{DWCC}_T(\tau^l - \tau^k) = \frac{2}{T \cdot T_c}} \tag{A.6}$$

A.3 Double Differential Multiple Access Interference

The $\mathcal{Z}_T^{l,k}$ represents the Double Differential Multiple Access Interference (D2MAI) and is defined as:

$$\mathcal{Z}_T^{l,k} = \int_0^T \frac{\partial c^k(t-\tau^k)}{\partial \tau^k} \cdot \frac{\partial c^l(t-\tau^l)}{\partial \tau^l} \, \mathrm{d}t$$

Since the sequences $c^k(.)$ and $c^l(.)$ are independent:

$$\mathcal{E}\left[\mathcal{Z}_T^{l,k}\right] = 0$$

A.3.1 General Case

This term $\mathcal{Z}_T^{l,k}$ can be developed by using the spreading code signals. Then it follows:

$$\begin{aligned}
\mathcal{Z}_T^{l,k} &= \sum_{n=-\infty}^{+\infty} \sum_{m=-\infty}^{+\infty} c_n^l \cdot c_m^k \cdot \int_0^T \frac{\partial p(t-nT_c-\tau^l)}{\partial \tau^l} \cdot \frac{\partial p(t-mT_c-\tau^k)}{\partial \tau^k} \, \mathrm{d}t \\
&\approx \sum_{n=0}^{T/T_c-1} \sum_{m=-\infty}^{+\infty} c_n^l \cdot c_m^k \cdot \int_{-\infty}^{+\infty} \frac{\partial p(t-nT_c-\tau^l)}{\partial \tau^l} \cdot \frac{\partial p(t-mT_c-\tau^k)}{\partial \tau^k} \, \mathrm{d}t
\end{aligned}$$

Then by using the Parseval identity:

$$\mathcal{Z}_T^{l,k} = \sum_{n=0}^{T/T_c-1} \sum_{m=-\infty}^{+\infty} c_n^l \cdot c_m^k \cdot \int_{-\infty}^{+\infty} (2\pi f)^2 \cdot |P(f)|^2 \cdot e^{j2\pi f(\tau^l - \tau^k + T_c \cdot (n-m))} \, \mathrm{d}f$$

The waveform $p(.)$ is real, then:

$$\mathcal{Z}_T^{l,k} = \sum_{n=0}^{T/T_c-1} \sum_{m=-\infty}^{+\infty} c_n^l \cdot c_m^k \cdot \int_{-\infty}^{+\infty} (2\pi f)^2 \cdot |P(f)|^2 \cdot \cos\left(2\pi f(\tau^l - \tau^k + T_c \cdot (n-m))\right) \mathrm{d}f \quad \text{(A.7)}$$

The variance is not computed because it is required neither in chapter 3 nor in chapter 4.

A.3.2 BPSK Case

The case of a BPSK signal will be now analysed. Note that here the effect of the filter can not be neglected (otherwise the signal would have an infinite spectrum). Before filtering, the chip modulation waveform is:

$$p(t) = \begin{cases} 1 & \text{if } -\frac{T_c}{2} < t < \frac{T_c}{2} \\ 0 & \text{else} \end{cases}$$

The filtered chip waveform is $p_F(t) = p(t) * h(t)$, where $h(t)$ is the impulse response of the low-pass filter with cut-off frequency B. Then in the case of a brick-wall filter, the Fourier transform of $p_F(t)$ is:

$$P(f) = \begin{cases} T_c \cdot \mathrm{sinc}\left(\pi f T_c\right) & \text{if } f \in [-B; B] \\ 0 & \text{otherwise} \end{cases}$$

Let $\delta = \tau^l - \tau^k + T_c \cdot (n-m)$ as before. Then it follows:

$$\begin{aligned}
&\int_{-\infty}^{+\infty} (2\pi f)^2 \cdot |P(f)|^2 \cdot e^{j2\pi f\delta} \,\mathrm{d}f \\
&= 4 \cdot \int_{-B}^{+B} \sin\left(\pi f T_c\right)^2 \cdot \cos\left(2\pi f\delta\right) \mathrm{d}f \\
&= 4 \cdot \int_{0}^{B} \left(1 - \cos\left(2\pi f T_c\right)\right) \cdot \cos\left(2\pi f\delta\right) \mathrm{d}f \\
&= 4 \cdot \int_{0}^{B} \cos\left(2\pi f\delta\right) \mathrm{d}f - 2 \cdot \int_{0}^{B} \cos\left(2\pi f(\delta - T_c)\right) \mathrm{d}f \\
&\quad - 2 \cdot \int_{0}^{B} \cos\left(2\pi f(\delta + T_c)\right) \mathrm{d}f \\
&= 4 \cdot B \cdot \mathrm{sinc}\left(2\pi B T_c\right) - 2 \cdot B \cdot \mathrm{sinc}\left(2\pi B(\delta - T_c)\right) - 2 \cdot B \cdot \mathrm{sinc}\left(2\pi B(\delta + T_c)\right)
\end{aligned}$$

Finally:

$$\begin{aligned}
\mathcal{Z}_T^{l,k} = 2 \cdot B \cdot \sum_{n=0}^{T/T_c-1} \sum_{m=-\infty}^{+\infty} c_n^l \cdot c_m^k \\
\cdot \big(2 \cdot \mathrm{sinc}\left(2\pi B(\tau^l - \tau^k + T_c \cdot (n-m)\right) \\
-\mathrm{sinc}\left(2\pi B(\tau^l - \tau^k + T_c \cdot (n-m-1))\right) \\
-\mathrm{sinc}\left(2\pi B(\tau^l - \tau^k + T_c \cdot (n-m+1))\right)\big)
\end{aligned} \quad \text{(A.8)}$$

Appendix B

Early Minus Late Discriminator

The Delay Locked Loop (DLL) tracks and estimates the misalignment between the locally generated PRN code replica and the incoming signal, within the tracking loops. For that purpose, the DLL uses a discriminator.

The DLL actually uses two additional correlators: one of them correlates the input signal with an advance replica of the prompt code, the other one with a late replica. The difference between the Early and Late correlators produces the so called S-curve. The DLL actually tracks the zero-crossing of this S-curve, in order to estimate the current error, which is then fed back to the local code generation block to correct the previous estimation of the incoming code delay.

An Early minus Late power discriminator is considered. The discriminator is in open loop, in order to make the computations easier. If the signal from pseudolite l is tracked, then the discriminator is:

$$D(\Delta\tau^l) = C_E(\Delta\tau^l)^2 - C_L(\Delta\tau^l)^2$$

Where $C_E(.)$ (respectively $C_L(.)$) represents the correlation of the received signal and the early (respectively late) local replica of the tracked code signal:

$$C_E(\Delta\tau^l) = \frac{1}{T} \cdot \int_0^T r(t) \cdot c^l \left(t + \frac{d_{\mathrm{EL}} \cdot T_c}{2} \right) \mathrm{d}t$$
$$C_L(\Delta\tau^l) = \frac{1}{T} \cdot \int_0^T r(t) \cdot c^l \left(t - \frac{d_{\mathrm{EL}} \cdot T_c}{2} \right) \mathrm{d}t$$

It is shown in [16] that the expectation of the correlator discriminator output is:

$$\mathcal{E}\left[D(\Delta\tau^l)\right] = \begin{cases} 2 \cdot \mathcal{P}^l (2 - d_{\mathrm{EL}}) \cdot \frac{\Delta\tau^l}{T_c} & \text{if } \left|\Delta\tau^l\right| < \frac{d \cdot T_c}{2} \\ 0 & \text{otherwise} \end{cases}$$

Then an estimator of the delay $\Delta\tau^l$ is:

$$\Delta\hat{\tau}^l = \frac{D(\Delta\tau^l)}{2 \cdot (2 - d_{\mathrm{EL}}) \cdot T_c \cdot \mathcal{P}^l}$$

The efficiency of this estimator can be characterized by its variance. It is also shown in [16] that the variance of this estimator can be expressed as:

$$\mathrm{var}\left[\tau^l - \hat{\tau}^l\right] \approx \frac{d_{\mathrm{EL}} \cdot T_c^2}{4 \cdot \mathrm{SNIR}^l} \cdot \left(1 + \frac{2}{(2 - d_{\mathrm{EL}}) \cdot \mathrm{SNIR}^l}\right)$$

Bibliography

[1] B. D. Elrod and A. J. Van Dierendonck, *Pseudolites, In Global Positioning System: Theory and Applications*. American Institute of Earonautic and Astonautics Inc, 1996.

[2] C. O'Driscoll, D. Borio, and J. Fortuny-Guasch, "Investigation of Pulsing Schemes for Pseudolite Applications," *Proceedings of the 24th International Technical Meeting of The Satellite Division of the Institute of Navigation (ION GNSS 2011), Portland, OR*, pp. 3480–3492, September 2011.

[3] D. Borio, *A statistical theory for GNSS signal acquisition*. PhD thesis, Politecnico di Torino, 2008.

[4] A. Mezghani, F. Antreich, and J. Nossek, "Multiple parameter estimation with quantized channel output," in *Smart Antennas (WSA), 2010 International ITG Workshop on*, pp. 143 –150, feb. 2010.

[5] M. K. Varanasi and B. Aazhang, "Multistage detection in asynchronous code-division multiple-access communications," *IEEE Transactions on Communications*, vol. 38, pp. 509–519, 1990.

[6] D. S. Chen and S. Roy, "An adaptive multiuser receiver for CDMA systems," *Selected Areas in Communications, IEEE Journal on*, vol. 12, pp. 808 –816, jun 1994.

[7] M. Pursley and D. Sarwate, "Performance Evaluation for Phase-Coded Spread-Spectrum Multiple-Access Communication–Part II: Code Sequence Analysis," *Communications, IEEE Transactions on*, vol. 25, pp. 800 – 803, aug 1977.

[8] J. Morrow, R.K. and J. Lehnert, "Bit-to-bit error dependence in slotted DS/SSMA packet systems with random signature sequences," *Communications, IEEE Transactions on*, vol. 37, pp. 1052 –1061, oct 1989.

[9] P. Patel and J. Holtzman, "Analysis of a simple successive interference cancellation scheme in a DS/CDMA system," *Selected Areas in Communications, IEEE Journal on*, vol. 12, pp. 796 –807, jun 1994.

[10] P. Madhani, P. Axelrad, K. Krumvieda, and J. Thomas, "Application of successive interference cancellation to the GPS pseudolite near-far problem," *Aerospace and Electronic Systems, IEEE Transactions on*, vol. 39, pp. 481 – 488, april 2003.

[11] P. Patel and J. Holtzman, "Performance comparison of a DS/CDMA system using a successive interference cancellation (IC) scheme and a parallel IC scheme under fading," in *Communications, 1994. ICC '94, SUPERCOMM/ICC '94, Conference Record, 'Serving Humanity Through Communications.' IEEE International Conference on*, pp. 510 –514 vol.1, may 1994.

[12] A. Kaul and B. Woerner, "An analysis of adaptive multistage interference cancellation for CDMA," in *Vehicular Technology Conference, 1995 IEEE 45th*, vol. 1, pp. 82 –86 vol.1, jul 1995.

[13] T. A. Stansell, Jr., "RTCM SC-104 Recommended Pseudolite Signal Specification," *NAVIGATION*, vol. 33, pp. 42–59, 1986.

[14] K. Borre, D. M. Akos, N. Bertelsen, P. Rinder, and S. r. H. Jensen, *A Software-Defined GPS and Galileo Receiver: A Single-Frequency Approach*. Applied and Numerical Harmonic Analysis, Birkhäuser, 2007.

[15] F. Soualle, M. Cattenoz, K. Giger, and C. Zecha, "Improved Analytical Models of SNIR Degradation in Presence of Pulsed Signals and Impact of Code-Pulse Synchrony," *Proc. GNSS Signals 2011, Fifth European Workshop on GNSS Signals and Signal Processing, IAS (Institut Aero Spatial), Toulouse, France*, 2011.

[16] A. J. Van Dierendonck, P. Fenton, and T. Ford, "Theory and Performance of Narrow Correlator Spacing in a GPS Receiver," *Journal of the Institute of Navigation*, vol. 39, pp. 265–283, Fall 1992 1992.